TRANSPLANTATION STRATEGIES FOR THE ANALYSIS OF BRAIN DEVELOPMENT AND REPAIR

BY

MILES G. CUNNINGHAM

B.A., PHYSIOLOGICAL PSYCHOLOGY, UNIVERSITY OF ARKANSAS

(1985)

SUBMITTED TO THE DEPARTMENT OF BRAIN AND COGNITIVE SCIENCES

IN PARTIAL FULFILLMENT OF THE REQUIREMENTS

FOR THE DEGREE OF

DOCTOR OF PHILOSOPHY

IN NEUROSCIENCE

AT THE

MASSACHUSETTS INSTITUTE OF TECHNOLOGY

MAY 1993

Signature of Author _____.
Department of Brain and Cognitive Sciences
May 17, 1993

Certified by _____.
Dr. Ronald D.G. McKay, Thesis Supervisor

Accepted by _____.
Dr. Emilio Bizzi
Chairman, Department of Brain and Cognitive Sciences

TRANSPLANTATION STRATEGIES FOR THE ANALYSIS OF BRAIN DEVELOPMENT AND REPAIR

By

Miles G. Cunningham

Submitted to the Department of Brain and Cognitive Sciences on May 19, 1993 in partial fulfillment of the requirements for the degree of Ph.D.

ABSTRACT

The series of experiments presented herein are based on novel approaches to neural transplantation as a means to advance our understanding of development, function, and repair in the central nervous system. Part I of this thesis presents new techniques which helped make possible the experiments which were to follow. A scaled-down stereotaxic instrument is described which allows for precision surgery in newborn and very small rodents. The instrument permits the administration of long-term hypothermic anesthesia and is designed to accomodate animals of varying sizes. The instrument has proven practical while allowing a level of accuracy and reproducibility that exceeds any previously described device or technique. This is supplemented by detailed protocols for transplantation into the neonate as well as the adult. A micrografting approach is introduced for enhancing placement accuracy and cell survival. Considerations prior to and after transplantation surgery are also discussed. The methods for neonatal stereotaxic surgery are

applied in the following report which describes the reconstitution of the nigro-striatal system with embryonic ventral mesencephalic grafts implanted into the substantia nigra of the 6-OHDA-lesioned neonate. The next report is a formal investigation of the efficacy of the micrografting approach as compared to the traditional grafting technique. This study demonstrated that, in contrast to grafting a subject with cell suspensions in relatively large volumes (two 1.8 µl deposits), multiple microvolume (eighteen 0.2 µl deposits) grafts increased cell survival some 2.8-fold, dopamine production was increased 2.5-fold, and fiber extension was markedly increased as well. The improved efficiency seen with multiple micrografts may be attributable to factors such as the increased surface area of the implanted tissue, which may allow a greater level of graft-host interaction, and a decrease in trauma during the grafting procedure.

Part II describes the detailed characterization of a nestin-positive cell line, HiB5, derived from embryonic hippocampus and immortalized using a temperature-sensitive allele of SV40 T-antigen. This oncogene enables the cells to divide indefinitely at 33°C, but not at 39°C, the body temperature of rodents. Upon grafting into the developing dentate gyrus, HiB5 cells differentiate into neurons and astrocytes typical of the dentate gyrus. Interestingly, if grafted into the developing cerebellum, these cells differentiate into neurons and astrocytes characteristic of the cerebellum. These conclusions, however, are based primarily on morphological and positional criteria. The subsequent study establishes the clonality of the cell line and analyzes the gene expression of HiB5 after differentiating in the hippocampus and cerebellum. It is shown that the cell line down-

regulates the stem cell-specific gene, nestin, and proceeds to express neuronal and astrocytic genes. The functional integration of the engrafted cells is then indirectly assessed by inducing the up-regulation of the immediate early gene, c-*fos*, in the grafted dentate gyrus through seizure activity produced by systemic kainic acid. The ultrastructural characteristics and capacity for grafted cells to establish appropriate synapses is reported in the following chapter. Cells labeled with electron-dense colloidal gold-conjugated nanospheres were examined with electron microscopy, which revealed the engrafted cells having stereotypical neuronal phenotypes. Induction of long-term potentiation (LTP) of the perforant path - granule cell synapse in grafted animals resulted in transplanted cells up-regulating the LTP-specific gene, NGFI-A, in a manner identical to endogenous dentate gyrus granule neurons.

The question then arises as to whether the pluripotency seen with HiB5 is due to the special conditions in which HiB5 was produced and maintained, or is such plasticity an inherent characteristic of neural precursors in general. To help address this, single cell suspensions from the newborn cerebellum were grafted into the developing dentate gyrus. Cerebellar primordia were harvested from two sources: 2-day-old rats labeled with tritiated thymidine and 3-day-old transgenic mice carrying the *lacZ* gene driven by a neuron-specific enolase promoter. Therefore, two independent labeling methods were used, a DNA marker and a transgene. With both approaches, cerebellum-derived cells integrated into the host site and differentiated into region-specific neurons and astrocytes. These studies provide evidence that pluripotent neural precursor cells can

be sustained in culture indefinitely and that the systematic manipulation and control of such cells may be realized in the future. This capability would provide a powerful approach to the study of brain development and perhaps serve as an abundant tissue source for research and therapy in neurodegenerative diseases.

TABLE OF CONTENTS

ACKNOWLEDGEMENTS

I wish to warmly acknowledge the following individuals for their contributions to my education, my research, and the enrichment of my life. . .

The esteemed members of my thesis committee:

Ron McKay, for believing in a kid from Arkansas; whose knowledge, wit, and charm I can only hope to match; and because of whom there has never been a dull moment.

Anders Björklund, whom my respect for as a scientist and as a person is immense, and whom I have been so fortunate to work with.

Arthur Lander, for a sense of security and for level-headed advice from the beginning. There was always Arthur.

Mriganka Sur, a strong scientist and a trustworthy colleague, for making the mistake of caring.

Past and present members of the McKay research group for their friendship and support: Diana Collazo, Tim Hayes, Richard Josephson, Urban Lendahl, Martha Marvin, Patricia Renfranz, George Vaughn, Carlos Vicario, and Lyle Zimmerman.

My mother and my father, who have given their unconditional love and encouragement and helped me maintain my perspective on life.

My beloved Jeanie, who has given to me her warmth and cheerfulness, even during the dark days.

INTRODUCTION

Grafting cells into specific sites of the mature and developing brain is in many ways the ultimate assay for the functional capacities of the cells of interest. While neural grafting has become important in many aspects of neurobiology and is showing promise as a therapy in neurodegenerative diseases, surprisingly little attention has been given to the details of the grafting technique itself. The delivery method and the placement of cells at precise targets in the brain is of crucial importance. Such technical conscientiousness may determine the success or failure of a neural graft - whether it is in a newborn rodent or a patient with Parkinson's disease.

Stereotaxic surgical techniques enable researchers to locate and manipulate structures in the adult brain with great accuracy. Such surgical precision in the very young newborn rodent would allow researchers to elegantly investigate neural systems in the developing animal. However, there are many considerations one must take into account when devising a neonatal stereotaxic technique. Because ossification is incomplete in the newborn, the skull is very thin and elastic, and thus poses a number of difficulties. The greatest problem is securing the head in a fixed and rigid position which is reproducible, while not distorting or shifting the brain in the cranium. Stabilizing the head is difficult in the newborn since the external auditory meati, which accept earbars in the adult, are underdeveloped. Very young neonates lack front incisors as well,

which in adult stereotaxic surgery are hooked over a tooth bar. The cartilaginous nature of the skull also becomes troublesome when attempting to penetrate the skull or produce a craniectomy without damaging the underlying tissue. Moreover, skull sutures are not yet fully established and the identification of landmarks such as bregma and lambda can be ambiguous.

Special consideration must also be given to the method of anesthesia used for newborns. Immature animals have lower levels of serum albumin and body fat which contribute to the diminished efficacy of conventional anesthetics, such as barbiturates used in adults (2). The method of choice for reliable anesthesia of neonatal rodents is hypothermia (7). However after the animal is about seven days of age, this method is no longer safe and practical, and alternative methods must be used.

The potential importance of the newborn developing brain as a model system for the study of brain disorders has, by and large, been slighted in contemporary thought in neural transplantation as a therapeutic approach. The majority of studies have been conducted in the adult for evident reasons. These disorders occur in the adult, usually the aged, and so it is the mature brain which must be studied and manipulated if the disease is to be treated. The data presented in Chapter 3 challenges this trend. Embryonic tissue taken from the ventral mesencephalon and grafted into the substantia nigra of the 6-OHDA lesioned newborn survives and reinnervates the striatum. This is the first demonstration of the reestablishment of the nigro-striatal pathway to date. Future studies will be directed toward elucidating

the factors which allow this reconstruction to occur in neonates but not in the adult.

For many years, transplantation scientists have known that grafts of fetal nigral tissue implanted into the dopamine (DA) denervated striatum can restore DA neurotransmission in the grafted area and reverse some of the behavioral deficits induced by a neurotoxic lesion of the nigrostriatal DA pathway (for reviews, see Refs 3,4,17). The efficacy of the standard transplantation approach, however, has several clear-cut limitations: First, with current grafting procedures the survival rate of the grafted DA neuroblasts and young postmitotic DA neurons is only in the range of 5-10%. Secondly, although graft-derived DA release (as measured by microdialysis) can be close to normal in the area surrounding the grafts (12,16) the striatal tissue DA levels are restored, on average, only to about 10-20% of normal (6,13,15). Finally, the behavioral recovery seen in the grafted animals is incomplete; while certain aspects of the lesion-induced deficits (such as drug-induced motor asymmetry and simple sensorimotor orienting responses) show complete or almost complete recovery, the deficits in more complex tasks (e.g., skilled paw use and disengage behavior) have remained unaffected (6,11). By disseminating multiple microvolume grafts into the lesioned striatum, these limitations are beginning to be addressed. However, complete recovery of the complex behavioral deficits is only being approached, and may necessitate a more comprehensive reconstruction of the mesostriatal system.

Surprisingly, little effort has been made toward grafting fetal nigral tissue homotopically; that is, transplanting the tissue from the

fetus with precision into the adult substantia nigra. The main reason for this is the difficulty in the procedure. This target is small relative the striatum; the size of the graft must be reduced and the insult to the target tissue must be minimized. The aforementioned micrografting technique is now allowing tissue to be implanted not only into the nigra, but into subregions of this structure. Preliminary results indicate that these transplants produce amelioration of more complex behavioral deficits which as of yet have not been improved with transplants into the striatum. Ongoing studies involve multiple micrografts placed into the nigra, the striatum, and the nucleus accumbens to effect a more complete recovery in this model of Parkinson's disease.

Although these results show promise, transplantation of fetal tissue is faced with inherent ethical and technological pitfalls. The use of human tissues, particularly of the unborn, will invariably cause social reaction, even violent reaction. Complicating this is the impending need for more tissue. As reviewed by Björklund (5), to achieve a significant level of recovery, approximately 10-15 fetuses may be necessary to treat a single patient. It also must be considered that many of the aborted fetuses cannot be used due to defacement and/or contamination during extraction or because of maternal diseases.

Culturing tissues, and perhaps expanding the cells of interest, is becoming a more realistic alternative. Immortalized cell lines have been derived from the developing brain by a variety of methods (1,8,10,14). Some of these cell lines express the neural epithelial stem cell antigen (nestin) for prolonged periods in culture, though

nestin expression in vivo is transient (9). The stable expression of the nestin protein in immortalized cells suggests that they retain some features of primary stem cells, but also suggests that they may not be able to progress beyond the precursor cell state easily. To facilitate the differentiation of nestin-positive immortal stem cells, they have been immortalized using a temperature-conditional oncogene, the *tsA58* allele of SV40 Large T-antigen (T-antigen). Such immortal cell lines have been established from the early postnatal cerebellum ((9); Redies et al., submitted for publication) and optic nerve (Almazan and McKay, submitted for publication), and they grow well at 33°C. Placing the cells at 39°C can result in the loss of precursor properties and the acquisition of morphological and biochemical characteristics of differentiated cells. However, this transition is difficult to observe in simple *in vitro* systems. For a full assessment of the developmental capacity of a cell line, it may be critical to place the cells into a suitable environment. Since the non-permissive temperature of the *tsA58* allele of T-antigen is the same as the body temperature of rodents, stem cells immortalized with this gene can theoretically be implanted into the developing brain, where the temperature should inhibit oncogene function and the cells will be exposed to appropriate extracellular cues. This served as the incentive for the present studies involving the *in vivo* characterization of the immortalized hippocampal cell line, HiB5.

The fate and organization of the cells comprising the central nervous system is determined by a complex orchestration of genetic and epigenetic factors. This becomes evident when considering the myriad transplantation observations either promoting the

importance of environmental influence or providing evidence that cell fate is determined by its lineage. McConnell (12) emphasized that although at early stages, a stem cell may be pluripotential, as the brain structure develops, the cells become progressively less plastic. To what extent, though, are stem cells pluripotent? McConnell further stated (premonitorily), "it remains unclear whether individual precursors could be cajoled into altering their fates if transplanted individually or in small groups". The final study in this series of experiments addresses this issue.

REFERENCES

1 Bartlett, P. F., Reid, H. H., Bailey, K. A., and Bernado, O. (1988). Immortalization of mouse neural precursor cells by the c-*myc* oncogene. Proc. Natl. Acad. Sci. USA *85*, 3255-3259.

2 Benjamin, M.M. (1978) Outline of Veterinary Clinical Pathology, Iowa State University Press, Ames, Iowa, pp 108-115.

3 Björklund A., Lindvall O., Isacson O., Brundin P., Wictorin K., Strecker R. E., Clarke D. J. and Dunnett S. B. (1987) Mechanisms of action of intracerebral neural implants. *Trends Neurosci.* **10,** 509- 516.

4 Björklund A. (1992) Dopaminergic transplants in experimental parkinsonism: cellular mechanisms of graft-induced functional recovery. *Curr. Opin. Neurobiol.* **2,** 683-689.

5 Björklund A. (1993) Better Cells of brain Repair. *Nature* 362, 414- 415.

6 Dunnett S. B., Whishaw I. Q., Rogers D. C. and Jones G. H. (1987) Dopamine-rich grafts ameliorate whole body motor asymmetry and sensory neglect but not independent limb use in rats with 6-hydroxydopamine lesions. *Brain Res.* **415,** 63-78.

7 Flecknell, P. A. (1987) Laboratory Animal Anesthesia, Academic Press, Inc, San Diego, pp. 73-74.

8 Frederiksen, K., Jat, P. S. , Valtz, N., Levy, D., and McKay, R. D. G. (1988). Immortalization of precursor cells from the mammalian CNS. Neuron *1*, 439-448.

9 Frederiksen, K., and McKay, R. (1988). Proliferation and differentiation of rat neuroepithelial precursor cells in vivo. J. Neurosci. *8*, 1144-1151.

10 Lee, H. J., Hammond, D. N., Large, T. H., Roback, J. D., Sim, J. A., Brown, D. A., Otten, U. H., and Wainer, B. H. (1990). Neuronal properties and trophic activities of immortalized hippocampal

cells from embryonic and young adult mice. J. Neurosci. *10*, 1779-1787.

11 Mandel R. J., Brundin P. and Björklund A. (1990) The importance of graft placement and task complexity for transplant-induced recovery of simple and complex sensorimotor deficits in dopamine denervated rats. *Eur. J. Neurosci.* **2,** 888-894.

12 McConnell, S.K. (1991) The Generation of Neuronal diversity in the Central Nervous System. *Annu. Rev. Neurosci.* 14, 269-300.

13 Rioux L., Gaudin D. P., Bui L. K., Gregoire L., DiPaolo T. and Bedard P. J. (1991) Correlation of functional recovery after a 6-hydroxy-dopamine lesion with survival of grafted fetal neurons and release of dopamine in the striatum of the rat. *Neuroscience* **40,** 123-131.

14 Ryder, E. F., Snyder, E. Y., and Cepko, C. L. (1990). Establishment and characterization of multipotent neural cell lines using retrovirus vector-mediated oncogene transfer. J. Neurobiol. *21*, 356-375.

15 Schmidt R. H., Björklund A., Stenevi U., Dunnett S. B. and Gage F. H. (1983) Intracerebral grafting of neuronal cell suspensions. III. Activity of intrastriatal nigral suspension implants as assessed by measurements of dopamine synthesis and metabolism. *Acta Physiol. Scand.* **522,** 19-28.

16 Strecker R., Sharp T., Brundin P., Zetterström T., Ungerstedt U. and Björklund A. (1987) Autoregulation of dopamine release and metabolism by intrastriatal nigral grafts as revealed by intracerebral dialysis. *Neuroscience* **22,** 169-178.

17 Yurek D. and Sladek J. (1990) Dopamine cell replacement: Parkinson's disease. *Annu. Rev. Neurosci.* **13,** 415-440.

TRANSPLANTATION STRATEGIES FOR THE ANALYSIS OF BRAIN DEVELOPMENT AND REPAIR

PART I

NEW APPROACHES AND METHODOLOGY FOR NEURAL TRANSPLANTATION

CHAPTER 1

PRECISION SURGERY IN NEWBORN RODENTS USING A MINIATURIZED STEREOTAXIC INSTRUMENT

Summary

We describe a simple, scaled-down instrument which enables accurate, reproducible stereotaxic placements into specific sites in the brain of the newborn rat. The instrument is specially designed for the administration of long-term hypothermia, yet permits the use of alternative methods of anesthesia. The design of the head-stabilizing mechanism allows head positioning to be finely adjusted to achieve precise horizontal and vertical zero planes. This adaptability also allows the device to accomodate a large range of animal sizes and levels of maturity. Furthermore, the apparatus can be fitted onto a conventional adult stereotaxic frame or used by itself in combination with a free-standing manipulator. As a model preparation, we describe a procedure for stereotaxic surgery in the the post-natal day (P1) rat. The versatility of the instrument has permitted successful stereotaxic surgery in adolescent as well as neonatal rats, newborn and adult mice, and newborn hamsters.

This chapter was adapted from the paper, "A Hypothermic Miniaturized Stereotaxic Instrument for Surgery in Newborn Rats", by Miles G. Cunningham and Ronald D.G. McKay, in press in the Journal of Neuroscience Methods (1993).

INTRODUCTION

Precision stereotaxic surgery in the newborn rat has previously been attempted with variable success primarily through the modification of instruments designed for adults.

Plasticene clay has been used to stabilize the newborn animal by molding the clay to the animal's body. The clay mold is supported by a "tilt table" which is attached to an adult stereotaxic frame and can be adjusted in the anterior-posterior and medial-lateral planes (Valenstein et al., 1969; Johnson et al., 1974). Variations on this approach include molds made from plaster (Hoorneman, 1985) and dental stone lined with alginate (Lithgow et al., 1982).

Standard adult frames modified with a toothbar adaptor and with or without specialized smaller earbars have also been used (Sherwood et al., 1970; Herman et al., 1991). Another adapter has been designed which supports the newborn head with concave lateral head supports and an intraoral bar which which are in turn supported by standard adult ear and tooth bars (Sutherland et al., 1972). An adult frame has also been used for neonates by fixing the skull with cyanoacrylate glue to stainless steel tubing which fits onto standard adult ear bars (Nakamura et al., 1987).

A more elaborate head-holding device has been described, also for use with an adult frame, that employs a curved needle which hooks into the foramen magnum of the animal; the needle tip thus supports the skull from its inner surface. A taut wire mouth bar and lateral head blocks provide additional head support. A microscope is then placed over the preparation for final head positioning and

removed to allow free movement of an electrode carrier. The electrode is passed through the skull without prior drilling (Heller et al., 1979).

While these methods have been used with some success, each has aspects which can be improved. The disadvantages of body molds to secure the newborn include that a different mold must be made for animals of different sizes, and the entire mold then must be coursely rotated within the adult frame to approximate a standardized head position. Also, it has been reported that when using molds, accuracy in electrode placement is poor in neonates younger than 5 days due to a greater difficulty in stabilizing the head (Johnson et al., 1974). In the same report, it was shown that penetration of the skull by pressure of an electrode alone compresses the cranium resulting in distortion of the lesion site. This method of entry also produces trauma and brain damage (Lithgow et al., 1982).

The method by which the head is secured with cyanoacrylate glue onto an adult frame is primarily used for electrophysiological recording studies in which the subjects are sacrificed immediately thereafter. It is therefore inappropriate for many stereotaxic procedures in which the animals must survive after surgery.

The use of adult frames for neonates poses difficulties in obtaining a proper fit with the large adult earbars, particularly for very small animals. In addition, the ear bars are not adjustable vertically, resulting in the inability to finely adjust the head position in the medial-lateral plane. This adjustment is often necessary for very precise positioning since the neonatal skull is underdeveloped and less rigid and symmetrical than the adult skull.

Each method thus far reported for neonatal surgery requires an adult stereotaxic frame, an instrument intended for animals some 30 times the size of a typical newborn; each instrument is limited in its versatility; and no apparatus provides a built-in means for simple, safe, and consistent anesthesia.

The present paper describes a novel apparatus and technique which have adopted the advantages of previously-described methods while attempting to eliminate their shortcomings. The method we present here has many virtues. First, it can be used for a variety of animals at different levels of maturity, and for numerous techniques and surgical approaches. Second, it allows prolonged hypothermic anesthesia for lengthy surgical procedures, yet permits use of all other methods of anesthesia. Third, it is noninvasive and simple to use. Fourth, it is inexpensive to build. Fifth, it can be used effectively with or without an adult stereotaxic frame. Sixth, it assures the normal health and survival of animals post-operatively. And finally, it affords a very high level of accuracy and reproducibility in stereotaxic surgery.

The technique applies similar principles as those used for adult stereotaxic surgery, while addressing the unique problems associated with anesthesia and surgery in the neonate. The miniaturized hypothermic stereotaxic instrument has been developed, modified, and put to extensive use in our and other laboratories primarily as a dependable means of implanting cell suspensions into specific sites of the newborn and adolescent rat (Renfranz et al., 1991; Cunningham et al., 1992; Nikkhah et al., 1992) and newborn mouse (Cunningham, Vicario, & McKay, 1992). The employment of various other

anatomical and electrophysiological techniques used in combination with this methodology may prove useful in many lines of research, particularly in our understanding of developmental neurobiology and neural plasticity.

METHODS

Subjects

The method decribed here has been tested on a variety of animals, including newborn Syrian hamsters (Charles River), newborn and adult Black 6 mice (Jackson), and Sprague-Dawley rats (Taconic), which have ranged in age from the moment of delivery to 60 grams. For the tests formally presented, the subjects were post-natal day 1 (P1) male Sprague-Dawley rats weighing between 8.0 and 8.6 grams. The anteroposterior distance between bregma and lambda on the exposed skull of the animals ranged from 3.4 to 3.7 mm. All animals were housed in clear plastic cages with their mothers and maintained on a 12 hour light/12 hour dark schedule. Food and water were provided ad libitum.

Apparatus

The miniaturized hypothermic stereotaxic instrument is shown in Figure 1. It can be constructed from common, readily available and inexpensive materials, but requires machining of various components. It is also now commercially available (Stoelting Co., Wood Dale, IL). The device consists of a 140 X 70 X 5 mm brass plate

upon which are mounted three aluminum head stabilizers, one positioned on each side of the animal's head and one positioned at the animal's nose. At the front of the brass plate is welded a 20 ml-capacity copper reservoir into which is placed 50% ethyl alcohol and dry ice pellets. This dilution of alcohol is optimal for maintaining the temperature of the brass plate at 0-5°C when adding 10 grams of dry ice every 10 minutes (at normal atmospheric conditions). The temperature can be reduced by increasing the proportion of ethyl alcohol to water to 75% or 90%.

Similar to adult stereotaxic instruments, the neonatal instrument secures the head with earbars and a mouthpiece. However, these have been specially designed to fit a range of underdeveloped animals, and they are vertically as well as horizontally adjustable to accomodate animals of various sizes. The semicircular shape of the mouthpiece assures that the animal's mouth remains partially open enabling ventilation. It also is designed with a notch which accepts the incisors of more mature animals (and newborn hamsters). After placing the mouthpiece into the animal's mouth, an adjustable crescent-shaped bridge is tightened snugly over the animal's nose. The earbars are designed to fit into the premature external auditory meati of the newborn. They are machined from small blocks of lexon (Altec Plastics, Inc., So. Boston, MA), the ends having a 25° taper with a rounded tip 0.5 mm in diameter.

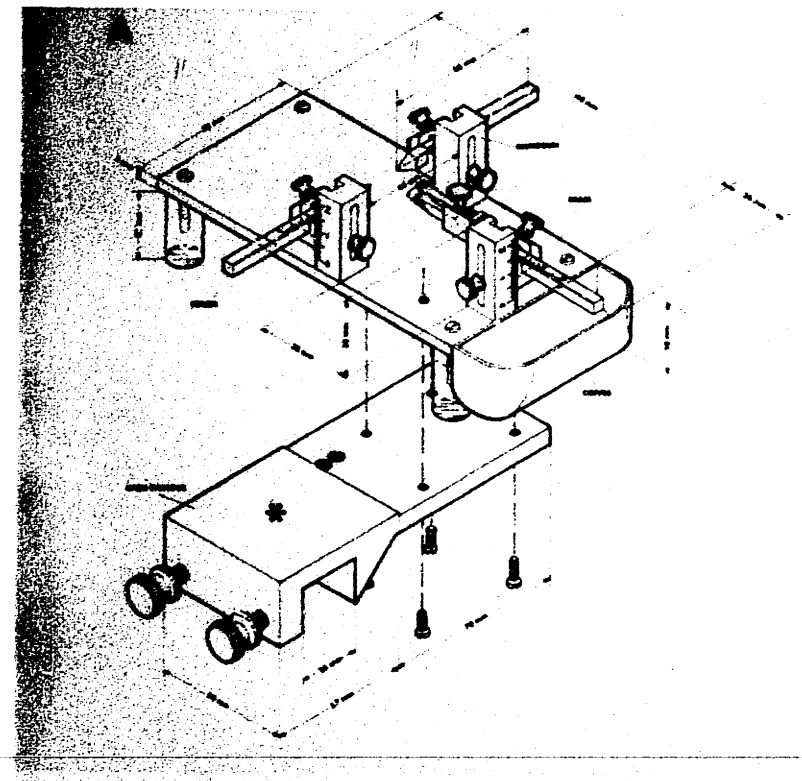

Fig. 1. The miniaturized hypothermic stereotaxic instrument and removable saddle (asterisk) viewed as a scale drawing (A), positioned in an adult stereotaxic frame (Stoelting Co., Wood Dale, IL) (B), and by itself combined with a free standing manipulator (C).

The instrument is equipped with a removable saddle which permits the device to be mounted onto a standard adult stereotaxic instrument (Fig. 1A & 1B). The tooth bar and the ear bars of the adult instrument are first removed, and the saddle, upon which is fastened the neonatal stereotaxic device, is fitted and secured onto the right arm of the adult frame. This configuration allows full use of the manipulator(s) accompanying the adult device. The saddle is made from a nonconducting linen phenolic material to prevent heat exchange between the neonatal device and the adult frame. For procedures where an adult frame is unavailable or unnecessary, the neonatal stereotaxic instrument can be removed from the saddle and used without an adult stereotaxic instrument. The device is then supported and isolated from heat transfer by acrylic legs (Fig. 1C).

Surgical procedure

The procedure we describe for the stereotaxic placement of an injection, electrode, lesion, etc., should be used first in testing the coordinates obtained from a previously-published atlas (Valenstein et al., 1969; Sherwood et al., 1970; Heller et al., 1979). Alternatively, a simple atlas can be constructed (e.g., see Heller et al., 1979) from a representative animal to determine the coordinates for the site of interest. These coordinates should be tested with ink injections or lesions and refined if needed.

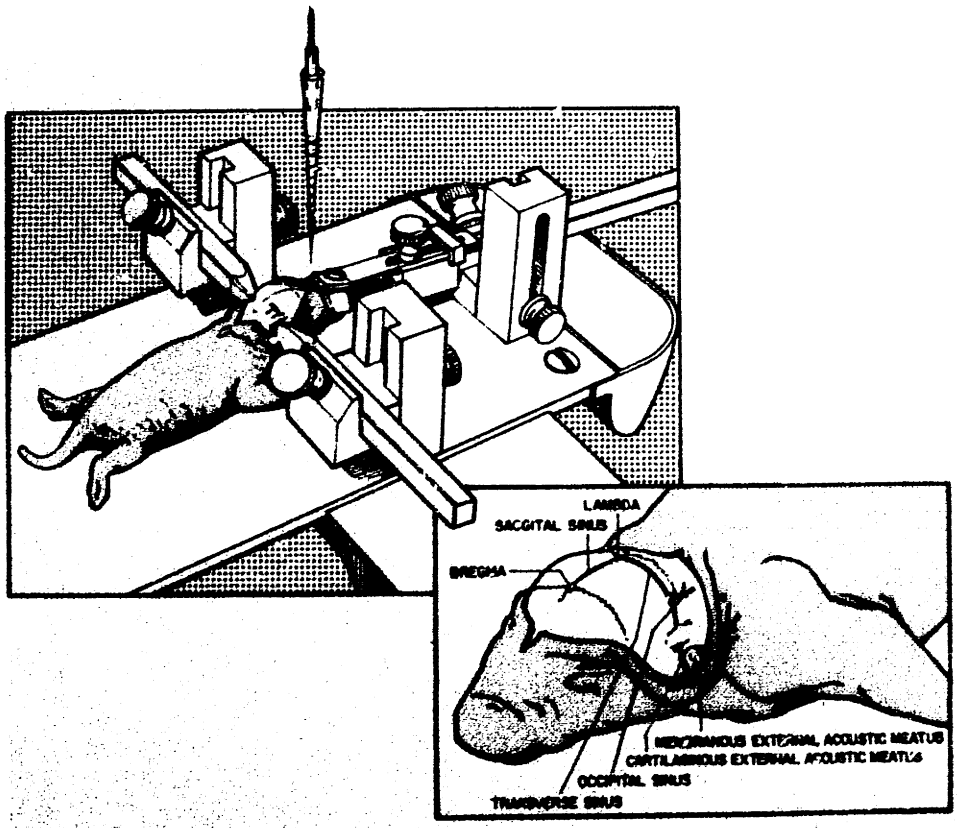
LAMBDA
SAGGITAL SINUS
BREGMA
OCCIPITAL SINUS
TRANSVERSE SINUS

Fig. 2. Drawing of newborn in apparatus. Inset, preparation of animal prior to stereotaxic procedure.

The subject is first hypothermically anesthetized by covering the animal with approximately 6 cm of crushed ice for a duration of one minute per gram body weight. A midline incision is then made which extends from the eyes to the back of the cranium. The skin is reflected downward, exposing the transverse and occipital sinuses and ventrally, the premature external auditory meati (see Fig. 2, inset). This dissection requires gentle removal of the loose connective tissue underlying the skin. The membranous external acoustic meatus can be seen as a delicate tube-like structure connecting the earbud to the cartilaginous external acoustic meatus. The membranous meatus should be left intact and the tip of the earbar gently inserted into the cartilaginous meatus. The earbars are moved inward until met with resistance. Care should be taken not to apply excessive force as this may distort the animal's head. Such distortion constricts the sinuses and blood can no longer be seen therein; therefore the disappearance of blood (particularly from the transverse sinus) serves as an indicator of excessive force. The mouthpiece is positioned and the nose bridge tightened, firmly stabilizing the head. The level of the earbars and mouthpiece can be positioned using the scale engraved on the side of each stabilizer.

Head positioning is then finely adjusted such that bregma and lambda have the same vertical coordinate (i.e., are on the same anterior-posterior plane), and the points 3 mm (for 8 gm rats, 2 mm for 3 gm mice) on either side of lambda have the same vertical coordinate (i.e., are on the same medial-lateral plane). These coordinates can be determined by simply reading the vertical scale where the electrode, pipette, or other probe makes contact with the

surface of the skull (Hoorneman, 1985). Also, proper alignment of the sagittal plane requires head positioning such that anterior-posterior movement of the probe precisely traces the midline of the skull (from lambda to 2-3 mm anterior to bregma). Note that this is standard positioning, and that variations on orientation of the head are possible and reproducible since the earbars and mouthpiece can slide upward or downward.

At this point in the surgical procedure, the stereotaxic methods used in adults can be applied, with some modification, to the newborn. Determination of bregma and lambda in the underdeveloped skull can be difficult as the skull sutures in the newborn are less distinct than in the adult. It is therefore essential that the experimenter remain consistent when determining the precise point which will be used as bregma or lambda (see Valenstein et al., 1979, for discussion). To aid in this determination, the bone plates around the landmark can be gently depressed to visualize where they meet.

The newborn skull also requires special care when attempting to penetrate the cartilaginous skull and enter the brain without causing trauma or contributing to loss of placement accuracy (as with a knife cut or puncture entrance with the probe). Ideally, the area of skull overlying the penetration site should be carefully removed without causing any damage to the underlying tissue whatsoever, including the dura. An intact dura serves as an accurate and reproducible vertical reference point and will therefore maximize the accuracy of vertical placement (Lithgow et al., 1982). We have found that, with practice, craniectomies can be routinely performed without

the slightest damage to the underlying dura using any standard miniature drill equipped with a 0.5 to 1.0 mm diameter high quality carbide dental burr (Brasseler U.S.A., Savannah, GA).

Using the miniaturized stereotaxic device, hypothermic anesthesia can be maintained safely for extended periods by staging the surgical procedure in approximately 30 minutes segments. After 30 minutes of hypothermic anesthesia, the animal should be removed from the apparatus and warmed to the point of being slightly responsive to a pinch to the tail or paw. This allows the animal a respite from extended hypothermia and also reassures the experimenter that the animal is surviving the procedure. The animal can then be returned to the ice for approximately four minutes and repositioned in the apparatus for the next phase of the surgical procedure. After the operation, the incision is sutured using 7-0 (10-0 for P3 mice) monofilament nylon suture. The animal should be cleaned of blood and slowly warmed to body temperature before returning it to the mother. For 90-minute-long procedures in P0-P3 rat pups, mortality using this method is less than 5%.

RESULTS

The level of accuracy that the present technique allows is demonstrated in Figure 3. Using the procedure described above, five consecutive animals were given bilateral injections of India ink. Microinjections of 30 nL were targeted for the hilar region of the dentate gyrus using the coordinates: 1.2 mm posterior to bregma, 1.9 mm lateral to midline, and 1.9 mm below dura. India ink was delivered using the micrografting technique (Nikkhah et al., 1992), in

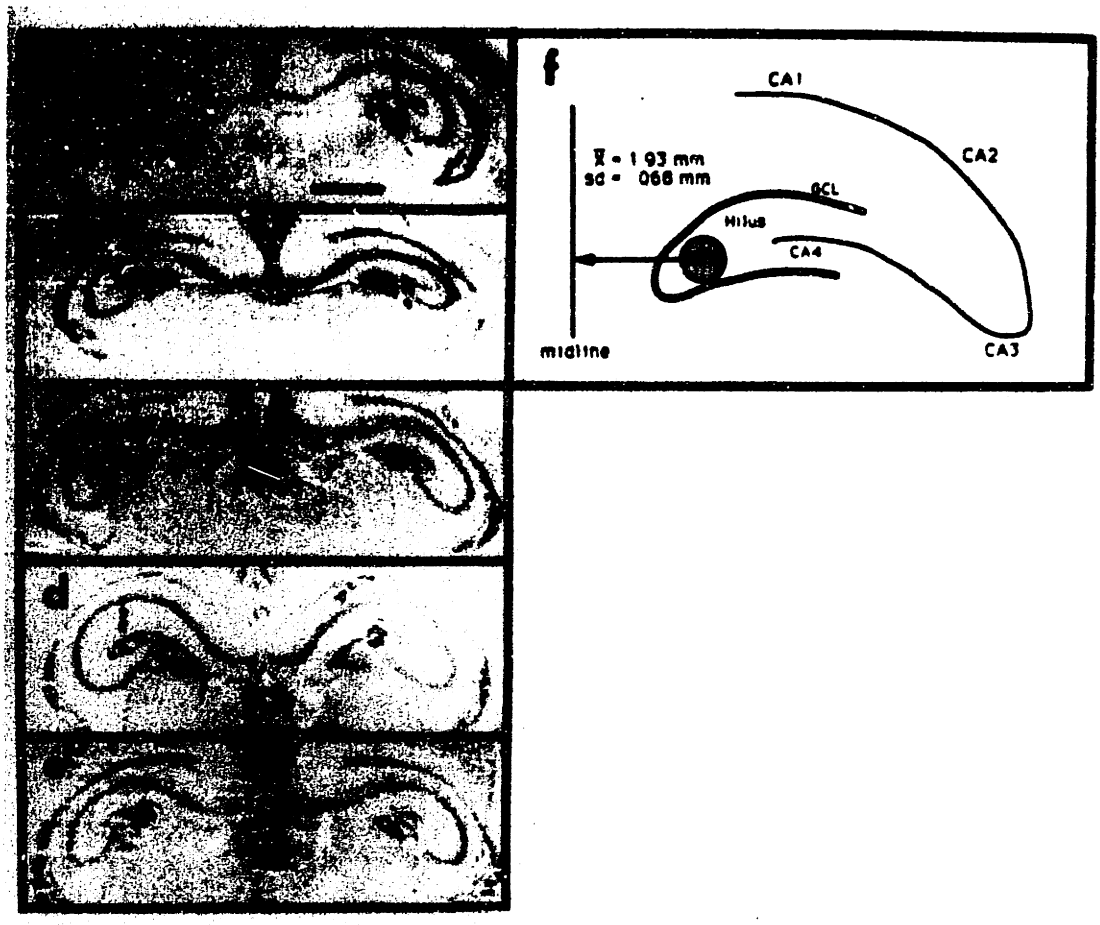
f
CA1
CA2
x̄ = 1.93 mm
sd = .068 mm
GCL
Hilus
CA4
midline
CA3

Fig. 3. Bilateral ink injections targeted for the hilar region of five consecutive P1 rats (a-e). The target site is approximately 0.5 mm in diameter. In ten attempts, the hilus was missed once (3c, right hemisection). (f) To provide a statistical account of the variability, the distance from the center of the injection site (stippled circle) to midline was measured for each of the 10 injections. The mean (X) and standard deviation (sd) are given. GCL, granule cell layer. Scale bar = 1mm.

which a pulled glass pipette with a final tip outer diameter (o.d.) of 30 - 50 mm was attached to a 1 mL Hamilton syringe. One hour after they recovered from the procedure, the animals were sacrificed. Fresh frozen cryostat sections were cut at 30 mm and stained with neutral red.

In a previously-described method for stereotaxic electrode placement into the developing rat brain, there was informally reported a success rate of 60 - 70% for unilateral lesions of a .7 mm-diameter target site in P3 rats (Heller et al., 1979). In another method, a 75% accuracy was estimated 35 days after the actual placement of a .7 mm-diameter electrode into a .8 mm-diameter target site of the P1 rat (Hoorneman, 1985). Here we show the raw data demonstrating a 90% success rate, targeting a predetermined site smaller in size (.5 mm in diameter) in 9 out of 10 attempts (see Fig. 3a-e). Note that this success rate is in the P1 rat using a noninvasive head-stabilizing method, which allows anesthesia to be safely extended to 90 minutes or longer. Moreover, bilateral 30 nL microinjections were produced with a micropipette having an o.d. of 50 mm as opposed to unilateral lesions produced by an electrode with an o.d. of approximately 100 mm (Heller et al., 1979) or bilateral lesions with a 700 mm-diameter electrode (Hoorneman, 1985).

In Figure 3 we show the actual ink injections in the test animals. The level of accuracy is self-evident upon inspection taking into consideration the position of the ink injection on each side of the brain (within and between animals) relative to the structure of the dentate gyrus. This is perhaps the most reliable indicator of accuracy since the tissue is often somewhat distorted during processing.

However, variability is also represented statistically using the lateral placement from midline (Fig. 3f). Measurements taken from tissue sections after processing indicate that the distance of the ink injections from midline range from 1.8 mm to 2.05 mm. The mean distance (X) is 1.93 mm, and the standard deviation (sd) is .068 mm. Discrepancies between injection sites may be attributed to a number of factors, including experimenter errors in determining bregma, midline, and the zero reference planes, variations in the shape of the newborn head, drift of the pipette during insertion, distortion of the tissue during freezing and processing, and variations in the plane of sectioning (Paxinos et al., 1982; Sherwood et al., 1970).

A practical application of this particular procedure is illustrated in Figure 4. In this example, a 250 nL cell suspension, as opposed to a 30 nL ink injection, has been placed in the hilus of the P1 rat using the same delivery system as that used for the ink injections. We have found that engrafting cells in precise regions of the developing brain, using an exacting method which can be systematically controlled, is in many ways the ultimate assay for characterizing the potential of the cells of interest. Moreover, virtually any other technique that requires stereotaxic placement can feasibly be coupled with the present method.

Fig. 4. Stereotaxic placement of a micrograft into the hilus of the dentate gyrus of the P1 rat. A 250 nL cell suspension of the HiB5 cell line (Renfranz et al., 1991) with a density of 30,000 cells / mL was engrafted, and the animal was sacrificed one hour after the procedure. The tissue and grafted cells are immunopositive for nestin illustrating their early developmental status (Lendahl et al., 1990). CA1, CA1 field of the hippocampus. CA3, CA3 field of the hippocampus. G, graft. gc, granule cell layer of the dentate gyrus. H, hilus of the dentate gyrus. Th, thalamus. PC, parietal cortex. Section thickness, 100 mm. Scale bar = 1mm.

DISCUSSION

In addition to the tests described above, the present technique has been used to accurately graft cell suspensions into sites in the newborn brain other than the dentate gyrus. These include the cerebellum (Renfranz et al., 1991), the striatum and substantia nigra (Nikkhah et al., 1992), the olfactory bulb, the cerebral peduncle, and various cortical areas (unpublished results). Moreover, we are presently using this method for precise graft placement into the hippocampus and cerebellum of postnatal-day-4, 3.5 gm, C57 Black 6 mice (Cunningham, Vicario, & McKay, 1992, submitted).

The apparatus can also be used for older or larger animals; however, hypothermic anesthesia is ineffective and unsafe in more mature rodents (> P7) and should be replaced with inhalant anesthetics or barbiturates. The device has allowed precise stereotaxic placement of grafts in P10 rats anesthetized with either halothane or a combination of Ketamine (30 mg/kg) and Xylazine (5 mg/kg) (Cunningham, Nikkhah, & Bjorklund, in preparation). Tests with neonatal hamsters and adult mice are preliminary, but indicate even greater accuracy in these larger animals as in P10 and older rats.

The equipment used to administer halothane anesthesia can easily be coupled with the miniaturized instrument. The advantage to this method is that halothane allows the level of anesthesia to be regulated quickly and precisely for any animal. Therefore, with a halothane anesthesia system combined with the device we present, animals of all ages can safely undergo lengthy stereotaxic surgical

procedures while maintaining normal body temperature. This capability is important for electrophysiological studies.

Note that correct placement of earbars requires a relatively large midline incision over the cranium. Complications, including infection, are never a problem when neat, clean surgical technique is practiced, and the incision is carefully closed with 7-0 monofilament nylon suture. Although previous reports have stated that ear bars cannot be used for newborn animals (Valenstein et al., 1969; Lithgow, 1982; Hoorneman, 1985), we have found that the use of the specialized ear bars is safe and effective. Occasionally, a mild hematoma is seen after surgery at the auditory canals as a result of trauma to the vasculature produced by the earbars. This trauma resolves within 24 hours. Also, there is no evidence of deficits in auditory function with the development of the animal.

Poor administration of hypothermic anesthesia can render the animal weak and thus less competitive for food. This weakness, combined with the surgical manipulation (e.g., foreign odors, presence of suture, traces of blood, etc.) can also make the newborn a victim of maternal neglect or cannibilization. Staging the procedure as we have described minimizes this risk. Our animals remain strong and healthy and develop normally. Pre-operative care, however, is also important for post-operative survival. Pregnant animals or mothers with their litters should be allowed to acclimate to the animal care facility and should be handled daily for at least one week before surgical procedures. Pregnant mothers, though, should not be disturbed during their delivery. Before using the animals in an

experiment, the mother should be carefully observed for her competence, particularly after routine handling of the newborns.

When the neonatal stereotaxic device is used without an adult frame, but in combination with a free standing micromanipulator (Fig. 1C), there is only a modest loss in efficacy of the apparatus. A greater amount of care must be taken, however, to insure that the device and the manipulator are properly aligned. The precision of the surgery is nevertheless optimal when the instrument is combined with an adult frame. Furthermore, the combination of the two instruments extends the researcher's ability to conduct studies with a virtually unlimited range in animal ages.

REFERENCES

1. Benjamin, M.M. (1978) Outline of Veterinary Clinical Pathology, Iowa State University Press, Ames, Iowa, pp 108-115.

2. Cunningham, M.G., Nikkhah, G., McKay, R.D.G., and Bjorklund, A. (1992) Transplantation of fetal dopaminergic neurons into the substantia nigra of neonates with bilateral 6-OHDA lesions, Rest Neurol and Neurosci, 4(3): 161.

3. Cunningham, M.G., Vicario, C., & McKay, R.D.G. (1992) Cerebellar primordial cells grafted into the developing facia dentata integrate and differentiate into region-specific neurons and glia. Submitted.

4. Flecknell, P. A. (1987) Laboratory Animal Anesthesia, Academic Press, Inc, San Diego, pp. 73-74.

5. Heller, A., Hutchens, J.O., Kirby, M.L., Karapas, F., and Fernandez, C. (1979) Stereotaxic electrode placement in the neonatal rat, J Neurosci Methods, 1: 41-76.

6. Herman, J.P., Abrous, D.N., and Le Moal, M. (1991) Anatomical and behavioral comparison of unilateral dopamine-rich grafts implanted into the striatum of neonatal and adult rats, Neuroscience 40(2): 465-475.

7. Hoorneman, E.M.D. (1985) Stereotaxic operation in the neonatal rat; a novel and simple procedure, J Neurosci Methods, 14: 109-116.

8. Johnson, D.A., Poplawsky, J.L., and Jackson, R. (1974) Techniques and problems in the stereotaxic placement of subcortical lesions in infant rats, Physiol Behav, 13: 465-470.

9. Lendahl, U., Zimmerman, L.B., McKay, R.D.G. (1990) CNS stem cells express a new class of intermediate filament protein, Cell, 60: 585-595.

10. Lithgow, T. and Barr, G.A. (1982) A method for stereotaxic implantation in neonatal rats, Dev Brain Res, 2: 315-320.

11. Nakamura, S., Kimura, F., and Sakaguchi, T. (1987) Postnatal development of electrical activity in the locus ceruleus, J. Neurophysiol, 58 (3): 510-521.

12. Nikkhah, G., Cunningham, M.G., Wictorin, K., Knappe, U., Jodicke, A., and Bjorklund, A. (1992) Microtransplantation of fetal dopaminergic neurons into the striatum and substantia nigra of 6-OHDA lesioned rats: morphological and functional features, Restor Neurol and Neurosci, 4(3): 161.

13. Paxinos, G., Watson, C. (1982) The Rat Brain in Stereotaxic Coordinates, Academic Press, New York.

14. Renfranz, P. J., Cunningham, M. G., and McKay, R. D. G. (1991) Region-specific differentiation of the hippocampal stem cell line HiB5 upon implantation into the developing mammalian brain, Cell, 66(4): 713-729.

15. Sherwood, N.M. and Timiras, P.S. (1970) A Stereotaxic Atlas of the Developing Rat Brain, University of California Press, Berkeley.

16. Sutherland, S.D. and Gorski, R.A. (1972) An evaluation of the inhibition of androgenization of the neonatal female rat brain by barbiturate, Neuroendocrinology, 10: 94-108.

17. Valenstein, T., Case, B., Valenstein, E.S. (1969) Stereotaxic Atlas of the Infant Rat Hypothalamus, Developmental Psychobiol, 2(2): 75-80.

CHAPTER 2

GRAFTING CULTURED CELLS INTO THE BRAIN OF THE ADULT AND THE NEWBORN RAT

This chapter provides detailed instructions for precision grafting of cells into the brain of the adult and neonatal rat. Although emphasis will be given to the actual transplantation procedure, preparation prior to grafting and evaluation after grafting are also discussed. A transplantation experiment can thus be divided into three phases: the pre-grafting phase, the grafting phase, and the post-grafting phase. The methods described herein have been used extensively to deliver the immortalized hippocampal cell line, HiB5 (1), into the brain of newborn and adult rats. Implantation of HiB5 cells will therefore serve as a model procedure for grafting cell lines; however, these methods can also be used to implant fresh tissue cell suspensions.

This chapter was adapted from a chapter written for the Academic Press publication "Neuroprotocols" authored by Miles G. Cunningham, Guido Nikkhah, and Ronald D.G. McKay.

The Pre-Grafting Phase

The HiB5 cell line - an example.

HiB5 was derived from a primary culture of embryonic day 16 (E16) rat hippocampus of the Sprague-Dawley strain (1). The line was immortalized using the temperature-sensitive allele tsA58 of SV40 large T antigen (2). With this immortalization strategy, the cells grow continuously at 33°C (the permissive temperature), but at 39°C (the non-permissive temperature) the oncogene product is rapidly degraded and the cells stop dividing. Neuroepithelial stem cells express a characteristic intermediate filament, nestin, that is not found in differentiated neurons or astrocytes (3,4). HiB5 cells are nestin-positive at either the permissive or non-permissive temperature (Fig. 1) and do not express markers characteristic of neurons and glia. These results suggest that the HiB5 cell line may represent neuroepithelial stem cells.

HiB5 cells were grown at 33°C in Dulbecco's Modified Eagle's medium (DMEM, Gibco), supplemented with 0.11 g/L NaPyruvate, 3.7 g/L $NaHCO_3$, 0.29 g/L glutamine, 3.9 g/L Hepes, penicillin, streptomycin, and 10% (v/v) fetal calf serum (hereafter referred to as DMEM + 10% FCS). Cells were grown on tissue culture plasticware precoated for at least 30' with 15 mg/ml polyornithine (Sigma). Prior to using the plates, the polyornithine was aspirated, and the plates rinsed at least 2 times with phosphate-buffered saline (PBS; 8 g/L

NaCl, 0.2 g/L KCl, 1.15 g/L Na_2HPO_4, 0.2 g/L KH_2PO_4). Under these culture conditions, the cells can be grown indefinitely and they remain nestin positive. There is strong evidence that neuronal precursor cells are multipotential and may generate different neurons in response to extracellular signals (1,5,6,7). The tsA58 allele of SV40 T-antigen was used to establish cell lines in the hope that nestin-positive cells might differentiate at the non-permissive temperature in response to the appropriate environmental cues. If HiB5 cells are capable of differentiation, as their expression of nestin suggests, then they should differentiate when placed back into their site of origin, the developing hippocampus. Our studies have indicated that indeed they do (1) (Fig. 1).

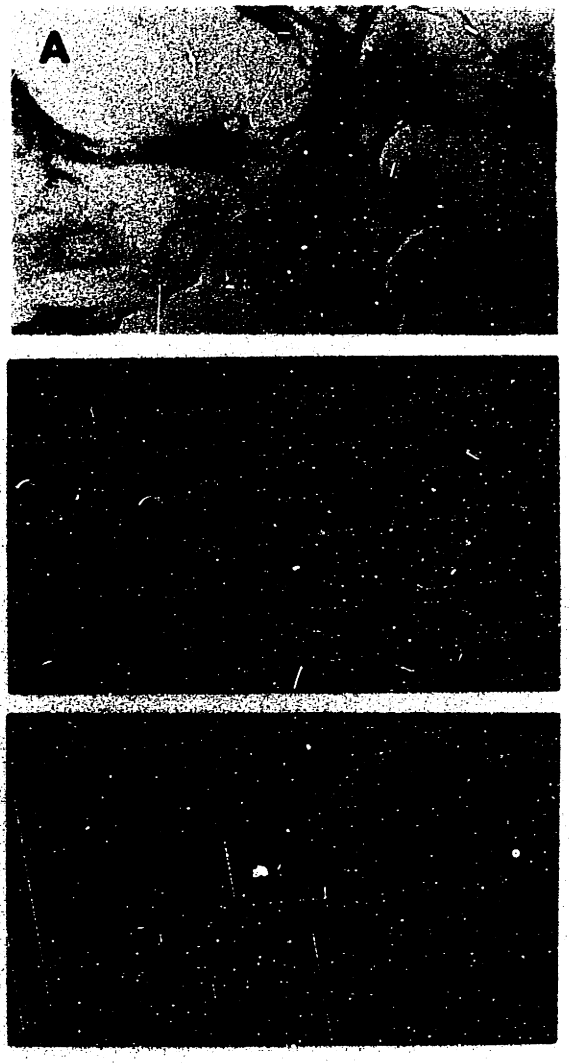
A

Fig. 1. Morphology of HiB5 cells *in vitro* and after grafting into the dentate gyrus. *a*, HiB5 cells at 33°C are immunopositive for the nestin protein. *b*, double exposure under rhodamine and fluorescein optics to visualize cultured HiB5 cells labeled with DiI-C_{18}-(3) and green fluorescent latex microspheres (green beads). The DiI-C_{18}-(3) signal is orange-red and is localized on external and internal membranes. The green beads are endocytosed and often seen in perinuclear aggregates; their yellow hue results from the double exposure of the green and orange-red fluorescent signals. *c*, a common morphology of HiB5 cells 1 - 3 weeks after grafting into the P2 dentate gyrus as seen in a double exposure. The cell body sits in the granule cell layer (gc) and extends processes (arrows) into the molecular layer (m).The cell body and processes are distinguished with DiI-C_{18}-(3) and appear orange-red and perinuclear aggregates of green beads appear yellow. Scale bars = 10 m.

Labeling cultured cells.

A primary concern in grafting experiments is distinguishing the engrafted cells from endogenous cells. For many transplantation studies, in which relatively large aspirative or neurotoxin lesions are produced followed by grafting into the lesioned area, it is assumed that the cells at this site are the transplanted ones. This is a reasonably safe assumption; however, the researcher must take into consideration the possibility of host cells migrating into the lesioned area. If however cells are grafted into an unlesioned site or they migrate out of the lesioned site, one must be able to follow and identify them. Numerous cell markers have been used, each of which has its advantages and pitfalls. We suggest using more than one labeling method, as this will increase the confidence level that the observed cells are indeed grafted ones. Here we describe labels which persist and allow the cell morphology and antigenicity to be determined. HiB5 cells have been labeled using four separate methods: a label contained in the cytoplasm (fluorescent microspheres), a label contained within the membrane (DiI-C_{18}-(3)), a DNA tag ([^{3}H]thymidine), and a genetic marker (*lacZ*). We have controlled for cell-to-cell transfer of each label by grafting freeze-thaw killed HiB5 cells as well as different cell lines labeled identically to HiB5 cells.

For a subset of grafts, cells were labeled with green fluorescent latex microspheres (green beads; Lumafluor, Inc., NJ or Interfacial Dynamics Corp. Portland, OR) combined with DiI-C_{18}-(3) (1,1'-dioctadecyl-3,3,3',3'-tetramethylindocarbocyanine perchlorate;

Molecular Probes, Inc., OR). This double labeling allows the cell's morphology to be appreciated since the lipophilic DiI-C_{18}-(3) can often be seen throughout the membrane of the cell, and the perinuclear arrangement of microspheres is further assurance that the DiI-C_{18}-(3) - labeled cell is one which was grafted (see Fig. 1). Cells were labeled with green beads *in vitro* for eight hours at 33 °C, using green bead stock solution (as it comes from Lumafluor) diluted 1000-fold in DMEM + 10% FCS. The cells were then rinsed three times with sterile PBS, trypsinized, and replated, so as to eliminate any free beads. A 1 mg/ml stock of DiI-C_{18}-(3) (Molecular Probes, Inc., OR) in 100% ethanol was diluted 1:200 in DMEM + 10% FCS. Eight to 24 hrs after passaging, the bead-labeled cells were rinsed with PBS, then incubated in the DiI-C_{18}-(3) solution for 2 hours at room temperature in darkness. The DiI-C_{18}-(3) solution was aspirated, and excess dye removed with 3 rinses in PBS. The cells were returned to 33°C in DMEM + 10% FCS for at least 2 hrs before being prepared for implantation.

In another set of grafts, cells were labeled with tritiated thymidine ([^{3}H]thymidine) (New England Nuclear, MA). [^{3}H]thymidine labeling of cells was accomplished by incubating them with 0.2 mCi [^{3}H]thymidine/ml of DMEM + 10% FCS over one length of the cell cycle (approx. 48 hrs for HiB5). The [^{3}H]thymidine-containing medium was replaced approximately every eight hours during this period.

[^{3}H]thymidine- or microsphere-labeling can be combined with standard immunohistochemistry so that gene expression can be

analyzed for transplanted cells. Immunoreactions utilizing the peroxidase reaction can be followed by autoradiography to visualize [^{3}H]thymidine - labeling, and immunoreactions utilizing a secondary antibody conjugated with a fluorescent tag can be combined with fluorescent microspheres (8).

In a third set of grafts, a subclone of HiB5 carrying the *lacZ* gene was implanted. An X-Gal reaction was then used to visualize the cells carrying the transgene. Moreover, immumohistochemistry can be conducted after the X-Gal reaction to examine the cell's antigenicity (9,10).

A variety of other methods have been used successfully to follow cultured cells or cells taken from donor animals. These include the fluorescent markers 4,6-diamidino-2-phenylindole (DAPI) and fast blue (11), gold particles combined with wheat germ agglutinin peroxidase (12) or latex microspheres (13), and BrdU to tag a cell's DNA (14, 15). Cultured cells can also be loaded with markers, such as rhodamine- or fluorescein-conjugated dextran or horse radish peroxidase, using glass beads to temporarily disrupt the cell membrane allowing molecules to enter the cell (15). Technology continues to progress enabling cells to be transfected to express a variety of genetic markers so that *in situ* hybridization and/or immunohistochemistry can be used to detect the cells in the host.

Choosing an animal model.

Although our focus here is on the rat, various other species have special features that may offer advantages. For example, many developmental events are delayed in marsupials. The availability of transgenic and mutant mice are of considerable value, yet mice are small and frail, making grafting experiments more difficult, particularly in the neonate. Cross-species transplantation can be useful if the grafted cells are to be identified using antibodies against species-specific antigens. Examples include the human specific anti-neurofilament (17) and the mouse specific anti-M6 which binds to glycoproteins on the surface of mouse neurons (18). Although xenografts may be subject to immunological rejection, the chances of this may be decreased if implanted into a newborn, in which the immune system has not completely developed. The rat is favored as an experimental host for many reasons: it is of ideal size and easily handled, inexpensive to maintain, and the most widely used experimental animal - many paradigms having already been characterized in this species. The gender of the newborn rats to be grafted should also be taken into consideration as there may be sex differences in anatomy or performance of behavioral tasks. The sexes in these newborns are distinguished based on the ano-genital space; this distance being greater for males (4-6 mm) than females (2-4 mm).

An alternative approach to grafting cells into the normal developing or mature brain is to implant into a lesioned host. The functional capabilities of a cell line can therefore be evaluated for the cells' ability to compensate for lesion-induced behavioral deficits in

the developing and adult host. Examples of standardized lesion models are given in Table 1. These models are particularly useful because the implantation of freshly dissociated brain tissue has been shown to accomplish a partial or complete recovery. Therefore, a direct comparison can be made between the time course and efficacy of fresh tissue grafts versus cell line implants.

Preparing animals.

It is good practice to take into consideration several issues regarding the care and preparation of the experimental subjects. The animals should be well maintained and free from disease, in a quiet, low stress environment, and placed on a 12 hour light/12 hour dark cycle. Procedures are usually conducted during the animals' light cycle since their level of metabolism and excitability is lower during this period. For adult animals which will receive an intraperitoneal anesthetic, many researchers food deprive their subjects to minimize possible absorbtion of drug by intestinal contents. Also, fresh bedding should not be given to adults or newborn litters for at least three days prior to surgery or delivery of a litter; because in adults, fresh bedding can influence their response to anesthetics, and for mothers with newborns, new odors should not be introduced near the time of surgery.

Table 1

Experimental Lesion of	Model	Method	Lesion effect	Graft effect	Reference
Neonate					
Nigrostriatal dopaminergic projection	Parkinson's Disease (PD)	Bilateral intraventricular injection of 6-OHDA	Exploration and Hoarding Behavior	Improved	(19)
				Unilateral turning to amphetamine and stress	(18)
Hippocampus	"HP damage"	X-ray lesion of the dentate gyrus	Impaired spatial learning in the water maze test	not tested	(20)
Adult					
Fimbria-Fornix	Alzheimers disease (AD)	Aspiration of the fiber bundle using a suction pipette	Cognitive and learning dysfunction	Improved performance in the water maze task	(21)
Hippocampus	"HP damage"	CA1 lesion by temporary occlusion of the common carotid arteries	Impaired spatial learning in the water maze test	Improved performance in the water maze task	(22)
Nigrostriatal dopaminergic projection	PD	Unilat. 6-OHDA injection into the ascending medial forebrain bundle	Spontaneous and drug-induced motor asymetry	Reduction or reversal of motor asymetry	(23)
			simple and complex sensorimotor neglect	improved simple but not complex sensorimotor functions	(24)
			impaired skilled forelimb use	not improved	(25)
Striatum	Huntington's disease (HD)	Ibotanic acid injections into the head of the caudate nucleus	Drug-induced circling behavior impaired skilled forelimb use	Improvement of drug-induced circling asymetry and skilled forelimb use	(24)

A common problem in neonatal surgery is the mother neglecting or cannabalizing her young after the procedure. This can almost always be avoided in rats, and can usually be avoided in mice. The single most important precautionary measure is to extensively handle the mother before and after her delivery. The mother should be petted and held for at least three minutes twice a day using the same kind of gloves which will be used in surgery. Handling should start about a week before delivery and continue until the day of surgery. However, the mother should not be disturbed the day of delivery. Animals which have changed environments and are new to the animal care facility should be allowed to acclimate to their new location for at least one week. The pups should also be handled after delivery to accustom the mother to the association of the scent of the gloved hand and her young. Also, before using a litter for an experiment, the behavior of the mother should carefully be observed. A good mother will keep her young grouped together and will position herself protectively over the litter. Scattered cold pups in a cage with a nervous mother should not be used in an experiment. Neglect can also be minimized by performing clean, neat surgery and using fine monofilament suture (7-0 for rats and 10-0 for mice). Avoid using any materials or substances that will introduce a foreign scent to the newborn. Furthermore, after surgery and prior to returning to the mother, the animal should be cleaned of blood and warmed to body temperature, either with a lamp or a heating pad. An added precaution is to keep the animal in soiled bedding from its original cage during this warm-up period.

Preparing a cell suspension for grafting.

Cells are first rinsed three times with PBS, then trypsinized and centrifuged identically as in the passaging procedure. The pelleted cells are resuspended in 5-10 mls of calcium- and magnesium-free Hank's balanced salt solution (CMF-HBSS) to remove residual proteins and antimicrobial agents present in the DMEM + 10% FCS. The cells are centrifuged a second time and the pellet is then resuspended in CMF-HBSS (or high glucose DMEM without fetal calf serum) at the desired density (we typically use a 30,000 cells/ml cell suspension). The final density can be measured by diluting an aliquot of the suspension in trypan blue and using a hemocytometer to determine the cell count and viability. During the course of a transplantation session, it may be necessary to gently triturate the cells to maintain a homogeneous suspension. To avoid introducing bubbles into the suspension, triturate slowly with a Pipetteman set to 1/2 the total volume of the suspension.

THE GRAFTING PHASE

The method of stereotaxic surgery is based on the principle that any given brain structure can be found by knowing the three-dimensional coordinates of that structure relative to a standard reference landmark on the skull. The three dimensional coordinates are the antero-posterior (AP) coordinate, which corresponds to the Z axis, the lateral (L) coordinate, which corresponds to the X axis, and the vertical (V) coordinate, which corresponds to the Y axis. The

landmarks typically used are the intersection of the coronal suture with the sagittal suture (bregma) and the intersection of the lambdoid suture with the sagittal suture (lambda). The stereotaxic instrument itself secures the subject's head in a rigid and reproducible manner and is equipped with a manipulator which is mobile in the three planes. Thus, any structure can be reached by determining the coordinates of the reference point (bregma or lambda) and calculating the location of the target site. A cannula, pipette, electrode, or other probe can then be advanced through a small craniectomy, through the brain tissue, and to the target site.

For grafting cell suspensions into the brain, stereotaxic surgery may not always be necessary. However, to optimize precision and reproducibility, stereotaxic placement of cells into specific structures of the brain has been the method of choice among transplantation scientists (26). We will therefore describe the standard method for stereotaxic implantation. This will be followed by a description of the micrografting technique, a modification of the standard procedure which allows grafts of very small volumes to be placed at precise targets with minimal trauma to the brain (27).

THE ADULT HOST

Apparatus and Anaesthesia.

The basic equipment needed for the stereotaxic implantation of cell suspensions into the brain of the adult host consists of a rat stereotaxic instrument (e.g., Stoelting Co. or Kopf Instruments); a small electric drill such as a dental drill or the less expensive hobby shop type (e.g., Dremmel), high quality drill bits - we recommend 1/2 or 1 mm diameter carbide dental burrs; surgical instruments including a scalpel, medium and fine forceps (jeweler's forceps are very helpful), small scissors, and hemostatic clamps; cotton swabs; animal sheers; and an injection syringe such as a 5 or 10 ml Hamilton microsyringe. An operating microscope is also very useful but expensive, and can be substituted by a magnification lens headset or simply a magnifying glass.

Adult rats can undergo safe general anesthesia for neural transplantation surgery by intraperitoneal (i.p.) injections of Equithesin (3 ml/kg), sodium pentobarbital (50 mg/kg), or a combination of Ketamine (80 mg/kg) and Xylazine (10 mg/kg). As an alternative method, we recommend inhalation narcosis by halothane, which offers an easily regulated level of anesthesia with minimal risk of animal overdose. In addition, a local anesthetic such as Xylocaine can be injected subcutaneously at the incision site prior to cutting the skin to reduce discomfort to an animal which may be under light anesthesia.

Determining target coordinates.

Coordinates for the target structure should first be taken from the literature or from a standardized stereotaxic atlas (28). Using a representative animal, implant the same volume and cell density as will be used in the future grafts but replace part of the solution used to dilute the cell suspension with India ink. Bilateral injections in the test animal should result in a near mirror image of the injections in the hemispheres upon sectioning. The same or identical instrument should be used as for the implantation experiment and the grafting protocol should be followed precisely.

After the marker injection has been made, the animal can be perfused with 4% paraformaldehyde (see Post-Grafting Phase) and the brain sectioned for observation on a vibrotome, or the brain can be cryoprotected in 20% sucrose and sectioned with a cryostat or sliding microtome. Alternatively, immediately after the injection, the brain can be removed and quickly frozen with crushed dry ice. Fresh frozen sections can then be cut, thaw mounted, air dried, postfixed with 4% paraformaldehyde, and Nissl stained. Any error in graft placement can be measured and corrected using additional animals. This procedure should be repeated until the coordinates have been optimized.

Note that we recommend using an ink-labeled cell suspension to test placement accuracy. The properties of such a suspension more closely mimic the fluid dynamics of the actual cell suspension that will be injected into experimental animals. Ink alone is thinner and more fluid than the suspension and can travel between cell layers (i.e., cleavage planes in the brain structure) more easily. It

should be noted here that for similar reasons, an injected cell suspension may not remain at the site of the pipette tip. Rather, the fluid will follow the path of least resistance. Such paths can include between cleavage planes, along the outer wall of the pipette, or into a ventricle. In many cases, the greater the volume of the graft or the greater the rate of injection, the more likely these pathways are to be opened and the more likely grafted cells will be forced away from the target site. A small volume of cells injected slowly may have a greater chance of staying at the site of the pipette tip, therefore resulting in more cells actually at the target site.

The standard neural transplantation method.

After the appropriate animal model has been chosen, any lesioning successfully performed, implantation coordinates optimized and the cell suspension prepared, the following steps should be performed for implantation into the adult host brain:

1) Clean the stereotaxic frame and all working surfaces with 70% alcohol.
2) Mount the microsyringe onto the syringe holder and flush 3 times with 70% alcohol, 3 times with distilled water, and 3 times with sterile saline. Make sure that the needle is absolutely straight. The syringe needle can be lined up with a ruler or a lined index card placed flush against a flat surface behind the needle.

3) Anesthetize the host. Administer subcutaneous local anesthetic if desired.

4) Shave the skin above the cranium with animal shears.

5) Mount the rat into the stereotaxic frame. Fix the head within the ear bars, adjust the tooth bar to the appropriate level and then secure the incisors in the tooth bar.

6) Clean the skin with 70% alcohol or an iodine solution.

7) Incise along the midline beginning approximately from the eyes and extending to the ears. Using blunt dissection, the connective tissue should be freed from the skull and pushed laterally from the midline. Apply retractors or heomostatic clamps to the subcutaneous tissue to clear the working area.

8) Dry the bone with a cotton swab and let air dry for about two minutes - this aids in a more precise identification of skull sutures. Bleeding which may occur on the surface of the skull can be stopped by placing a small piece of gelfoam or collagen over the bleeding point and applying firm pressure with a cotton swab.

9) Maneuver the syringe needle so that its tip is just above the reference skull landmark (bregma or lambda) and note the antero-posterior (AP) and lateral (L) reading. From these coordinates, calculate the position of the target site.

10) Perform a craniectomy being careful to not disturb the dura. With practice this can be done with skilled control of the drill. An alternative method is to drill partially through the skull until cortical blood vessels can be seen through a thin layer of bone. The remaining bone can then be removed using fine

forceps, the bevel of a small gauge hypodermic needle, or the craniectomy can be completed using a manual drill.

11) Slowly draw up the cell suspension and fill the syringe with the required volume plus 10% of the total syringe capacity.

12) Lower the syringe so that the needle just touches dura (see "-Neonatal Host", step #7). Note this vertical (V) coordinate. Incise the dura with the bevel of a hypodermic needle and penetrate this hole with the syringe cannula. Slowly lower the syringe the required vertical distance to the target. Leave in this position for 1 minute before beginning injection.

13) Inject the desired volume of the cell suspension at a rate of 0.5 µl/min, and leave the needle in place for an additional 2 minutes before slowly withdrawing it. If more than one graft is to be placed at different depths along the same tract, deposit the deepest graft first, followed by the next deepest, et cetera.

14) Levage the operation field with sterile saline and close the incision using 6-0 suture or wound clips. A topical antibiotic (e.g., Neosporin) can also be applied before closing the incision as prophylaxis against infection.

16) Lie the animal on its side in its cage with its head elevated slightly above its lower body. This will reduce the effort required for breathing and minimize accumulation of fluid in the lungs. To help maintain body temperature, place the cage on a temperature controlled 39°C heating pad or direct a 75 watt lamp at the animal from a distance of about 30 cm. If the animal remains depressed for more than 4 hours after the

operation, provide wet mash consisting of crushed rat food and water.

The microtransplantation technique.

To minimize the trauma inflicted by the transplantation procedure and to apply small graft deposits in the range of 50-500 nl, we use a modification of the implantation instrument and approach. Figure 2 illustrates the design of the microimplantation instrument. It is based on a 1µl Hamilton microsyringe (H7001), but can be adapted to a larger syringe (2, 5 or 10 µl) if greater volumes are to be injected. Using a pipette puller (Kopf Instruments), a micropipette is made from a glass capillary (ID 0.5 mm, OD 1.0 mm) having a long (8-10 mm) slowly tapering shank with a final tip diameter of 50-75 mm. The tip must be broken square with the sides of the pipette at the level which will give the desired internal diameter. This can be done easily with the aid of a dissecting microscope. If the tip is not broken squarely, any protrusion of glass at the tip may give a false reading for the reference vertical coordinate at dura. Note here that the tip diameter can be tailored to accomodate various types of cell suspensions. Cell aggregates or very dense suspensions may require a larger diameter to avoid clogging. The micropipette is connected to the end of blunt-end syringe cannula (OD 0.5 mm) using a cuff made from a segment of polyethylene tubing (ID 0.58 mm, OD 0.965 mm). The tubing can be pulled under warm air (e.g., a hair-dryer) to get a conical shape so that it fits tightly onto the syringe cannula and forms a seal with the inside surface of the shank of the the glass capillary. Alternatively, a

smaller diameter segment of tubing can be expanded when placed in chloroform, and all but 2 mm can then be slid onto the cannula. As the chloroform evaporates, the tubing shrinks resulting in the tubing fitting tightly around the cannula. The remaining 2 mm segment which overhangs the end of the cannula serves as the sealing interface between the pipette and the cannula.

To eliminate dead space, the system must then be completely filled with fluid (e.g., sterile saline or implantation medium) and devoid of air pockets. This can be achieved by removing the plunger and backfilling the syringe by forcing saline or the medium used for the cell suspension through the microsyringe (use a 1 cc injection syringe with the appropriate size tubing attached to its needle) until 5 - 10 drops pass through the pulled glass pipette tip.

When handling the microimplantation instrument, the following suggestions may be helpful: Because of the fragility of the tip of the glass capillary, care must be taken when moving the microsyringe or moving other instruments near the syringe. Cell suspensions are drawn up through the tip of the capillary (i.e., frontfilled). When moving the microsyringe or aspirating the cell suspension, extrude a small drop in order to visualize the tip of the glass cannula. Any contact of the tip with blood should be avoided as blood will coagulate quickly and clog the tip .

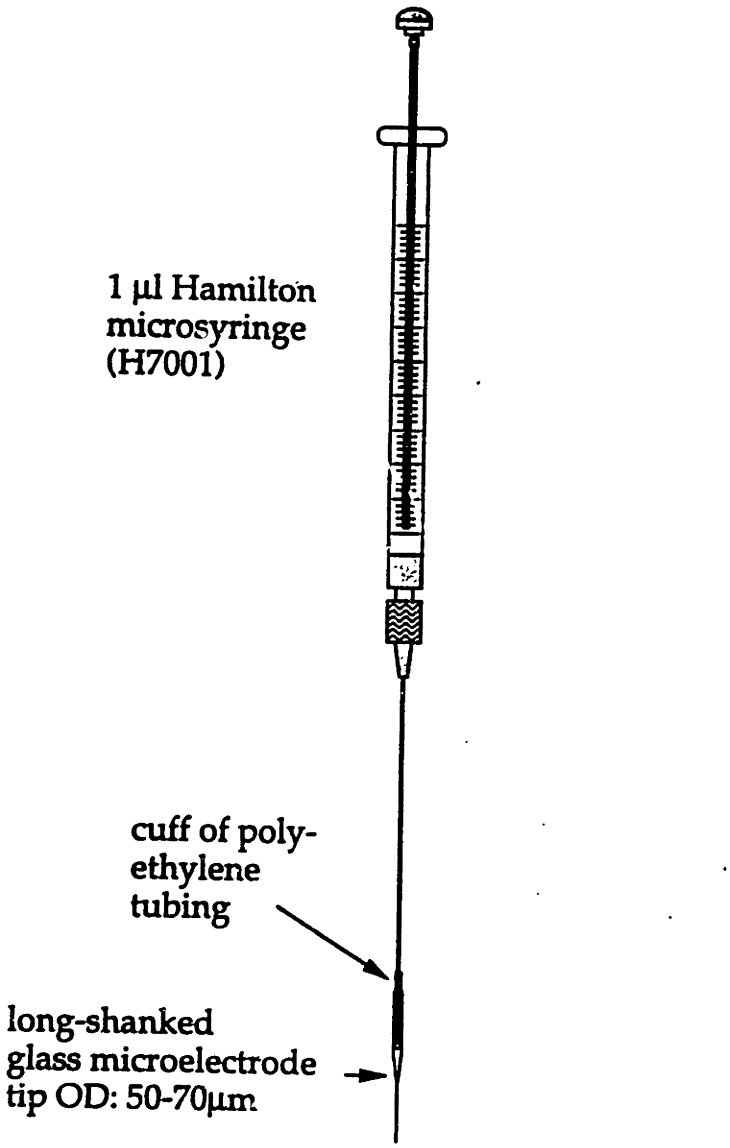
1 µl Hamilton
microsyringe
(H7001)
cuff of poly-
ethylene
tubing
long-shanked
glass microelectrode
tip OD: 50-70µm

Fig. 2. The microimplantation instrument. A long-shanked glass micropipette is fitted onto a 1 µl Hamilton microsyringe using a cuff of polyethylene tubing as an adapter.

Always incise or puncture the dura before advancing the glass capillary into the brain. After the microsyringe has been retracted from the brain, it should be rinsed immediately with the implantation medium to avoid aggregation and clogging of cells in the tip. By observing these precautions, many implantations can be made with a single glass capillary. If, however, the tip breaks or clogs, it can be replaced easily, but the system must be prepared as described above.

THE NEONATAL HOST

We will now describe in detail a method for neonatal surgery (0 to 7 days of age) which applies similar principles as those used for adult surgery. There are, however, a number of considerations one must take into account when devising a neonatal stereotaxic technique. The animal's underdeveloped cranium is a primary concern. As ossification is not yet complete, the skull itself is very thin and elastic. This poses difficulties when performing a craniectomy while preserving the underlying tissue; and since the skull sutures are not well formed, clear determination of landmarks such as bregma and lambda is often difficult. The external acoustic meatuses are immature as well and the neonate lacks front incisors which, when performing stereotaxic surgery in the adult, are hooked over a tooth bar further securing the head. Complicating these factors is that a heightened level of precision and care is needed to

perform precise surgical manipulations in the neonatal rodent brain due to its smaller size and frailty.

Another major concern in working with newborns is the method of anesthesia. Conventional anesthetics used in adults, such as barbiturates, give inconsistent results and are difficult to use effectively in very young animals. Dosage problems are largely attributable to these animals' lower levels of serum albumin and lower percentage of body fat (29). Hypothermia is the method of choice to reliably anesthetize very young animals (up to 8 days-old) (30). As the animal grows older, hypothermia becomes unsafe and impractical and alternative methods of anesthesia must be used.

We have developed a miniaturized hypothermic stereotaxic instrument (now available from Stoelting Co.) which allows for precision stereotaxic surgery in very young newborns (post-natal day 0). The virtues of this apparatus are that it enables prolonged hypothermic anesthesia, it is easy to use, and it is versatile - for a variety of animals and for numerous techniques and surgical approaches. Moreover, it affords a high level of accuracy and reproducibility. The instrument is shown in Fig. 1.1 and a detailed description appears elsewhere (31).

For stereotaxic placement of grafts in the neonate we recommend the following procedure:

1) Hypothermically anesthetize the subject by first covering it with about six cm of crushed ice for approximately seven minutes. Crushed ice allows ample ventilation but should not be saturated with water or packed down over the animal. The time the animal is in ice should be tested for the size and species used. One minute per gram body weight is usually appropriate.

2) The subject can then be taken from the ice and fixed and aligned in the stereotaxic device (see Chapter 1, Figure 2). Hypothermic anesthesia can be maintained safely for approximately 30 minutes by adding 10 gm of dry ice every 10 minutes to a 50% ethyl alcohol bath in the instrument's reservoir. This will maintain the temperature of the instrument at approximately 5°C (under normal atmospheric conditions). Higher alcohol content of the solution in the reservoir will result in colder temperatures. For longer surgical procedures, the animal should be removed from the apparatus after 20 - 30 minutes and warmed to the point of being slightly responsive to a pinch to the tail or paw. This allows the animal a respite from extended hypothermia and also reassures the researcher that the animal is surviving the procedure. The animal can then be returned to the ice for approximately four minutes and then repositioned in the apparatus for the next phase of the surgical procedure. For 90-minute-long procedures using P0-P3 rat pups, mortality using this method is less than 5%.

3) After the subject has been hypothermically anesthetized, a midline skin incision is made from just behind the eyes over the length of the cranium. With fine forceps, the loose connective tissue underlying the skin is gently pulled away as the skin is pushed downward exposing the premature external acoustic meatuses, which are located ventral and anterior to the transverse and occipital sinuses (see Fig. 3, inset). The delicate tube-like membranous external acoustic meatus can be seen connecting the earbud to the cartilaginous external acoustic meatus. The membranous meatus is left intact and reflected downward, and the tip of the earbar is gently inserted into the cartilaginous meatus. The earbars are moved inward until met with resistance. Care should be taken to not apply excessive force as this may distort the animal's head. Such distortion constricts the sinuses and blood can no longer be seen therein; therefore the disappearance of blood (from particularly the transverse sinus) serves as an indicator of excessive force. The animal's snout is stabilized by inserting the mouthpiece and tightening the nose bridge. Using the scale engraved on the side of each stabilizer, the level of the earbars and mouthpiece can be positioned at any level.

4) Final head positioning is then finely adjusted such that bregma and lambda have the same vertical coordinate (are on the same longitudinal plane), and the points 3 mm (for 7 gm rats, 2 mm for 3 gm mice) on either side of lambda have the same vertical coordinate (are on the same horizontal plane). This can be

determined by simply reading the vertical scale of the manipulator where the pipette makes contact with the surface of the skull. Proper alignment also requires head positioning such that anterio-posterior movement of the pipette precisely traces the midline of the skull. Note that this is standard positioning. Variations on head orientation are possible because the earbars and mouthpiece can slide upward or downward.

5) The skull surface is cleared of loose connective tissue using fine forceps followed by gentle abrasion with a slightly dampened cotton swab. The coordinates of the appropriate landmark (e.g., bregma or lambda) are noted and the anteroposterior and lateral coordinates for the site of interest are calculated and marked in permanent ink on the surface of the skull. The skull sutures in the newborn are less distinct than in the adult. It is therefore essential that the experimenter remain consistent in determining the precise point which will be used as bregma or lambda (see Valenstein et al. for discussion (32)).

6) A 0.5 to 1.0 mm diameter craniectomy can be made using a drill equipped with a 0.5 mm carbide dental burr. Care must be taken not to damage the underlying dura. Before entering the brain with the pipette, accuracy can be enhanced by recalculating the precise site of entry through the craniectomy using the pipette as the pointer. This is done by positioning the pipette tip over the appropriate skull landmark and determining a refined set of coordinates for the site of interest.

7) The vertical coordinate for dura is determined by slowly advancing the pipette through the drill hole until it makes contact with the meninx. This can be detected directly by observation using an operating microscope or indirectly (without a microscope) by observing the onset of movement of fluid that usually accumulates in the bottom of the drill hole. That is, when a slowly advancing pipette makes contact with the dura, light reflecting off the fluid in the hole will move. Damage to the dura which causes excessive bleeding should be avoided as this can obscure accurate determination of the vertical coordinate at dura. If fluid fails to accumulate in the drill hole, it may be necessary to place a small drop of mineral oil (or saline) into the hole to visualize movement. In many cases, applying mineral oil should be a standard step, as this will keep the dura supple and prevent drying and clogging of the pipette tip.

8) After the vertical coordinate for dura is noted, the pipette is withdrawn, and the dura is carefully incised using the bevel of a high gauge hypodermic needle (e.g., 27 GA). The pipette is then slowly advanced under careful observation until it is lowered to the site of interest. The pipette is left in this position for about one minute before beginning an injection or other procedure to allow displaced brain tissue to recover or otherwise approximate its original position.

9) Using the previously discussed micrografting syringe, a cell suspensions is injected at a rate of 0.25 microliters per minute. The

pipette is left in position after the injection for two minutes before beginning a slow withdrawal (one mm per minute). After the pipette is removed, the exposed area is cleaned with sterile saline and the incision is sutured using 7-0 (10-0 for P3 mice) monofilament nylon suture. The edges of the incision are aligned, with the inside of the skin opposed, and interrupted knots of three throws each are made every 3 mm (1.5 mm in mice) along the incision. Avoid the use of larger diameter suture, which is less flexible and may tear the animal's delicate skin. The mother rat is also more sensitive to larger suture and is more likely to tear open the incision. Braided suture is also not ideal, as it may allow pathogens to wick into the wound, increasing the possibility for infection. Another method of closing an incision is to oppose the clean and dry edges and sparingly apply a cyanoacrylate glue, taking care to not allow the glue to flow onto the surface of the skull. The animal is then cleaned and warmed on a 39° C heating pad and returned to its mother.

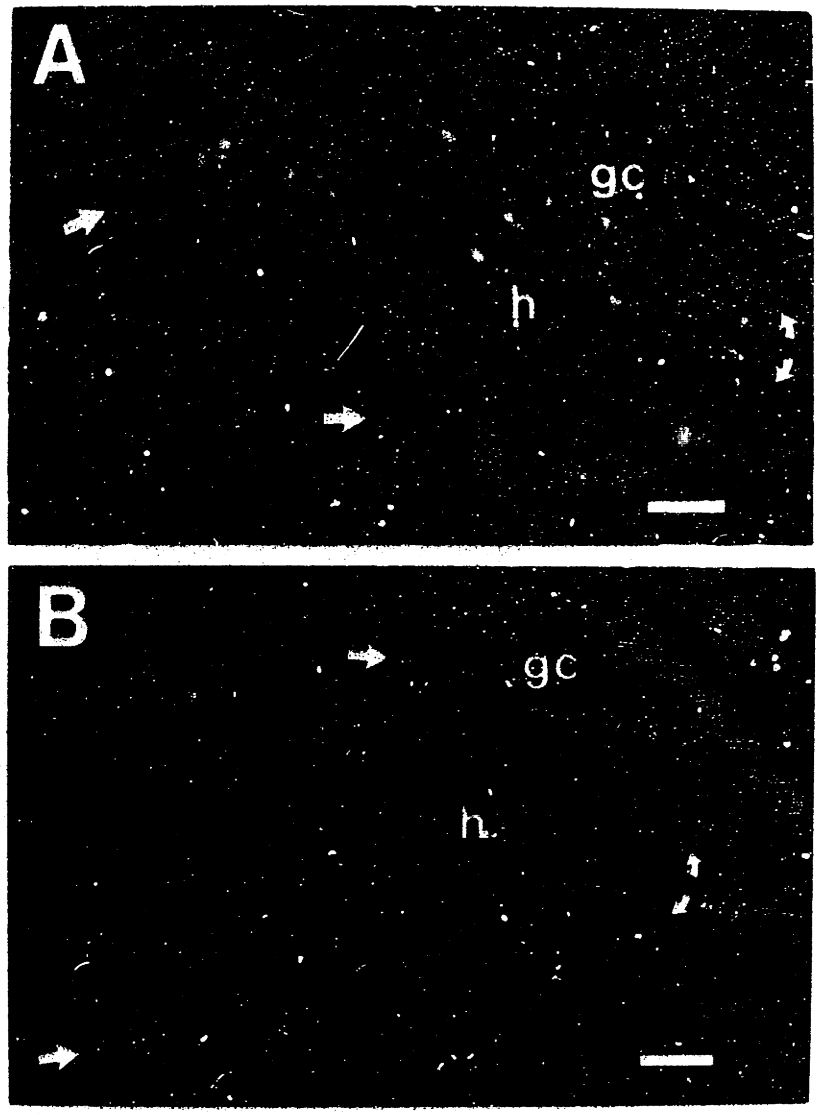
A
gc
h
B
gc
h

Fig. 3. Integration of HiB5 cells can be visualized with green bead labeling. *a*, green bead labeled HiB5 cells immediately after grafting into the hilar region (h) of the dentate gyrus of a P2 rat. The two curved arrows are positioned at the apex of the granule cell layer (gc) while the two straight arrows point toward the apex along the lateral horns of the granule cell layer. This section was counter stained with Hoechts stain. *b*, three weeks after grafting, labeled cells are seen dispersed through the granule cell layer, particularly in the infrapyramidal horn as this is the latest to develop. Scale bars = 100 μm.

Figure 3 shows green bead-labeled HiB5 cells grafted into the hilus of the dentate gyrus immediately after the surgical procedure (A) and after a three week survival (B). Grafted cells can easily be identified throughout the tissue, but are especially populous in the granule cell layer. In addition to the dentate gyrus, we have successfully targeted a variety of other structures in the P2 rat using this methodology. These sites include the lateral ventricles, various cortical areas, the striatum, substantia nigra, cerebral peduncle, cerebellum, and the olfactory bulb.

For injections into the cerebellum and olfactory bulb, the animals' heads are oriented in the neonatal stereotaxic instrument such that the pipette enters perpendicular to the surface of the brain, thus standard head positioning is modified to allow for easier access to these targets. This technique requires, in the case of olfactory bulb implants, that the animal's head be tilted with its nose elevated, and in the case of the cerebellar implantations, that the animal's nose be in a downward position allowing the pipette to enter the cerebellum from the back of the animal's head.

In many cases (e.g., the olfactory bulb, cerebellum, and some cortical areas) it is necessary to place a graft at a very small distance ventral to dura (i.e., $V \leq 1$ mm). Since the newborn brain tissue is underdeveloped and very soft, a common problem is that of the cell suspension escaping from the injection site along the needle tract out onto the surface of the brain. This is caused by the pressure of injection and withdrawal of the pipette combined with the very low resistance provided by the newborn brain tissue (Fig. 4A). A

solution to this problem involves taking advantage of the dura, which can provide support to the tissue and therefore the resistance necessary to hold the graft in place (Fig. 4B). To apply this technique, a dissecting microscope is very helpful; also a larger than normal craniectomy (~1.5 mm in diameter) is needed, exposing a large area of intact dura. The site where the pipette will penetrate should be clear of debris and the dura should be damp and supple yet without any accumulation of fluid or blood in the drill hole. The pipette is lowered so that it just touches the dura; the vertical coordinate is noted and the precise point where the pipette tip touched the dura is observed and memorized based on landmarks (e.g., blood vessels) on the dura's surface. The pipette is withdrawn a few millimeters and the contact point is slightly punctured using a 27 gauge hypodermic needle. The puncture should be just large enough to allow the tip of the micropipette through the dura. The micropipette is then carefully advanced through the puncture hole to the site of implantation and the injection can proceed as normal. It is especially important to inject very slowly, to leave the pipette in position for 2 minutes after the injection, and to withdraw the pipette very slowly.

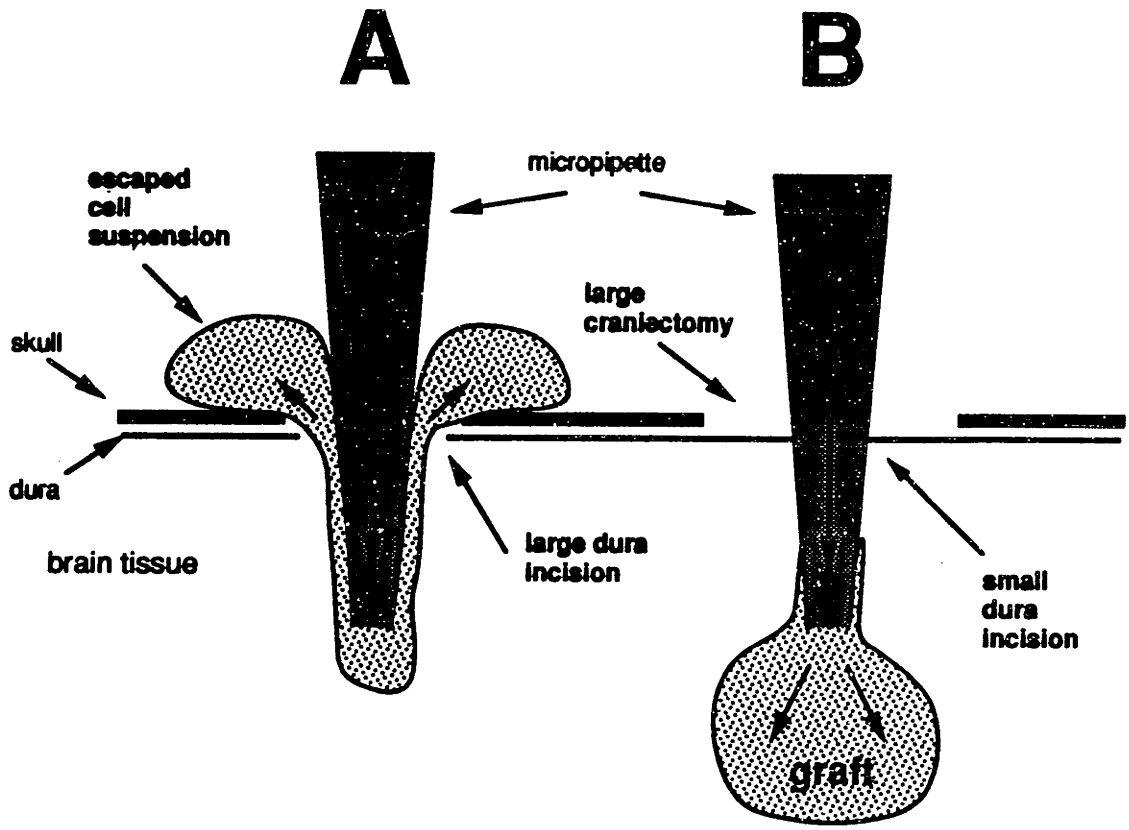
A
B
micropipette
escaped
cell
suspension
large
craniectomy
skull
dura
brain tissue
large dura
incision
small
dura
incision
graft

Fig. 4. Shallow cell suspension grafts can be prevented from escaping during implantation by exploiting the mechanical properties of the dura. In *A* the dura is shown to be opened with a relatively large incision. This reduces the tension in the grafting area and suspension is easily refluxed along the low-resistant pathway onto the surface of the brain. If however, a large craniectomy is produced so that the surface of dura can be visualized as in *B*, the dura can be punctured at the point where the micropipette will enter the brain. The dura can then fit snugly around the walls of the pipette as it is lowered into position thus increasing resistance and preventing escape of the cell suspension.

Other animals.

Although the focus here has been on stereotaxic surgery in the newborn rat, the apparatus and technique described herein have been used extensively in newborn mice (10). However, it is to be expected that the accuracy will be diminished in the mouse due to its smaller size. Conversely, in the hamster, one can expect equal if not greater precision than that obtained in the rat due to the hamster's larger size.

The miniaturized stereotaxic instrument is designed to accomodate larger, more developed animals (post-natal day 7 to 20) as well as neonates. For these older animals, however, anesthesia can be problematic. The animals are too old for hypothermic anesthesia and too young to be reliably anesthetized with most barbiturate anesthetics. However, a reduced dose of Ketamine (30 mg/kg) combined with Xylazine (5 mg/kg) is quite dependable. Halothane inhalant anesthesia is also very effective, and the apparatus required to administer halothane is easily adaptable to the miniaturized instrument.

THE POST-GRAFTING PHASE

Immediate post-operative considerations

Before the animals recover from anesthesia, it is usually desirable to mark them for future identification. For adults, this can be achieved by cutting notches in the ear(s) or marking the tails in permanent ink. Other methods include ear tags and tatoos. For neonates these methods are less effective due to their immaturity and rapid growth and skin renewal. Toe removal is a commonly used method, since the toe will not regrow, and the animal can be easily identified after reaching adulthood. Care should be taken, however, to amputate the toe(s) while the animal is still deeply anesthetized, and the severed tissue should be cauderized to stop any bleeding and reduce the risk of infection.

Post-operative complications are rare after most procedures in adult animals, particularly rats. After closing the incision, the experimenter should keep the animals warm and watch for irregularities in their breathing patterns. If an animal stops breathing, in many cases successful resuscitation can be performed using a segment of tubing which fits snugly over the animal's nose and mouth. The experimenter can then blow into the other end of the tube to expand the animal's lungs. This should be repeated if necessary. This problem is more common in neonates than in adults. If the newborn does not begin breathing within seven minutes after the rewarming period has begun, a similar resuscitation technique can be used. This will usually initiate the breathing reflex.

Another problem which can arise after procedures in neonates is maternal neglect - even though the aforementioned precautions were taken (see Pre-Grafting Phase). After a surgical procedure, the newborn is temporarily weaker than normal. The mother often instinctively separates weak or sick animals from the remaining strong, healthy ones. To prevent such separation, the unoperated newborns can be removed from the mother, therefore reducing the competition in the litter. If this fails, it is possible that another mother with a litter of a comparable age will adopt the operated newborns. However, the risk is that the new mother will perceive these pups as foreign and neglect or cannibalize them. The best solution for maternal neglect is prevention, as previously discussed.

Histological and behavioral assessment

After a graft has been successfully placed in the desired region of the brain of the adult or neonatal host, the cells must be given time to interact with their new environment. For many studies, particularly in the neonate, it is advisable to conduct a time course examination of possible integration, distance and pathway of cell migration, and cellular differentiation. This requires sacrificing and analyzing a subgroup of animals at various time points. Results may be observed as early as a couple of days or may require a period of months. Bear in mind that some assays will be weak if the cells have not fully differentiated. For example, expression of certain gene products such as calbindin protein by granule cells in the dentate gyrus is not maximal until after 3-4 weeks, the time point in which this structure has completed its development. On the other

hand, calbindin protein immunohistochemistry is very strong for the fully differentiated Purkinje cells in the cerebellum at the time of birth.

The methods for treatment of brain tissue after sacrificing the experimental animals vary extensively. The scientist should take into consideration several issues that are important for the success of tissue processing. These include: 1) the age at which the animals should be sacrificed (as mentioned above), 2) whether fresh frozen or fixed tissue should be processed, 3) which is the optimal fixative for further processing, 4) whether the animals should be transcardially perfused or the tissue be immersion fixed, 5) should the tissue be sectioned using a vibratome, sliding microtome, cryostat, etc., and 6) which methods will be most effective for examining the tissue. Again, it is advisable to carefully plan methods for histological analysis before beginning a grafting experiment.

Although it is beyond the scope of this chapter to address these issues in detail, we can direct the reader to sources on neuroanatomical methods (33,34,35); and in addition, we can offer a few helpful suggestions. If newborn animals are to be sacrificed, transcardial perfusion can be done in a similar manner as in the adult, but scaled down to size. A blunted 21 gauge needle can be used as the intraventricular cannula combined with a 20 cc syringe to deliver a smaller volume of perfusate (10-50 ml). Immunoreactions may be optimized by decreasing the concentration of fixative, as over-fixation can result in partial or total masking of the antigen of interest. However, with a reduction in fixation the tissue is softer and more friable. It is therefore more difficult to

handle as in free floating immunoreactions. This problem can be avoided by handling the tissue on glass slides: Tissue can be cut in very thin sections (6 mm) using a cryostat and thaw mounted onto glass slides coated with a poly-L-lysine solution (1mg poly-L-lysine / ml dH_2O spread evenly and air-dried on glass slides). Immunoreactions on the thaw mounted sections can then be performed on the slides. This allows single cell thick sections to be handled easily. Another advantage is that if the tissue has been grafted with [^{3}H]-thymidine labeled cells, an immunoreaction can be followed by autoradiography and the antigenicity of the grafted cells can be determined. The disadvantage of this technique is that only one side of the tissue section is exposed to reaction reagents as opposed to both sides in free floating sections. This can result in less intense staining. Note also that many cell markers lose there effectiveness when frozen (e.g., carbocyanine dyes), treated with alcohols or xylene (e.g., carbocyanine dyes and latex microspheres) or fixed with an inappropriate fixative (e.g., paraformaldehyde decreases the signal of X-gal reactions and the fluorescence of glutaraldehyde may obscure fluorescent signals).

The functional assessment of graft-induced behavioral effects should relate to the time-course of morphological differentiation and integration of cells into a specific target region of the host brain. For the behavioral tests applicable to the different lesion models, the reader is referred to Table 1. If little is known about the fate of the transplanted cells, behavioral assessment should at least be expanded over a period of six months with repeated testings. It can take a considerable period of time for the implanted cells to exert

functional effects, even though one may find earlier signs of morphological integration.

Final Comments.

Scientists have directed a great deal of thought and effort toward producing cell lines, characterizing them *in vitro*, and thoroughly evaluating, both behaviorally and histologically, animals grafted with such cells. It is of at least as much importance to devote the same effort to careful surgical placement of cells in specific brain structures. In this chapter we have focussed in detail on procedures for grafting cell suspensions into the adult and neonatal brain. We have described standard grafting methodology and a novel apparatus to aid in precision surgery in newborn rodents. We have also described a micrografting technique which enables controlled depositions of very small numbers of cells to be made at discrete foci. Using a pulled glass pipette, the tip at least one-tenth the diameter of the cannula of the typical syringe barrel. micrografting minimizes trauma to the brain tissue in the immediate vicinity of the graft. There is less hemorrhage, less gliosis, and greater preservation of the integrity of the blood brain barrier. Moreover, we have seen that the placement of several small grafts (e.g., 200 nL = 20,000 cells) as opposed to one or two large grafts ($\geq$ 1 mL) in the striatum of 6-OHDA lesioned adult rats increases cell survival and integration (27).

Transplantation has emerged as a powerful tool in neurobiology. Grafting of cultured cells adds a new dimension to the

field, allowing the cells to be manipulated in a variety of ways. Exploring the consequences of genetic alterations of cells can now be systematically controlled and performed. This technology will provide us with new and exciting potential to elucidate the complexities in the normal and compromised development and function of the central nervous system. Moreover, as the transplantation of fetal cells in patients with Parkinson's disease has shown encouraging clinical results, *in vitro* manipulations of tissue may become a valuable approach to the study and treatment of neurodegenerative diseases. Studies which involve implanting cultured cells into the brain offer great potential toward offering therapeutic alternatives as well as disclosing basic principles in neurobiology. These approaches will be confronted by a tremendous scientific and medical challenge over the forthcoming years.

REFERENCES

1. Renfranz, P. J., Cunningham, M. G., and McKay, R. D. G. (1991) Region-specific differentiation of the hippocampal stem cell line HiB5 upon implantation into the developing mammalian brain, *Cell*, 66(4), 713-729.

2. Almazan, G., McKay, R.D.G (1992) An oligodendrocyte precursor cell line from rat optic nerve, *Brain Res.*, 579, 234-245.

3. Frederiksen, K. and McKay, R.D.G. (1988) proliferation and differentiation of a rat neuroepithelial precursor cells in vivo. *J. Neurosci.* 8, 1144-1151.

4. Lendahl, U., Zimmerman, L.B., McKay, R.D.G. (1990) CNS stem cels express a new class of intermediate filament protein,*Cell* 60, 585-595.

5. Turner, D.L. & Cepko (1987) A common progenitor for neurons and glia persists in rat retina late in development, *Nature* 328, 131-136.

6. Holt, C.E., Bertsch, T.W., Ellis, H.M., Harris, W.A. (1988) Cellular determination in the Xenopus retina is independent of lineage and birth date, *Neuron* 1, 15-26.

7. Price, J., & Thurlow, L. (1988) Cell lineage in the rat cerebral cortex: a study using retroviral-mediated gene transfer, *Development* 104, 473-482.

8. Cunningham, M.C., Renfranz, P., Arel, L., & McKay, R.D.G. (1993) In vivo expression of neural or glial cell-specific antigens and up-regulation of c-fos by an immortal neuroepithelial cell line. Submitted.

9. Snyder, E.Y., Deitcher, D.L., Walsh, C., Arnold-Aldea, S., Hartwieg, E.A., & Cepko, C.L. (1992) Multipotent neuroal cell lines can engraft and participate in development of mouse cerebellum, *Cell*, 68, 33-51.

10. Cunningham, M.C., Vicario, C., & McKay, R.D.G. (1993) Fate shifting of cerebellar primordial cells upon transplantatioo the developing fascia dentata. Submitted.

11. McConnell, S.K. (1988) Fates of visual cortical neurons in the ferret after isochronic and heterochronic transplantation. *J. of Neuroscience*, 8(3), 945-974.

12. Cadusseau, J. & Peschanski, M., (1989) Direct neuronal and macroglial versus indirect macrophagic labeling in transplants of fetal neural tissue incubated with gold particles, *Exper. Neurology*, 106, 265-274.

13. Madison, R., Macklis, J.D., Thies, C. (1990) Latex nanosphere delivery system (LNDS): novel nanometer-sized carriers of fluorescent dyes and active agents selectively target neuronal subpopulations via uptake and retrograde transport. *Brain Research*, 522, 90-98.

14. Zimmer Doll, D. and Lehman, M.N. (1992) Bromodeoxyuridine as a label for fetal hypothalamic whole tissue and cell suspension grafts, *Rest. neurol. and Neuroscience*, 4(3), 209.

15. Takahashi, T., Nowakowski, R.S., and Caviness, V.S. Jr. (1992) BUdR as an S-phase marker for quantitative studies of cytokinetic behaviour in the murine cerebral ventricular zone. *Journal of Neurocytology* 21, 185-197.

16. McNeil, P.L. and Warder, E. (1987) Glass beads load macromolecules into living cells. *Journal of Cell Science* 88, 669-678.

17. Wictorin, K., Brundin, P., Sauer, H., Lindvall, O., and Björklund, A. (1992) Long Distance Directed Axonal Growth From Human Dopaminergic Mesencephalic Neuroblasts Implanted Along the Nigrostriatal Pathway in 6-Hydroxydopamine Lesioned Adult Rats. *J. Comp. Neurol.* 322, 1-20.

18. Snyder-Keller A.M., Carder R.K. and Lund R.D. (1989) Development of dopamine innervation and turning behavior in dopamine-depleted infant rats receiving unilateral nigral transplants. *Neuroscience* 30 (3), 779-794

19. Herman J.-P., Choulli K ., Geffard M., Nadaud D., Taghzouti K. and Le Moal M. (1986) Reinnervation of the nucleus accumbens and frontal cortex of the rat by dopaminergic grafts and effects on hoarding behavior. *Brain Research* 372, 210-216

20. Sunde N., Laurberg S. and Zimmer J. (1984) Brain grafts can restore irradiation-damaged neuronal connections in newborn rats. *Nature* 310, 51-53

21. Dunnett S.B. (1991) Cholinergic grafts, memory and aging. *TINS* 14 (8), 371-375

22. Onifer, S., and Low, W.C. (1990) Spatial memory deficit resulting from ischemia-induced damage to the hippocampus is ameliorated by intra-hippocampal transplants of fetal hippocampal neurons. In Dunnett SB and Richards SJ (eds.) Prog Brain Res 82, Elsevier, Amsterdam, 359-366

23. Björklund A., Stenevi U., Dunnett S.B., Iversen S.D. (1981) Functional reactivation of the deafferented neostriatum by nigral transplants. *Nature* 289, 497-499

24. Mandel R., Brundin P. and Björklund A. (1990) The importance of graft placement and task complexity for transplant-induced recovery

of simple and complex sensorimotor deficits in dopamine denervated rats. *Europ. J. Neurosci.* 2, 888-894

25. Dunnett S.B., Isacson O., Sirinathsinghji D.J.S., Clarke D.J. and Björklund A. (1988) Striatal grafts with unilateral neostriatal lesions. III. Recovery from dopamine-dependent motor asymmetry and deficits in skilled paw reaching. *Neuroscience* 24, 813-820

26. Björklund, A., and Dunnett, S.B. (1992) Neural transplantation in adult rats. In Dunnett SB and Björklund A (eds.) Neural Transplantation A Practical Approach, Oxford University Press, New York, 58-78

27. Nikkhah, G., Cunningham, M.G., Björklund, A., Microtransplantation technique for the implantation of dopaminergic grafts into the 6-OHDA lesioned adult and neonatal nigrostriatal system. (manuscript in preparation).

28. Paxinos, G., Watson, C. , *The Rat Brain in Stereotaxic Coordinates*, Academic Press, New York, 1982.

29. Benjamin, Maxine M., (1987), Outline of Veterinary Clinical Pathology, Iowa State University Press, Ames, Iowa, pp. 108-115.

30. Flecknell, P. A. (1987) Laboratory Animal Anesthesia, Academic Press, Inc, San Diego, pp. 73-74.

31. Cunningham, M.G. and McKay, R.D.G. (1992) A hypothermic miniaturized stereotaxic instrument for surgery in newborn rats. *J. Neurosci. Meth.* In press.

32. Valenstein, T., Case, B., Valenstein, E.S.(1969) , Stereotaxic Atlas of the Infant Rat Hypothaiamus, *Developmental Psychobiology*, 2(2), 75-80.

33. Nauta, W.J.H. and Ebbesson, S.O.E. (Eds.) (1970) Contemporary Research Methods in Neuroanatomy Springer-Verlag Berlin, Heidelberg, New York.

34. Lahue, R. (Ed.) (1981) Methods in Neurobiology, Volume 2. Plenum Press, New York and London.

35. Björklund, A., Hökfelt, T., Wouterlood, F.G., and van den Pol A.N. (Eds.) (1990) Analysis fo Neuronal Microcircuits and Synaptic Interactions in Handbook of Chemical Neuroanatomy. Elsevier, Amsterdam, New York, Oxford.

CHAPTER 3

RECONSTRUCTION OF THE MESOSTRIATAL SYSTEM IN THE 6-OHDA-LESIONED NEONATE

ABSTRACT

The present study was designed to elucidate the dynamic influence of the developing brain on the anatomical and functional capacities of intranigral dopaminergic grafts into the 6-OHDA lesioned neonate. Postnatal-day-one (P1) animals received bilateral intraventricular injections of 6-OHDA. P3 pups were then grafted with E14 ventral mesencephalon unilaterally into the substantia nigra. 40,000 cells were injected at two sites (150 nl/site) using a glass capillary (OD 50-70 mm). For a subset of grafts the cell suspension was prelabelled with green-fluorescent latex microspheres. After 10 weeks, animals were injected with amphetamine to up-regulate the immediate early gene (IEG), c-*fos*. The tissue was then processed for TH- and FOS-immunohistochemistry. TH-positive cells were found integrated in the neonatal host brain, with no indication of graft-host segregation, and to extend projections along the mesostriatal pathway which terminate in the striatum. Large numbers of FOS-positive cells were also found in the striatum on the side of the transplant suggesting that the projections from the graft terminate with functional synapses. The organotypic reconstruction of the mesostriatal system in the neonate provide a new approach to our understanding the factors influencing dopaminergic graft integration and function.

This brief report was adapted from a presentation at the IVth International Symposium on Neural Transplantation, authored by Miles G. Cunningham, G. Nikkhah, R.D.G. McKay, & A. Björklund.

INTRODUCTION

Transplantation studies of dopaminergic (DA) grafts into the neonatal and the adult brain have focussed on the ectopic graft placement into the 6-OHDA denervated corpus striatum (Herman et al., 1986). One reason for this is that behavioral effects have not been observed when attempts were made to graft into the substantia nigra. Striatal grafts, nevertheless, have been shown to provide partial restoration of the behavioral and biochemical 6-OHDA lesion syndrome (Rioux et al., 1991).

The lack of a more complete recovery of the 6-OHDA-lesion induced deficits by DA grafts could be at least partially due to the absence of physiological afferent input. More recently, it has been pointed out that the dopaminergic innervation of the substantia nigra pars reticularis plays an important role in the information processing directed outward from the basal ganglia (Robertson, 1989).

While there have been a few attempts to transplant DA grafts homotopically into the substantia nigra in the adult host, which have failed to show any functional effects, there has been no report on the organotypical implantation of DA grafts into the developing neonatal brain. The present study was therefore designed to elucidate the influence of the developing brain on the anatomical and functional capacities of intranigral dopaminergic grafts into the 6-OHDA lesioned neonate.

METHODS

Postnatal-day-1 (P1) male and female Sprague-Dawley rats received bilateral intraventricular injections of 2 X 5µl 6-OHDA (110 µg of 6-OHDA HCl in 0.2 mg/ml ascorbic acid/saline) using the following coordinates: AP -0.6 mm; L ± 0.8 mm; V 2.1 mm. Animals were then allocated into three groups: Normal (n=9), 6-OHDA (n=20) and Graft (n=22) groups. Neural microtransplants of dopamine-rich cell suspensions were prepared from central mesencephalic (VM) tissue of 14-day old rat fetuses (Björklund et al., 1983). The tissue was incubated in 0.1% trypsin/0.05% DNase/DMEM at 37° C for 20 min, rinsed 4 times in 0.05% DNase and mechanically dissociated using a 1 ml Eppendorf pipette. The tissue was then centrifuged at 600 rpm for 5 min and the pellet resuspended in 0.05% DNase/DMEM. The cell number of this suspension was 140,000 cells/µl and the viability was >95% as determined by the trypan blue dye exclusion method.

The transplantation surgery on P3 animals was performed as described in detail elsewhere (Cunningham & McKay, in press). Briefly, P3 animals were fixed in the Cunningham hypothermic miniaturized stereotaxic device (Stoelting Co.). The micrografts were implanted using a glass capillary with an OD of 50-70 µm connected to a 1 ml Hamilton microsyringe. 150 nl of the cell suspension was implanted at each of two sites:

AP:	-3.7	-4.3
L:	1.6	1.6
V:	4.3	4.3

At P72 14 animals (5 grafted, 5 lesioned and 4 normal) were sacrificed 2 hours after receiving 5 mg/kg amphetamine to up-

regulate the expression of c-*fos*. Tissue was processed for tyrosine hydroxylase and FOS immunohistochemistry using standard techniques (see methods in Chapters 4 & 6) and were examined microscopically under dark and bright field illumination.

RESULTS AND DISCUSSION

Figure 1 illustrates the integration of the graft in the right substantia nigra (Fig. 1D) as compared to the non-grafted contralateral side (Fig. 1C). The top panels in Figure 1 show the numerous TH-positive fibers infiltrating the striatum on the grafted side and the absence of fibers in the contralateral striatum. The presence of TH-immunoreactive fibers in the lesioned striatum ipsilateral to the graft suggests some level of graft-derived reinnervation. This was further evaluated by examining the amphetamine-induced up-regulation of the immediate early gene, c-fos. Administration of amphetamine results in the expression of FOS by many striatal cells, particularly in the striasomal compartment (Graybiel, 1990). This induction is blocked by the NMDA-receptor antagonist, MK801 (Johnson & Robertson, 1989) and the dopamine receptor antagonist, SCH23390 (Moratalla et al., 1992). Since the mechanism of action of amphetamine is stimulating the presynaptic release of catecholamines, and the FOS response appears to be receptor-mediated, the up-regulation of c-fos upon challenge with amphetamine would indicate the presence of functional synapses.

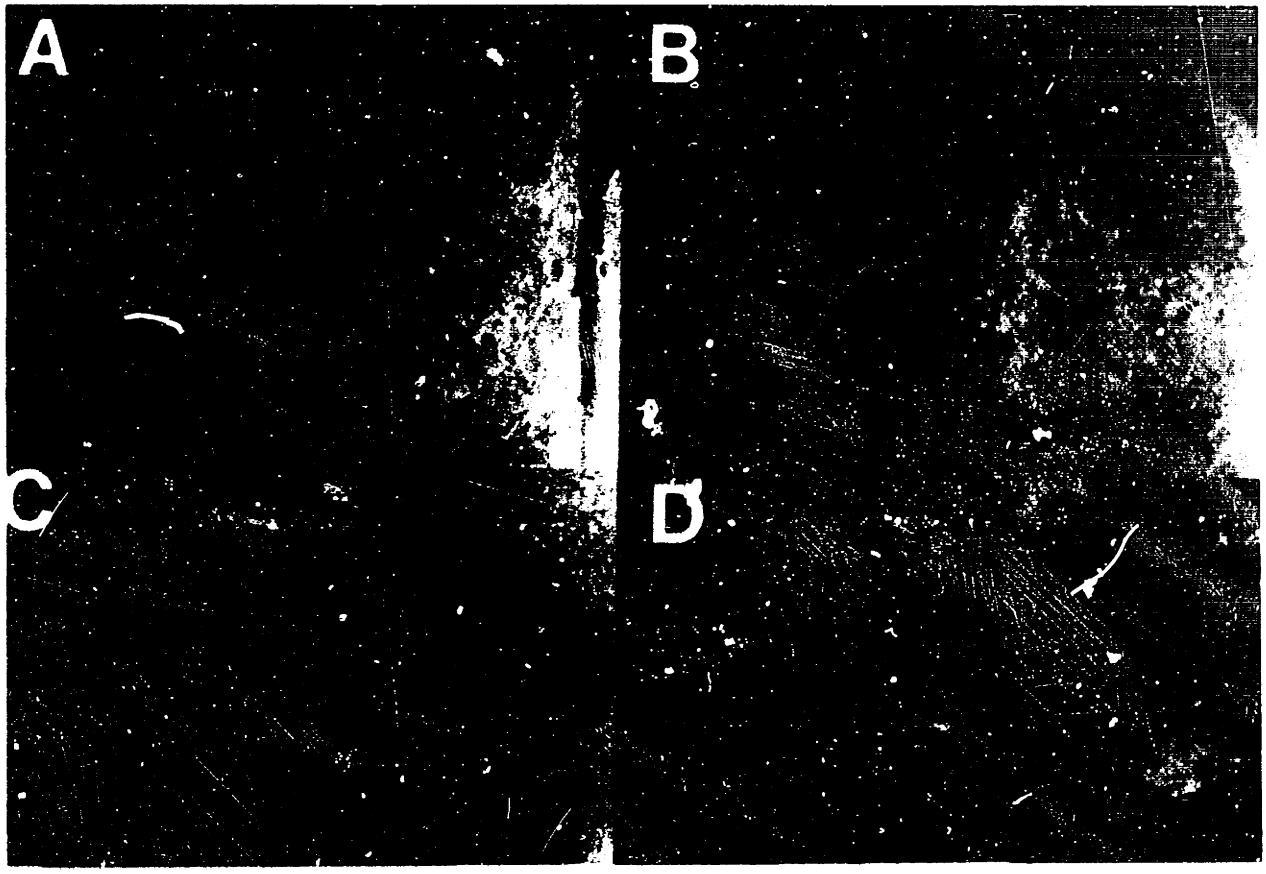
A
B
C
D

Figure 1. Integration and projection of homotopically placed nigral grafts in the lesioned neonate.

Left (C) and right (D) substantia nigra correspond to their respective striata shown in (A) and (B), respectively. There is seen a robust survival of the DA micrograft and an abundant arborization in its vicinity on the right side. The left side illustrates the permanent disappearence of the intrinsic DA neurons in the substantia nigra after intraventricular 6-OHDA administration.

Extensive TH immunoreactive terminals are seen in the right striatum (B), predominately in the medial part, compared to an almost absent staining on the left side (A).

Figure 2. The striatum of the corresponding grafted substantia nigra contains more cells immunoreactive for FOS after administration of amphetamine. Panels **A** and **C** represent (at low and higher magnification, respectively) the left striatum, and **B** and **D** the right striatum of a 6-OHDA lesioned rat which received grafts into the right substantia nigra. Approximately two-fold more FOS-positive cells are found in the striatum receiving projections from the grafted substantia nigra.

Figure 2 illustrates the extent of FOS expression in the striatum of a lesioned animal which received transplants into the ipsilateral substantia nigra. The grafted side (right, B & D) contains many more FOS-positive cells than the non-grafted control side (left, A & C). This result is consistent with the data shown in Figure 1 and suggests that the striatum has become functionally reinnervated.

This report provides the first evidence to date demonstrating the capability of an allograft placed in the substantia nigra of an animal Parkinson's model to integrate and project to the striatum. As this has not been witnessed in the adult, it seems probable that the mature brain has lost or become inhibitory to this capability during development. Nevertheless, the factors which regulate reinnervation may, at some level, be accessible.

In a related study, Wictorin et al. (1990) showed that human telencephalic neuroblasts, when grafted into the ibotenic acid-lesioned adult rat striatum, extend processes along striato-nigral and cortico-spinal tracts. A species-specific antibody against human neurofilament (HNF) was used to visualize fibers extending to many targets, including the cervical spinal cord, the pontine nuclei, and the substantia nigra. The authors suggest that human, as opposed to rat, embryonic tissue may have this capability because the neuroblasts have a longer developmental period in which axon elongation can occur. In addition, they point out that human cells normally extend processes far greater distances. These results imply that any process-extension inhibitory factors which exist in the adult are avoided or not recognized by the human neuroblasts. The present

data suggest that embryonic rat mesencephalic cells are also capable of growing axons over long distances, but they are not capable of avoiding environmental restrictions present in the adult, and therefore depend on the developmental stage of the host in order to extend processes.

The prevention of axon growth in the adult has been attributed to the presence of myelin-associated neurite growth inhibitors. Intracerebral application of the monoclonal antibody, IN-1, against the myelin-associated proteins , NI-35 and NI-250, results in prolific sprouting at the site of a cortico-spinal tract transection (Schnell & Schwab, 1990). Since we now know that embryonic ventral mesencephalic cells are capable of restoring the nigro-striatal path in the neonate but probably not the adult, perhaps altering the host environment, as with IN-1, will permit similar restoration in the mature brain.

REFERENCES

Björklund A., Stenevi U., Schmidt R. H., Dunnett S. B. and Gage F. H. (1983) Intracerebral grafting of neuronal cell suspensions. I. Introduction and general methods of preparation. *Acta Physiol. Scand.* **522,** 1-7.

Graybiel, A.M., Moratalla, R., Robertson, H.A. (1990) Amphetamine and cocaine induce drug-specific activation of the c-fos gene in striosome-matrix an dlimbic subdivisions of the striatum. *Proc. Natl. Acad. Sci. USA* 87, 6912-6916.

Herman J. P., Choulli K., Geffard M., Nadaud D., Taghzouti K. and LeMoal M. (1986) Reinnervation of the nucleus accumbens and frontal cortex of the rat by dopaminergic grafts and effects on hoarding behavior. *Brain Res.* **372,** 210-216.

Johnson, K. & Robertson, H.A. (1989) The NMDA antagonist MK-801 reverses d-amphetamine-induced activation of the protooncogene c-fos in rat striatum. Soc Neurosci Abstr 15: 782.

Rioux L., Gaudin D. P., Bui L. K., Gregoire L., DiPaolo T. and Bedard P. J. (1991) Correlation of functional recovery after a 6-hydroxy-dopamine lesion with survival of grafted fetal neurons and release of dopamine in the striatum of the rat. *Neuroscience* **40,** 123-131.

Robertson, G.S. & Robertson, H.A. (1989) Evidence that L-DOPA-induced rotational behavior is dependent on both striatal and nigral mechanisms, J. Neurosci. 9, 3326-3331.

Schnell, L. & Schwab, M.E. (1990) Axonal regeneration in the rat spinal cord produced by an antibody against myelin-associated neurite growth inhibitors. *Nature* 343, 269-272.

Wictorin, K., Brundin, P., Gustavii, B., Lindvall, O., & Björklund, A. (1990) Reformation of lon axon pathways in adult rat CNS by human forebrain neuroblasts. *Nature* ,

CHAPTER 4

IMPROVED GRAFT SURVIVAL AND STRIATAL REINNERVATION BY MICROTRANSPLANTATION OF FETAL NIGRAL CELL SUSPENSIONS IN THE RAT PARKINSON MODEL

ABSTRACT

A microtransplantation approach has been used in order to achieve more complete reinnervation of the dopamine denervated rat striatum by fetal nigral cell suspensions injected into multiple striatal sites. A total of 450,000 cells, obtained from the ventral mesencephalon of embryonic day 14 rat fetuses, were implanted either in the conventional way as two 1.8 µl deposits centrally in the head of the caudate-putamen ("Macro grafts"), or as eighteen 0.2 µl deposits disseminated over six needle penetrations in the same area using a 50-70 µm glass capillary tip ("Micro grafts"). Non-grafted lesioned rats served as controls. Dopamine neuron survival (as assessed by tyrosine hydroxylase immunohistochemistry at 4 months after transplantation) was 2.8-fold greater in the Micro grafts as compared to the Macro grafts.

This chapter was adapted from a manuscript submitted to the Journal of Neuroscience authored by Guido Nikkhah, Miles G. Cunningham, A. Jodicke, U. Knappe, and Anders Björklund.

Striatal dopamine tissue levels (determined in a separate group of rats) were increased 2.5-fold in the head of the caudate-putamen (from 12.5% of normal in the Macro graft group to 30% of normal in the Micro graft group). Consistent with this, the overall graft-derived tyrosine hydroxylase positive fiber outgrowth was more extensive in the Micro graft group and covered larger areas of the previously denervated caudate-putamen.

The results show that distribution of the fetal nigral tissue in multiple small deposits provides for increased dopamine neuron survival, probably because of a closer contact between the implanted cells and the surrounding host striatal tissue in the small-sized graft deposits. Less bleeding and necrosis at the implantation site may also have contributed to this effect. The present microtransplantation procedure is an efficient means to increase overall dopamine neuron survival and to achieve more complete reinnervation of the denervated striatum in the rat Parkinson model. It also substantially increased the reproducibility of DA graft survival between animals.

Introduction

In a recent quantitative autoradiographic study, Doucet et al. [10] have shown that the DA fiber outgrowth from a single nigral cell suspension graft is dense only in a narrow zone close to the graft (up to about 0.5 mm) and that the density declines sharply over the next millimeter. Moreover, overall fiber outgrowth was correlated with the graft size only up to a volume of about 0.5 - 1 mm^3. Larger sized grafts did not result in any further increase in fiber outgrowth, which is consistent also with the previous biochemical data of Schmidt et al.[22]

These observations suggest that the efficacy of intrastriatal nigral grafts might be increased if the tissue is distributed as multiple small deposits, dispersed over a wider area of the striatal target. In the present series of experiments we have tested this possibility using a new microtransplantation approach (Nikkhah et al, in preparation) which allows reliable and reproducible implantation of sub-microliter volumes of fetal neural cell suspension at multiple sites with minimal tissue damage. The functional effects of intrastriatal nigral microtransplants on the recovery of complex spontaneous sensorimotor and drug-induced behavioral deficits are reported in a parallel paper. [18]

EXPERIMENTAL PROCEDURES

Animals

Thirty adult female Sprague-Dawley rats (200-225 g body weight at the beginning of the experiment) (ALAB, Stockholm, Sweden) were used. They were housed under a 12: h light-dark cycle with access to food and water ad libitum. All animals were subjected to unilateral 6-hydroxydopamine (6-OHDA) lesion and intrastriatal transplantation under equithesin anaesthesia. Following lesion and transplantation surgery a battery of tests for spontaneous and drug-induced behaviour was performed, as described in detail elsewhere.[18] The animals were sacrificed for either morphological or biochemical analysis at 15 weeks post-transplantation.

6-OHDA lesion surgery

All 30 rats were given two stereotaxic injections of 6-OHDA using a 10 µl Hamilton syringe into the right ascending mesostriatal DA pathway at the following coordinates (in mm, with reference to bregma and dura): First, 2.5 µl of 6-OHDA (3.6 µg/µl in 0.2 mg/ml L-ascorbate-saline) at: AP: -4.4, L: 1.2, V: 7.8. (TB: -2.4). Second, 3 µl of 6-OHDA at AP: -4.0, L: 0.8, V: 8.0 (TB: + 3.4). The injection rate was 1 µl/min and the cannula was left in place for an additional 5 min before slowly retracting it. Two weeks after 6-OHDA lesion surgery, the animals were given 5 mg/kg d-amphetamine (in saline) i.p. and their rotational scores collected over a 90 min period. The rotational behavior of the rats was monitored in automated

"rotometer" bowls according to Ungerstedt and Arbuthnott.[24] Only rats exhibiting a mean net ipsilateral rotation of at least 6.1 fully body turns/min, ipsilateral to the lesion, over the 90 min observation period were included in the study. This criterion secures that the 6-OHDA induced denervation of the caudate-putamen was complete. This test (as well as tests for rotation in response to apomorphine and D1- and D2-receptor agonists) was repeated at 6-7 weeks and 14-15 weeks after transplantation (see Ref. [18]).

Transplantation surgery

The 6-OHDA lesioned animals were divided into three equal groups, balanced with respect to their amphetamine-induced rotation asymmetry scores: a 6-OHDA (lesion only) group; a Micro graft group; and Macro graft group; with ten animals in each group.

Dopamine-rich cell suspensions were prepared from ventral mesencephalic (VM) tissue of 14-day old rat fetuses according to a modified version (Nikkhah et al, in preparation) of the cell suspension technique described by Björklund et al. [3] and Herman et al. [15] To obtain a sufficient working volume for the cell suspensions, 41 (Micro) and 37 (Macro) ventral mesencephalons were dissected in DMEM (Gibco) and the tissue was incubated in 0.1% trypsin/0.05% DNase/DMEM (Trypsin: Worthington, DNas: Sigma DN-25) at 37°C for 20 min, then rinsed 4 times in 0.05% DNase/DMEM. The mechanical dissociation of the tissue pieces was performed in 250 µl of 0.05% DNase/DMEM by repeated tituration starting with a 1 ml Eppendorf pipetteman. After the suspension became milky a 200 µl Eppendorf pipetteman was used with its smaller tips for a second trituration in

order achieve a homogeneous single cell suspension. The tissue was then centrifuged at 600 rpm for 5 min and the pellet resuspended in a final volume of 130-140 µl of 0.05% DNase/DMEM. The cell number of this cell suspension was 125,000 cells/µl and the viability was >97% prior to transplantation, and >84% post-transplantation, as determined by the trypan blue dye exclusion method.

Micro- and macrografts were prepared at two equivalent surgical sessions. The Macro grafts consisted of 2 deposits of 1.8 µl each and were implanted with a 10 µl Hamilton syringe equipped with a 0.5 mm O.D. metal cannula. The Micro grafts were implanted using a glass capillary with an OD of 50-70 µm connected to a 1 µl Hamilton microsyringe. Three deposits of 200 nl were placed along each of six implantation tracts resulting in a total of 18 micrografts with a total graft volume of 3.6 µl (see Fig. 1). For the coordinates used, see Table 1. Over the course of both transplantation sessions the cells were gently triturated to maintain a homogeneous suspension.

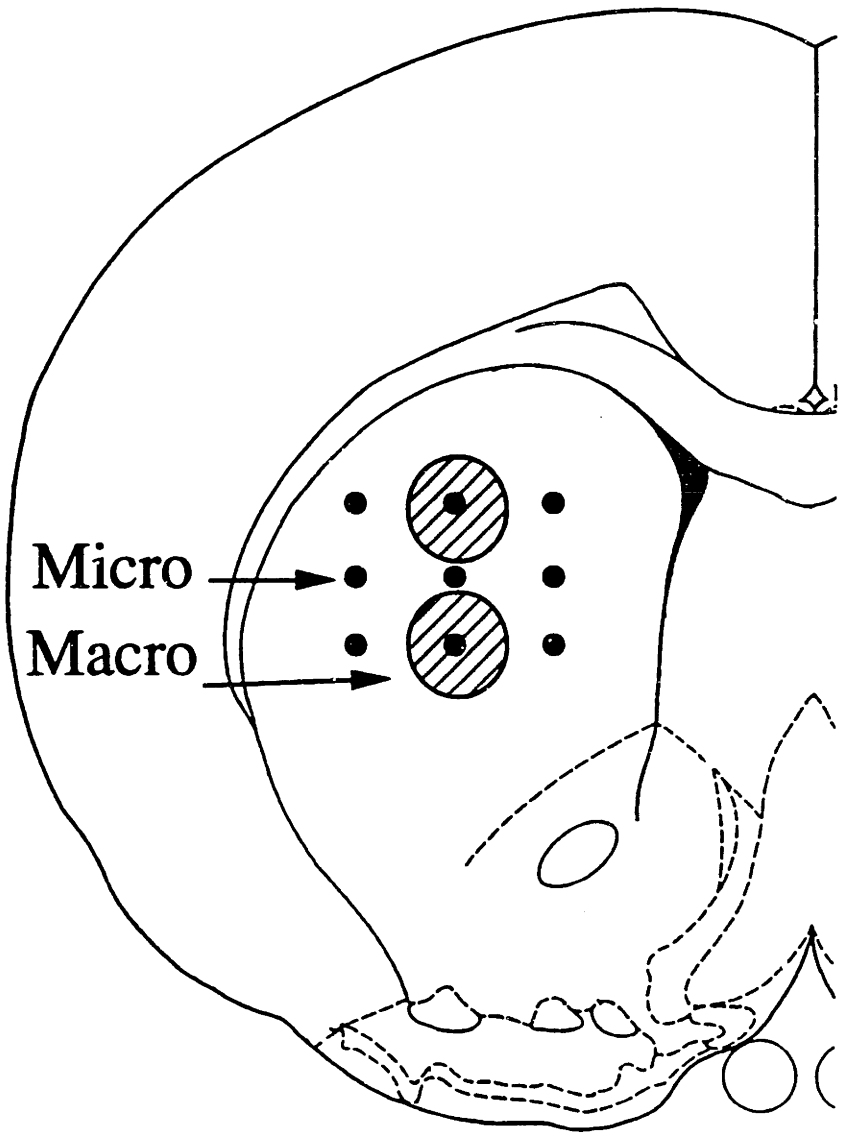
Micro
Macro

Fig. 1. Schematic representation of the intrastriatal implantation sites used for the Micro grafts (black dots) and Macro grafts (hatched circles) as projected onto a single coronal plane. For coordinates see Table 1.

Table 1: Coordinates used for the intrastriatal implantation of the nigral Micro and Macro grafts (Tooth bar = 0; numbers are given in mm)

	Micro grafts						Macro grafts
Tract	1	2	3	4	5	6	1
Anterior to bregma:	1.3	1.0	0.7	0.6	0.3	0.0	0.5
Lateral:	2.1	2.9	3.7	2.1	2.9	3.7	3.0
Ventral:	5.5 + 4.9 + 4.3 each tract						5.0 + 4.1
Volume:	200 nl each						1.8 µl each

Tyrosine hydroxylase (TH) immunohistochemistry

At 15 weeks postgrafting, 4 animals from each group were deeply anaesthetized with choral hydrate and perfused transcardially with 30 ml of 0.9% saline, followed by 300 ml of ice-cold 4% paraformaldehyde in 0.1 M phosphate buffer (PB, pH 7.4) over 9 min. The brains were postfixed for 2 hours and dehydrated overnight in 20% sucrose/0.1 M PB. Serial coronal sections were cut on a freezing microtome at 30 µm thickness and every third section was processed for TH immunohistochemistry as follows: Free-floating sections were rinsed three times with 0.2 M PB, quenched with 3% H2O2/10% methanol/PB for 10 min and rinsed three times with PB. Following a preincubation of 1 hr in 5% normal swine serum (NSS)/0.3% Triton-X/PB, the sections were incubated with the primary TH antiserum (Pel Freez; diluted 1:500 in 2% NSS/0.3% Triton-X/PB) overnight at room temperature. After three rinses with PB, sections were incubated with a biotinylated swine-anti-rabbit IgG (1:200, Dakopatts)/0.3% Triton-X/PB for 1 hr, rinsed again three times and transferred to a Vectastain ABC solution/PB for 1 hr. The labeling was visualized by a chromogen solution of 0.05% 3,3-diaminobenzidine and 0.01% H2O2. Sections were mounted onto chromalum-coated slides , dehydrated in ascending alcohol concentrations, and coverslipped in DPX.

Morphometry

TH-immunoreactive graft neurons in the striatum were counted microscopically under bright field illumination, and an approximation of the final graft cell number was calculated according to the formula of Abercrombie.[1] Graft volumes were determined according to the Cavalieri principle[13, 16] with the help of a computerized stereology system (Bico AS, Denmark) equipped with the GRID software (MedicoSOFT, Denmark)

Dopamine and noradrenaline levels

At 15 weeks postgrafting 6 animals in each group were killed by decapitation under choral hydrate anaesthesia. The brains were removed quickly and the caudate-putamen, nc. accumbens and anteromedial frontal cortex were dissected bilaterally. The head of the caudate-putamen (defined as the area rostral to the crossing of the anterior commissure) was divided into a medial and lateral portion. The caudal caudate-putamen contained the part of the nucleus located caudal to the crossing of the anterior commissure, and dorsally and laterally to the globus pallidus. The dissected pieces were immediately frozen in liquid nitrogen. Dopamine (DA) and noradrenaline (NA) levels were assayed according to the radioenzymatic method of Schmidt et al.[22] Test samples demonstrated that there was < 0.1% crossover actitivity between DA and NA in this method.

Statistical analysis

Results are expressed as mean ± SEM of the different treatment groups. For statistical evaluation, data were subjected to one-way analysis of variance (ANOVA) and Fisher PLSD post-hoc test. Statistical significance level was set at $p<0.05$.

RESULTS

TH Immunohistochemistry

The Macrografts, which were implanted as two 1.8 µl deposits along a single injection tract, appeared as a single elongated tissue mass, 0.5-0.6 mm wide and 2-2.5 mm long, which usually extended into and through the corpus callosum (Fig. 2 A). These grafts reached a mean volume of 1.06 mm^3 (range: 0.86-1.20 mm^3) and contained an average of 1996 TH-positive neurons (range: 1904-2064), corresponding to a TH-positive cell density of 1914 cells/mm^3 (Table 2).

The TH-positive neurons occured preferentially in clusters in the peripheral areas of the grafts, leaving the deeper core areas relatively sparsely supplied with such cells (Fig. 4). The transplant-associated TH-positive fiber outgrowth was dense in a 0.5-0.6 mm wide zone surrounding the graft, but the density of the terminal network declined sharply at greater distances from the graft-host border (Fig. 3A). The anterior-most portion of the caudate-putamen

(Fig. 3A), as well as the nc. accumbens (Fig. 5C) had no or very few TH-positive fibers.

The Micrografts were implanted as three 0.2 µl deposits along each of the six needle tracts, giving the same total injected graft volume (3.6 µl) and number of implanted cells as in the Macro graft group. Similar to the Macro grafts the deposits had fused to form single elongated tissue strands along each needle tract, approx. 0.3-0.5 mm wide and 1.5-2 mm long (Fig. 2B). In addition, the grafts at the three rostral needle tracts had grown to merge with the grafts at each of the three posterior tracts. Since the rostral and the caudal grafts of each pair could not be readily distinguished in the coronal sections, the medial, intermediate and lateral grafts were combined in the morphometric analysis (Table 2). Each of these three subportions (corresponding to six 0.2 µl deposits) had a mean volume ranging between 0.55 and 0.69 mm^3. The total graft volume (the three subportions combined) reached an average of 1.83 mm^3 (range: 1.27-2.63). The mean total cell number of surviving TH-positive neurons was 5608 (range: 4246-7272), which is almost 3-fold greater than that obtained in the Macro graft group ($p<0.005$; ANOVA with post-hoc Fisher PLSD test). The density of TH-positive cells in the Micro grafts (3151 TH-positive cells/mm^3) was also significantly higher (+65%) than in the Macro grafts ($p<0.05$, ANOVA with post-hoc Fisher PLSD test). Similar to the Macro grafts, the TH-positive neurons tended to be clustered in the periphery of each implant. However, the cell-sparse core area was overall smaller and less pronouced (Fig. 3). The graft-host border was less distinct in the Micro grafts and the peripherally

located TH-positive neurons appeared to be more closely integrated with the surronding host striatal tissue.

In the Micro grafts the TH-positive fiber outgrowth was more pronounced around each of the subtransplants compared to the Macro grafts (Figs. 3B, 5A). As a result, the entire head of the caudate-putamen was supplied with a dense TH-positive terminal network (Fig. 3B), and the graft-derived fibers were seen to extend also into the nc. accumbens and parts of the underlying olfactory tubercle (Fig. 5).

Table 2: Number of TH+ cells, graft volumes, and density of TH+ cells

	Micro grafts				Macro grafts	Micro/ Macro ratio
	medial part	*intermediate part*	*lateral part*	total		
No. of TH+cells	2032±280	1823±197	1753±175	5608±624*	1996±36	2.81
Graft volume(mm3)	0.693±0,15	0.55±0,086	0.585±0,074	1.83±0,3*	1.064±0,076	1.72
TH+ cell density per mm3	2932	3315	2997	3151*	1914	1.65

Each value represents the mean ± S.E.M. of four animals.

* indicates significant difference between Micro and Macro graft groups; $p<0.05$, ANOVA with post hoc Fisher PLSD test

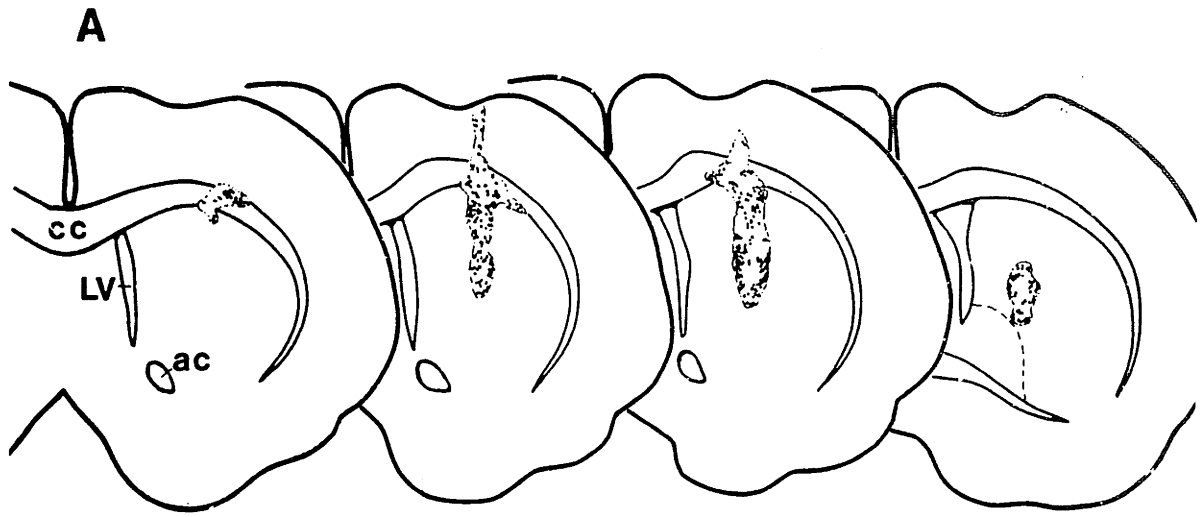
A
cc
LV
ac

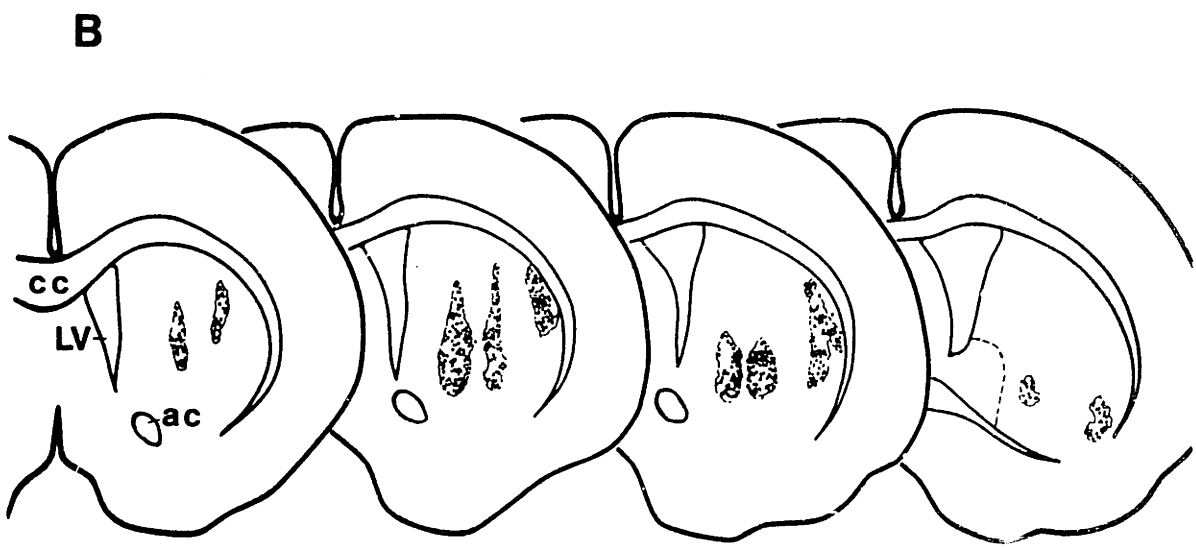
B
cc
LV
ac

Fig. 2. Camera lucida drawings of intrastriatal nigral Macro (A) and Micro (B) grafts at four representative rostro-caudal levels through the host striatum. Dots represent the distribution of implanted TH-positive cells within the transplants. LV, lateral ventricle; ac, anterior commissure; cc, corpus callosum.

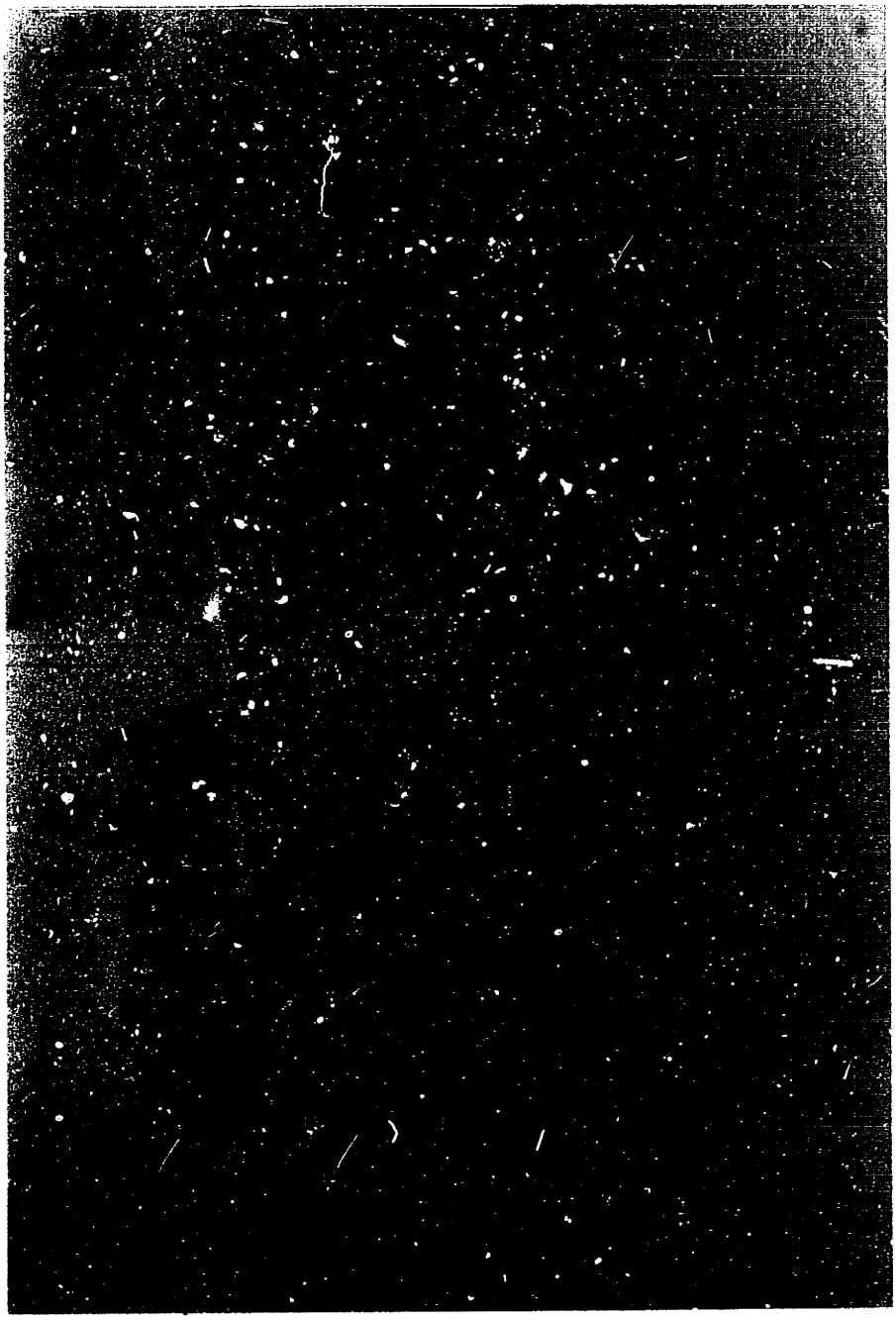

Fig. 3. TH immunostained sections illustrating the 6-OHDA denervated caudate-putamen 4 months after Macro (A) or Micro (B) grafting of a nigral cell suspension. The photomicrographs are from sections passing through the anterior graft-host border. Note the difference in intensity and extent of the TH positive fiber network around the Macro and the Micro grafts. LV, lateral ventricle. Scale bar = 400 μm.


A
C

Fig. 4. Details of the Macro grafts (A), where surviving DA neurons are preferentially located in clusters at the periphery of the implants and the core is relatively free of DA neurons. In contrast, the DA neurons in the Micro grafts (B, C) were more evenly distributed throughout the graft tissue, and the cell-sparse core areas were smaller and less prominent than in the Macro grafts. D (Nomarski optics) illustrates, in a section passing tangentially through the periphery of a Micro graft, the close integration of the TH positive graft neurons with the fiber bundles and the neuropil of the surrounding host striatum. Scale bars = 100 μm (A, B); 50 μm (C, D).


ac
Acb
Tu
C

Fig. 5. Darkfield photomicrographs illustrating the extensive TH positive fiber outgrowth from a Micro graft into the area of the caudate-putamen surrounding the implants (A). The TH positive fiber outgrowth derived from the Micro grafts extended ventrally also into the nc. accumbens and the olfactory tubercle (B), i.e., into areas that remained essentially free of TH positive fibers in the animals with Macro grafts (C). Acb, nc. accumbens; ac, anterior commissure; Tu, olfactory tubercle. Scale bars = 100 μm (A); 200 μm (B, C).

Biochemistry

In the lesion-only rats DA levels were reduced ipsilateral to the lesion by over 99% throughout the caudate-putamen and the nc. accumbens, and by 94% in the anteromedial frontal cortex (Table 3). Consistent with previous data [22] the 6-OHDA-lesion produced marked reductions also in NA (Table 4). In the Macro graft group striatal DA levels were increased to 10-15% of normal, but neither nc. accumbens nor frontal cortex were significantly affected. The NA levels were also unaffected. DA recovery in the Micro graft group amounted to 25-35% of normal in the head of the caudate-putamen (medial and lateral parts), and there was also a significant, though smaller, recovery in the nc. accumbens (to 4.5% of normal) and frontal cortex (to 28% of normal) (Table 3). In both the medial and the lateral caudate-putamen the DA levels in the Micro graft group were significantly higher (2.3-2.6 fold) than in the Macro graft group ($p<0.01$, ANOVA with post-hoc Fisher PLSD test). Significant graft-induced recovery in NA levels were observed in the caudate-putamen (to between 20-75% of normal) and to a minor extent in the frontal cortex (5.9%) (Table 4).

Table 3: Regional dopamine levels (pmol/mg wet weight) in 6-OHDA lesioned and intrastriatally nigra-grafted brains

	Lesion only			Macro grafts			Micro grafts			Micro/ Macro
	contralat. side	ipsilat. side	% of normal	contralat. side	ipsilat. side	% of normal	contralat. side	ipsilat. side	% of normal	ratio (ipsilateral side)
Frontal cortex	0.26 (±0.04)	0.02 (±0.01)	6	0.36 (±0.05)	0.08 (±0.02)	22	0.45 (±0.11)	0.13+ (±0.04)	28	1.62
Nc. accumbens	12.17 (±3.08)	0.11 (±36)	0.9	20.07 (±4.67)	0.36 (±0.12)	1.8	10.46 (±2.77)	0.47+ (±0.16)	4.5	1.29
Caudate-putamen:										
medial	39.78 (±4.21)	0.35 (±0.29)	0.9	42.38 (±1.1)	6.45+ (±1.68)	15.2	42.08 (±0.89)	14.89+* (±2.49)	35.4	2.3
lateral	40.85 (±2.76)	0.02 (±0.02)	0.04	50.70+ (±2.97)	5.07 (±3.3)	10	51.33+ (±2.49)	12.95+ * (±2.40)	25.2	2.6
caudal	46.93 (±2.12)	0.26 (±0.07)	0.5	48.65 (±2.01)	5.09 (±2.83)	10.5	47.23 (±3.96)	3.20 (±1.09)	6.8	0.63

Each value represents the mean ± S.E.M. of six animals.

* indicates significant difference between Micro and Macro graft groups; $p<0.05$, ANOVA with post hoc Fisher PLSD test

+ indicates significant difference from lesion-only group; $p<0.05$, ANOVA with post hoc Fisher PLSD test

Table 4: Regional noradrenaline levels (pmol/mg wet weight) in 6-OHDA lesioned and intrastriatally nigra-grafted brains

	Lesion only			Macro grafts			Micro grafts			Micro/ Macro
	contralat. side	ipsilat. side	% of normal	contralat. side	ipsilat. side	% of normal	contralat. side	ipsilat. side	% of normal	ratio (ipsilateral side)
Frontal cortex	1.29 (±0.12)	0.03 (±0.01)	2.6	1.62 (±0.14)	0.06 (±0.01)	3.5	1.83+ (±0.22)	0.11+* (±0.01)	5.9	1.88
Nc. accumbens	1.88 (±0.22)	0.12 (±0.02)	6.5	1.61 (±0.21)	0.24 (±0.06)	15.2	2.25 (±0.18)	0.28 (±0.08)	12.3	1.14
Caudate-putamen:										
medial	0.47 (±0.17)	0.08 (±0.02)	17.7	0.40 (±0.08)	0.09 (±0.03)	21.1	0.37 (±0.04)	0.29+* (±0.05)	74.6	3.46
lateral	0.44 (±0.06)	0.02 (±0.01)	5	0.45 (±0.06)	0.03 (±0.01)	6.5	0.36 (±0.02)	0.11+* (±0.03)	30.2	3.72
caudal	0.39 (±0.04)	0.03 (±0.01)	7.8	0.47 (±0.04)	0.05 (±0.01)	11.1	0.44 (±0.05)	0.09+* (±0.01)	20.6	1.75

Each value represents the mean ± S.E.M. of six animals.

* indicates significant difference between Micro and Macro graft groups; $p<0.05$, ANOVA with post hoc Fisher PLSD test

+ indicates significant difference from lesion-only group; $p<0.05$, ANOVA with post hoc Fisher PLSD test

DISCUSSION

The results of the present study show that distribution of the intrastriatal nigral graft tissue over larger numbers of implantation sites (18 versus 2 deposits) promotes overall graft survival and growth as seen in terms of graft volume, DA neuron cell numbers, DA fiber outgrowth, and striatal DA levels. The study was designed such that the same amount of graft tissue (a total of about 450.000 cells in 3.6 µl corresponding to the amount of cells obtained from approx. one fetal ventral mesencephalon piece), was implanted into two experimental groups. In the Macro graft group two deposits were placed along a single injection tract, using the standard needle (OD 500 µm), which is similar to the nigral suspension grafts described in our previous biochemical[22] or quantitative immunohistochemical and autoradiographic studies.[9] In the Micro graft group the technique used for implantation of the tissue was modified in two ways: First, three small (200 nl) graft deposits were distributed over each of six different needle tracts in the same area of the head of the caudate-putamen. Second, a thin glass capillary (OD 50 µm) was used for the Micro graft implantation. A modified cell suspension procedure, in which the fetal tissue pieces were dissociated in a larger volume, in the presence of DNase, was used in order to obtain a complete single-cell suspension (necessary when using the thin capillaries for implantation).This procedure also allows for more precise determination of numbers of cells implanted at each site, and hence for more reproducible graft sizes.

Overall graft survial

In the Micro graft group there was a significant 72% increase in total graft volume when compared to the grafts in the Macro group. This fact is interesting in the context of the diversity of cell types included in the grafted mesencephalic cell suspension. The DA neurons constitue only a few percent (estimated at 8-10% in smear preparation by Nikkhah et al.[17]), the rest representing a mixture of non-dopaminergic types of neurons and glial precusors contained in the ventral mesencephalon. The increase in total graft size thus cannot be accounted for exclusively on basis of increased DA cell number, but must be due to an improved overall graft survival. This effect may be attributable to any one, or a combination, of several features inherent in the microtransplantation technique. Reducing the graft size of a single deposit 9-fold, and the scaling-down of the size of the tip of the implantation instrument 10-fold, is likely to reduce bleeding and necrosis as well as the acute traumatic reaction of the surrounding host brain tissue. In fact, in a recent study Emmett et al. [11] have reported that bleeding and necrosis associated with small deposits of astrocytes (1000 cells in 100 nl) implanted into the hippocampus, were substantially reduced when a thin glass capillary was used. This most likely results in less macrophage invasion and reactive gliosis, and promotes diffusion of nutrients and early vascularization of the transplant from host blood vessel. Improved local conditions at the implantation site may be particularly important during the initial phase of graft survival, when the fetal cells are recovering from the dissociation procedure, are in a state of proliferation and rapid growth,[2] and lacking a direct

blood supply. That the development and extent of graft vascularization is important for the growth of nigral transplants is supported by the results obtained by Finger et al.[12] In that study, treatment with nimodipine, a calcium channel antagonist which dilates cerebral blood vessels and thus increases blood flow, was seen to increase the density of graft vascularization associated with a 2-fold increase in graft volume. The effect was most prominent under suboptimal grafting conditions (i.e. older donor tissue or prolonged storage of the tissue before grafting).

DA neuron survival and growth

The total number of surviving TH-positive neurons was almost 3-fold greater in the distributed Micro grafts than in the Macro grafts. Similarly, striatal DA levels were about 2.5-fold greater in the Micro grafts compared to the Macro graft group. The effect on the total graft volume (+72%) was less than half of the increase seen in TH-positive cell number. This indicates that the Micro graft procedure was particularly beneficial for DA neuron survival. With the current procedure each row of Micro grafts (3 deposits of 0.2 µl along a needle tract, equivalent to a total of 75.000 implanted cells) gave as many surviving TH-positive neurons as one of the 1.8 µl Macro graft deposits (equivalent to 225.000 cells). Consistent with previous observations [10, 22] these data indicate that the efficacy of intrastriatal nigral grafts does not increase linearly with the amount of cells (or volume of cell suspension) implanted at a single site. In the present Micro grafts the yield of surviving DA neurons was about 1.2 DA neuron per 100 cells implanted, which should be compared to

a yield of about 0.4 surviving DA neurons per 100 cells implanted obtained in the Macro graft procedure. Based on the estimation that each mesencephalic tissue piece contains a total of about 30,000 - 40,000 DA neurons[5] this represents a survival rate for the grafted DA neurons in the range of 15 - 20% in the Micro grafts, as compared to 5 - 10 % seen in the present Macro grafts as well as in earlier quantitative studies using the standard cell suspension procedure.[6]

A possible mechanism underlying the graft-volume effect is suggested by the difference in microscopic appearance of the Micro and the Macro grafts. As reported earlier in the standard type of Macro grafts[10, 15] most surviving TH-positive neurons are localized at the graft-host border in the periphery of the graft tissue mass, and only scattered TH-positive cells occur in the central core region. With single, small-sized graft deposits (in the range of 15-30 x 10^3 cells injected) this cell-sparse core is almost absent and TH-positive cell density is more even throughout the graft (Nikkhah et al., in preparation). In the present Micro grafts the individual deposits had fused to form larger aggregates of about 0.5 mm^3 in size. Although the TH-positive neurons tended to be more numerous in the periphery also in these aggregates, the cell-sparse core areas were overall clearly smaller and less prominent. This suggests that the conditions for DA neuron survival is favored by close contact with the surrounding host tissue (eg, by more rapid vascularization and/or access to striatum-derived trophic factors). The wide-spread distribution of the implanted cells obtained in the Micro grafts would undoubtedly favor such close graft-host interaction. This hypothesis is consistent with previous in vitro studies,[7,8, 21, 23] in which the

addition of striatal extracts or membrane preparations to mesencephalic cell cultures specifically promoted survival and/or maturation of the cultured DA neurons. More recently, O'Malley et al. [19] have reported that mesencephalic cell grown on top of a support cell monolayer derived from striatal tissue show a 3.5-fold increase in TH cell numbers after 7 days in vitro. This effect, which was similar in magnitude to that seen in the present study, seemed to be due to a prevention of TH cell loss rather than to an increased proliferation of the cultured TH cells.

Improved graft-host interaction may also explain the overall greater TH-positive fiber outgrowth (and increased striatal DA levels) obtained in the Micro graft procedure. Although dense graft-derived fiber outgrowth occurred around both the Micro and the Macro graft deposits, the overall fiber outgrowth was more extensive in the Micro graft group. This was particularly evident in the rostral aspect of the caudate-putamen and the nc. accumbens area which were more densly innervated by the more dispersed Micro graft deposits. This is consistent with the biochemical data showing a significant recovery of DA in the nc accumbens and the frontal cortex in the Micro graft, but not the Macro graft group. In addition there were significant increases in NA levels in the Micro graft group. This effect, which has been reported earlier in biochemical studies of standard type grafts,[22] was most probably due to the inclusion of low numbers of noradrenergic neurons in the fetal mesencephalic dissection.

Previous in vitro studies provide support for the idea that striatal tissue can exert a direct growth stimulatory effect on fetal

mesencephalic DA neurons. In mixed aggregate cultures[14] and in postnatal nigral and striatal organotypic slice cocultures,[20] the appropiate target tissue, striatum, has been observed to exert a stronger stimulus for TH-positive fiber outgrowth from nigral DA neurons than different types of non-target tissue (cortex, hippocampus or cerebellum).

Observations on fiber outgrowth from fetal nigral transplants in adult rats[4, 10] have indicated that also the mature striatal target tissue may exert a stimulatory effect on DA fiber outgrowth, and that this effect is particularly pronounced if the target is dennervated of its intrinsic dopaminergic afferent input.[10]

CONCLUSIONS

The present results show that wider distribution of fetal nigral tissue in the DA denervated striatum, combined with a microtransplantation approach which minimizes the implantation trauma and maximizes the opportunities for graft-host interactions, is an effective means to increase DA neuron survival and to achieve more complete graft-derived reinnervation and recovery of DA levels throughout larger areas of the host striatal complex. The behavioural analysis of the present animals, reported elsewhere,[18] shows that the improved DA neuron survival and growth obtained in the microtransplant procedure is associated with a more extensive functional recovery of spontaneous sensorimotor behaviour, such as skilled paw-reaching and complex sensorimotor orienting responses.

The present microtransplantation technique should be particulary useful for studies in adult recipients where the nigral grafts are implanted into small target areas, such as the substantia nigra itself, as well as for studies on nigral grafts in neonatal hosts. Studies along these lines are now in progress.

REFERENCES

1 Abercrombie M. (1946) Estimation of nuclear population from microtome sections. *Anat. Rec.* **94,** 239-247.

2 Abrous N., Guy J., Vigny A., Calas A., Le M. M. and Herman J. P. (1988) Development of intracerebral dopaminergic grafts: A course and environmental influences. *J. Comp. Neurol.* **273,** 26-41.

3 Björklund A., Stenevi U., Schmidt R. H., Dunnett S. B. and Gage F. H. (1983) Intracerebral grafting of neuronal cell suspensions. I. Introduction and general methods of preparation. *Acta Physiol. Scand.* **522,** 1-7.

4 Björklund A., Stenevi U., Schmidt R. H., Dunnett S. B. and Gage F. H. (1983) Intracerebral grafting of neuronal cell suspensions. II. Survival and growth of nigral cell suspensions implanted in different brain sites. *Acta Physiol Scand* **522,** 9-18.

5 Björklund A. and Lindvall O. (1986) Catecholaminergic brain stem regulatory systems. In *Handbook of physiology: The nervous system. Intrinsic regulatory systems in the brain* (ed. Bloom F. E.), Vol. **4,** pp. 155-235. American Physiological Society, Bethesda.

6 Brundin P. and Björklund A. (1987) Survival, growth and function of dopaminergic neurons grafted to the brain. In *Neural regeneration. Progress in Brain Research* (ed. Seil F. J., Herbet E. and Carlson B. M.), Vol. **71,** pp. 293-308. Elsevier, Amsterdam.

7 Carvey P. M., Ptak L. R., Lo E. S., Lin D., Buhrfiend C. M., Goetz C. G. and Klawans H. L. (1991) Levodopa reduces the growth promoting effects of striatal extracts on rostral mesencephalic tegmentum cultures. *Exp. Neurol.* **114,** 28-34.

8 Dal Toso R., Giorgi O., Soranzo C., Kirschner G., Ferrari G., Favaron M., Benvegnu D., Presti D., Vicini S., Toffano G., Azzone G. F. and Leon A. (1988) Development and survival of neurons in dissociated fetal mesencephalic serum-free cell cultures: I. Effects of cell density and of an adult mammalian striatal-derived neuronotrophic factor (SDNF). *J. Neurosci.* **8,** 733-745.

9 Doucet G., Brundin P., Seth S., Murata Y., Strecker R. E., Triarhou L. C., Ghetti B. and Björklund A. (1989) Degeneration and graft-induced restoration of dopamine innervation in the weaver mouse neostriatum: A quantitative radioautographic study of [(3)H]dopamine uptake. *Exp. Brain Res.* **77,** 552-568.

10 Doucet G., Brundin P., Descarries L. and Björklund A. (1990) Effect of prior dopamine denervation on survival and fiber outgrowth from intrastriatal fetal mesencephalic grafts. *Eur. J. Neurosci.* **2,** 279-290.

11 Emmett C. J., Jaques B. W. and Seeley P. J. (1990) Micro-transplantation of neural cells into adult rat brain. *Neuroscience* **38,** 213-222.

12 Finger S. and Dunnett S. B. (1989) Nimodipine enhances growth and vascularization of neural grafts. *Exp. Neurol.* **104,** 1-9.

13 Gundersen H. J. G., Bendtsen T. F., Korbo L., Marcussen N., Moller A., Nielsen K., Nyengaard J. R., Pakkenberg B., Sorensen S. B., Vesterby A. and West M. J. (1988) Some new, simple, and

efficient stereological methods and their use in pathological research and diagnosis. *Acta Path., Microbiol. Immunol. Scandinavia* **96,** 379-394.

14 Hemmendinger L. M., Garber B. B., Hoffmann P. C. and Heller A. (1981) Target neuron-specific process formation by embryonic mesencephalic dopamine neurons in vitro. *PNAS* **78,** 1264-1268.

15 Herman J. P., Choulli K., Geffard M., Nadaud D., Taghzouti K. and LeMoal M. (1986) Reinnervation of the nucleus accumbens and frontal cortex of the rat by dopaminergic grafts and effects on hoarding behavior. *Brain Res.* **372,** 210-216.

16 Mayhew T. M. (1992) A review of recent advances in stereology for quantifying neural structure. *J. Neurocytol.* **21,** 313-328.

17 Nikkhah G., Odin P., Smits A., Tingström A., Othberg A., Brundin P., Funa K. and Lindvall O. (1993) Platelet-derived growth factor promotes survival of rat and human mesencephalic dopaminergic neurons in culture. *Exp. Brain Res.* **92,** 516-523.

18 Nikkhah G., Duan W.-M., Knappe U., Jödicke A. and Björklund A. (1993) Restoration of complex sensorimotor behavior and skilled forelimb use by a modified nigral cell suspension transplantation approach in the rat Parkinson model. *Neuroscience* **in press.**

19 O'Malley E., Black I. and Dreyfus C. (1991) Local support cells promote survival of substantia nigra dopaminergic neurons in culture. *Exp. Neurol.* **112,** 40-48.

20 Ostergaard K., Schou J. P. and Zimmer J. (1990) Rat ventral mes-encephalon grown as organotypic slice cultures and co-cultured with striatum, hippocampus, and cerebellum. *Exp. Brain Res.* **82,** 547-565.

21 Prochiantz A., Daguet M., Herbet A. and Glowinski J. (1981) Specific stimulation of in vitro maturation of mesencephalic dopaminergic neurons by striatal membranes. *Nature* **293,** 570-572.

22 Schmidt R. H., Björklund A., Stenevi U., Dunnett S. B. and Gage F. H. (1983) Intracerebral grafting of neuronal cell suspensions. III. Activity of intrastriatal nigral suspension implants as assessed by measurements of dopamine synthesis and metabolism. *Acta Physiol. Scand.* **522,** 19-28.

23 Tomozawa Y. and Appel S. H. (1986) Soluble striatal extracts enhance development of mesencephalic dopaminergic neurons in vitro. *Brain Res.* **399,** 111-124.

24 Ungerstedt U. and Arbuthnott G. (1970) Quantitative recording of rotational behavior in rats after 6-hydroxy-dopamine lesions of the nigrostriatal dopamine system. *Brain Res.* **24,** 485-493.

TRANSPLANTATION STRATEGIES FOR THE ANALYSIS OF BRAIN DEVELOPMENT AND REPAIR

PART II

THE CHARACTERIZATION OF AN IMMORTALIZED CELL LINE

CHAPTER 5

REGION-SPECIFIC DIFFERENTIATION OF THE HIPPOCAMPAL STEM CELL LINE HIB5 UPON IMPLANTATION INTO THE DEVELOPING MAMMALIAN BRAIN

Summary

Proliferating precursors to the distinct cell types comprising the mammalian brain can be identified by the presence of the nestin intermediate filament. We report the establishment of a nestin-positive cell line, HiB5, from embryonic precursor cells to the rat hippocampus. Since it was immortalized using the temperature-sensitive allele *tsA58* of SV40 T-antigen, these cells grow continuously at 33°C, but not at 39°C, the body temperature of rodents. To test the developmental capacity of HiB5 cells, they were implanted into both the neonatal hippocampus and cerebellum. The cells integrated into the host tissue and acquired morphologies characteristic of the neurons and glial cells found at the implant site. HiB5 cells might thus be useful in characterizing the signals regulating cell type determination in the mammalian brain.

This chapter was adapted from the manuscript authored by Patricia J. Renfranz, Miles G. Cunningham, and Ronald D. G. McKay appearing in **Cell**, Vol. 66, pp. 713-729 (1991).

Introduction

The adult mammalian brain comprises many functionally distinct neuronal types. Fate mapping has shown that multipotential stem cells give rise to different neuronal types (Turner and Cepko, 1987; Gray et al., 1988; Holt et al., 1988; Price and Thurlow, 1988; Wetts and Fraser, 1988; Temple, 1989; Galileo et al., 1990; Turner et al., 1990). The commitment to a specific fate occurs close to the last cell division, prior to the migration of a cell away from the mitotic zone (McConnell, 1988). Autoradiographic studies (Altman, 1963; Altman and Das, 1965; Angevine, 1965; Altman, 1972a,b,c; Rakic, 1974; Schlessinger et al., 1975; Schlessinger et al., 1978; Bayer, 1980; Altman and Bayer, 1990) have shown that distinct types of neurons become post-mitotic at different times in embryonic life, suggesting that stem cells respond to local, temporally controlled signals to produce successive waves of neurons committed to different fates. A young post-mitotic neuron then migrates to its appropriate site in the brain, where the axon and dendrites are formed, giving the neuron a distinctive morphology and function. This differentiation process determines both the number and types of neurons and glial cells found in the adult brain. Thus, the mechanisms by which multipotential precursors become committed to particular fates are of great interest.

To understand these mechanisms, it is important to be able to define at the cellular level the transition from stem cell to young neuron. Cells in either state can be defined by the characteristic set

of gene products expressed. For example, the proliferating stem cells express a distinct intermediate filament protein, nestin (Hockfield and McKay, 1985; Frederiksen and McKay, 1988; Lendahl et al., 1990; Cattaneo and McKay, 1990), whereas neurons express a set of neurofilaments (Yen and Fields, 1982; Kaplan et al., 1990), and many glial cells express glial fibrillary acidic protein (Yen and Fields, 1982). The regulated expression of these genes can be observed in primary cultures of cells from different embryonic brain regions where nestin-positive cells proliferate and generate daughter cells that can differentiate into neurons or glial cells (Cattaneo and McKay, 1990; P.R. and R.M., unpublished). Although primary cultures of neuroepithelial stem cells have many advantages, they have two disadvantages: Firstly, it is difficult to obtain large numbers of cells, limiting biochemical analysis, and secondly, genetic manipulations, which will be crucial in dissecting the mechanisms involved, are difficult to carry out in primary cells. In principle, immortalized cell lines offer a solution to these technical difficulties (reviewed in Cepko, 1988, 1989, and Lendahl and McKay, 1990).

In this paper, we report an extensive series of implant studies with a conditionally immortalized, nestin-positive cell line derived from the embryonic rat brain. This cell line, HiB5, was derived from a primary culture of embryonic day 16 (E16) rat hippocampus. Embryonic day 16 coincides with the beginning of a wave of neurogenesis in the hippocampus that extends into early postnatal life (Altman, 1963; Altman and Das, 1965; Angevine, 1965; Schlessinger et al., 1978; Bayer, 1980). Postnatal neurogenesis occurs

in the hippocampal region, predominantly in a subregion called the dentate gyrus (Altman and Das, 1965; Angevine, 1965; Schlessinger et al., 1975; Altman and Bayer, 1990). HiB5 cells can thus be placed back into the hippocampus while neurogenesis is still occurring. Since neurogenesis also continues in the rat cerebellum during the first postnatal week (Altman, 1972a, b, c), this region was also chosen as an implant site. In addition to the immortalization strategy, the key technical features of these experiments include a stereotaxic implantation procedure for neonatal rats and the use of multiple labelling procedures for identification of immortalized cells in the host brain. These labelling methods indicate that conditionally immortalized HiB5 cells integrate into the host tissue, where their proliferation is controlled. Moreover, the morphologies of these cells suggests that they differentiate into neuronal and glial types appropriate to the location and developmental stage of the implant site.

Experimental Procedures

Animals and Cell Lines

Timed-pregnant (E16) Sprague Dawley or Fischer rats were purchased from Taconic, Inc. Psi2 cells transducing the *tsA58/U19* Large T-antigen (T-antigen) vector (gift of G. Almazan), as well as all derived cell lines, were grown in Dulbecco's Modified Eagle's medium (DMEM, Gibco), supplemented with 0.11 g/L NaPyruvate, 3.7 g/L $NaHCO_3$, 0.29 g/L glutamine, 3.9 g/L Hepes, penicillin, streptomycin,

and 10% (v/v) fetal calf serum (hereafter referred to as DMEM + 10% FCS). All cell lines were grown on tissue culture plasticware; for all derived cell lines, the dishes were also precoated for at least 30' with 15 mg/ml polyornithine (Sigma). Prior to using the plates, the polyornithine was aspirated, and the plates rinsed at least 2 times with phosphate-buffered saline (PBS; 8 g/L NaCl, 0.2 g/L KCl, 1.15 g/L Na_2HPO_4, 0.2 g/L KH_2PO_4).

Primary Cultures and Establishment of Cell Lines

Immortalized cell lines from the hippocampus were isolated from three separate primary cultures and infection paradigms, two from Sprague Dawley and one from Fischer rat strains. The HiB5 cell line was established from the Sprague Dawley strain. The general procedure was as follows: Timed-pregnant females were sacrificed by decapitation, and the E16 fetuses removed into ice-cold calcium- and magnesium-free Hanks' Balanced Salt Solution (CMF-HBSS) (Gibco), supplemented with 15 mM Hepes. Hippocampal anlagen, as described by Banker and Cowan (1977), were dissected from the fetal brain, and the choroid plexus and most of the meninges were removed. The cells were dispersed by a 10' incubation in 0.04% trypsin in CMF-HBSS, and, following the addition of DMEM + 10% FCS, gently triturated. The cell suspension was plated onto coated tissue culture dishes, at concentrations of 50,000 to 200,000 cells/cm^2, and incubated at 33 ^oC. Experiments not discussed here showed that these cells were capable of proliferating, and then differentiating into neurons and glial cells.

The following day, the primary hippocampal cells were infected for two hours with filtered conditioned medium from psi2 cells packaging the retrovirus encoding *tsA58/U19* T-antigen and neomycin resistance (F4 subclone), to which had been added 8 mg/ml polybrene. After infection, the virus-containing medium was replaced with fresh DMEM + 10% FCS, and the cells were placed at 33 ^{o}C, the permissive temperature of the oncogene. One to two days later, some of the cultures were passaged, and all were fed with complete medium along with the selective agent, neomycin analog G418 (Geneticin, Gibco) at 200 mg/ml. The selective medium was replaced every four days. Within three weeks, G418-resistant colonies were observed. Colonies were picked using cloning rings, and expanded into 96-well plates. The clones were subsequently grown at 33 ^{o}C in DMEM + 10% FCS, and expanded up through several 10 cm plates, whereupon they were cryopreserved. From a total of 14.5 x 10^{6} primary cells infected, 48 "Hi" clones were selected, a frequency of 3.3 x 10^{-4}%. "Hi" indicates hippocampal derivation and also provides a cheerful greeting each day. The letter following "Hi" designates the plate from which the colony was picked, and the following number indicates the colony per se.

Most all of these clones grow slowly (approximately 48 hr doubling time), and growth in all but one line is contact inhibited. Subsequent tests on a large subset of established cell lines included the following: examination of the cells at 33 ^{o}C and at 39 ^{o}C, in both serum-containing and various defined media, followed by an immunohistochemical detection for the expression of a variety of

antigens, including nestin, neurofilament, and glial fibrillary acidic protein. Under the culture conditions used, the growth and differentiation of primary cultures could be supported. The HiB5 cell line was selected for further study because it fell into a class of lines that reflect properties of primary hippocampal precursor cells in vitro (data not shown). Among the properties are the following: a morphologically heterogeneous cell population that is immunopositive for nestin, changes morphology (in the lines, at 39 ^{o}C), and appears responsive to basic fibroblast growth factor (in the lines, at both temperatures). Details of these results and those from other cell lines will not be described here.

Immunohistochemistry

HiB5 cells were grown at 33 ^{o}C to ~70% confluence on 12 mm glass coverslips. Cells were fixed 15' in 4% paraformaldehyde in 0.1 M phosphate buffer, pH 7.4, followed by two rinses in PBS, pH 7.4. After blocking and permeabilizing the cell for 15' in 5% goat serum, 0.2% triton X-100 in PBS, the cells were stained for the presence of the nestin protein by a 2 hr incubation at room temperature in monoclonal antibody Rat401 with 0.1% triton X-100. Coverslips were rinsed 3 times in PBS, then incubated for 60' in goat anti-mouse IgG coupled to horseradish peroxidase (Biorad), diluted 1:100 in 3% goat serum, 0.1% triton X-100 in PBS. The cells were rinsed four times in PBS, then the immune complex was visualized by a 10' reaction in 0.1 mg/ml diaminobenzidine (Sigma), 0.01% hydrogen peroxide in PBS. Reacted coverslips were mounted in Immunomount (Shandon).

Isolation of HiB5 Subclones Expressing the Bacterial *LacZ* Gene

HiB5 cells were infected with the BAG retrovirus (Price et al., 1987) (Subclone 7, gift of Xandra Breakefield), by incubating the cells at 33 °C with filtered producer cell conditioned medium (in this series of infections, the inclusion of polybrene did not seem to increase the infection frequency). Cells were infected over a total of two weeks, with multiple medium changes daily. Also, the virus-containing medium was supplemented with fresh medium, to counteract adverse effects of growing HiB5 cells in depleted medium. The cells were passaged during the infection period. Despite a high titer of retrovirus, as seen after infection of a more rapidly growing cell line, only 5-10% of the cells successfully incorporated the vector, as visualized with X-gal histochemistry (see below).

To increase the probability of obtaining *lacZ*-positive subclones, a population of infected cells was subjected to the FACS-FDG procedure of Nolan et al. (1988). The cells were harvested by trypsinization from ~70% confluent plates. Approximately 1.5 x 10^6 cells at a concentration of 10^7 cells/ml of medium were aliquoted into a polystyrene tube. A 200 mM stock of fluorescein-di-b-D-galactopyranoside (FDG, Molecular Probes) in 1:1 H_2O:DMSO was diluted 100-fold into H_2O. Both this stock and the cells were warmed for 10' to 37 °C. The cells were then diluted 1:1 with 2 mM FDG, and incubated 1' at 37 °C. The hypotonic loading of FDG was stopped upon the addition of 3 ml of ice-cold DMEM + 10% FCS. The cells were kept on ice for the remainder of the procedure in order to

lessen the leakage of the free fluorescein out of positive cells. The cells were briefly pelleted, and resuspended in DMEM + 10% FCS to a concentration of 5 x 10^6 cells/ml. All cells were then stained with propidium iodide.

This cell population was then subjected to fluorescence-activated cell sorting (MIT Center for Cancer Research), and fluorescein-positive cells, about 2% of the total population, were collected onto a 35 mm tissue culture dish. The cells adhered in one area of the dish, so they were dispersed, then expanded and cryopreserved. This population is called HiB5B, for Blue.

The HiB5B cells were plated at various dilutions (18 - 28 cells/cm^2) and grown for about three weeks at 33 ^oC. The cells were fed every four to six days with 1:1 fresh medium: HiB5B-conditioned medium. (The addition of conditioned medium greatly enhanced the viability of the cells at this low of a cell concentration.) At this time, FDG-visualization of b-galactosidase activity was repeated *in situ* on the colonies as above, except that the hypotonic loading occured for 2' at 39 ^oC, and the FDG-containing medium was replaced with complete medium at room temperature. Each colony was examined via epifluorescence microscopy on a Zeiss Axiovert. Although the signal was relatively weak, fluorescing colonies were readily differentiated from non-fluorescing ones; about 66% of the colonies were scored as positive, and about 58% of those were isolable from others. These colonies were subcloned and expanded much as the original Hi clones were; different subclones were designated by a number. These subclones were analyzed by X-gal histochemistry

(see below) at both the permissive and nonpermissive temperatures of the T-antigen, as well as for the stable maintenance of nestin expression throughout the subcloning procedure. Of the 41 subclones picked, all those tested retained nestin, but only 27 were found to deposit the X-gal reaction product at both temperatures, and eight of these were judged to warrant further analysis, among these the subclone HiB5B-27 used here.

Implants

Subjects

Implants were placed in two-day-old (P2) male and female Sprague Dawley rat pups. Each mother with her litter (8-12 pups) was housed in a clear plastic cage and maintained on a 12 hour light/12 hour dark schedule. Food and water were provided *ad libitum*. Sixteen litters were used in these studies. Animals usually received unilateral implants into both their right cerebellar hemisphere, their right hippocampus, and, less frequently, into their right cortex. The total number of implants for the various cell lines and conditions are depicted in Table 1.

Table 1. The Number of Implants by Cell Line and Label

Label	Site	Cell Type			
		HiB5	Dead HiB5	Rat2	HiA4
dil-C18-(3) and green beads	HP	26	9	15	6
	CB	31	14	15	4
[^{3}H]Thymidine	HP	17	4	4	6
	CB	17	4	4	4

CB, cerebellum; HP, hippocampus.

Cell Labelling

Cells were labelled with green fluorescent latex microspheres (green beads) (Lumafluor, Inc., NJ) in vitro for eight hours at 33 ^{o}C, using green bead stock solution diluted 1000-fold in DMEM + 10% FCS. The cells were then rinsed three times with sterile PBS, trypsinized, and replated, so as to eliminate any free beads. A 1 mg/ml stock of 1,1'-dioctadecyl-3,3,3',3'-tetramethylindocarbocyanine perchlorate [DiI-C_{18}-(3)] (Molecular Probes, Inc., OR) in 100% ethanol was diluted 1:200 in DMEM + 10% FCS. Eight hours after passaging, the bead-labelled cells were rinsed with PBS, then incubated in the DiI-C_{18}-(3) solution for 2 hr at room temperature in darkness. The DiI-C_{18}-(3) solution was aspirated, and excess dye removed with 3 rinses in PBS. The cells were returned to 33 ^{o}C in DMEM + 10% FCS for at least 2 hr before being prepared for implantation.

Tritiated-thymidine (^{3}H-thymidine; New England Nuclear, MA) labelling of cells was accomplished by incubating them with 0.2 mCi ^{3}H-thymidine/ml of DMEM + 10% FCS over one length of the cell cycle (approx. 48 hrs for HiB5 and 24 hr for Rat2 fibroblasts). The ^{3}H-thymidine-containing medium was replaced approximately every eight hours during this period.

Cell Implantation

After trypsinizing and pelleting the cells gently, the resulting pellet was rinsed once with 10 mls of CMF-HBSS to remove residual proteins and antimicrobial agents present in the DMEM + 10% FCS, and repelleted. This pellet was resuspended in CMF-HBSS at a

density of ~75,000 cells/ml, which was loaded into a glass pipette (ID 0.5 mm, OD 1.0 mm) with an 8 mm-long, gently tapering shank having a final internal tip diameter of 50 mm.

For these implants, a scaled-down stereotaxic device was designed to accomodate rodent neonates, allowing for accurate and reproducible implantation. This miniature stereotax consists of a muzzle for the pup's snout and rubber cushions that oppose each side of the animal's head; all three can be independently adjusted horizontally and vertically. The head can therefore be firmly fixed in a number of positions. The muzzle and the head cushion adjustments are mounted on a copper platform, under which is welded a copper tubing system for circulating 75% ethanol at 0 ^{o}C. This system permits prolonged hypothermic anesthesia.

P2 subjects were anesthetized by placing on ice for six minutes. Each animal was then aligned and fixed in the stereotaxic device. A midline incision was made over the cerebellum or the hippocampus; the skull surface was cleared of connective tissue and marked at the appropriate coordinates. Cerebellar implants were placed 1 mm lateral to midline, 1 mm caudal to the parietal-occipital fissure, and 0.6 mm below the dura. Hippocampal implants were placed 1.8 mm lateral to midline, 1.5 mm posterior to bregma, and 1.8 mm below the dura. In each case, a 1.0 mm diameter area of skull was removed using a low-speed drill equipped with a dental burr. The dura was reflected, and, using a manual microdrive, the pipette tip was slowly lowered perpendicular to the surface of the brain to the implant site. A Picospritzer (General Valve Corp.) was used to

pressure-inject 1 ml of cell suspension over 2', in 4 ms pulses at a pressure of 10 psi. The pipette was left in this position for one minute and then withdrawn over three minutes to minimize loss of cells from the injection site. Gel foam was placed in the skull cavity; the animal was sutured, revived on a warm heating pad, and returned to its mother.

After variable survival times (one to six weeks) animals were deeply anesthetized with ethyl ether, then transcardially perfused with 0.9% saline followed by 4% paraformaldehyde in 0.1 M phosphate buffer, pH 7.4. For HiB5B-27 transplants, the fixation used was 0.5 % glutaraldehyde, 2 mM MgCl2, 5 mM EGTA in 0.1 M Pipes buffer, pH 6.9 (see below). For fluorescent label observations, tissue was cut in 50-100 mm vibratome sections, examined, and photographed within 6-36 hr to minimize any dye dispersion that may occur upon processing.

All photographs were taken on a Zeiss Axiophot photomicroscope using 400 ASA Ektachrome film (Kodak). Selected slides were then converted to color print film.

Retrograde Filling

Three weeks after implanting ^{3}H-thymidine-labelled HiB5 cells into the cerebellum, the animal was sacrificed and 500 mm vibratome sections of the cerebellum were cut. Using a dissecting microscope, small crystals (approx. diameter 100 mm) of DiI-C18-(3) were embedded in the molecular layer at arbitrary points in each section. The tissue was then incubated at 39 ^{o}C for three to seven days in the

paraformaldehyde fixative. Progression of the dye was monitored visually by epifluorescence microscopy. When a field of granule cells became adequately filled, the fluorescent label was converted to a diaminobenzidine product, using the photoconversion technique of Sandell and Masland (1988). The tissue was then allowed to sink in 50% sucrose in 0.1 M phosphate buffer and cut in 10 mm cryostat sections. These sections were then processed using standard autoradiography methods (Rogers, 1967).

Animals implanted with ^{3}H-thymidine-labelled HiB5 cells into the hippocampus were allowed to reach a weight of 150 g (about 6 weeks) to maximize accuracy of Fluoro-Gold injections. Thirty nl of 10% Fluoro-Gold in H_2O was stereotaxically pressure-injected over one minute into the lateral aspect of CA3 in the dorsal hippocampus. The coordinates used for this site were empirically determined to be 3.1 mm posterior to bregma, 3.2 mm lateral to midline, 3.0 mm below dura, with a tooth bar setting of -2.4. After a survival time of 36 hours, the animal was sacrificed, 10 mm cryostat sections were cut, and then were processed using standard autoradiography methods.

Cell Killing Methods

Two methods were used to kill labelled cells for control implants. The first was through microwave fixation (Login and Dvorak, 1985). A cell suspension of known density was diluted 1:300 in CMF-HBSS, then microwaved at high power in a 750 watt conventional microwave oven for 8 sec. The suspension was then cooled for 1' on

ice. After five cycles, the suspension was centrifuged and resuspended to its original volume.

The second method was through diluting the suspension 1:300 in dH_2O, followed by five cycles of freeze-thaw, using a dry ice/ethanol bath and warm running water. After this treatment, the suspension was centrifuged and resuspended to its original volume before implantation as described.

LacZ Histochemistry

The histochemical reaction for *lacZ* b-galactosidase activity was visualized using 5-bromo-4-chloro-indoxyl-b-D-galactoside (X-gal, Bachem), following the procedure of Price and Thurlow (1988). Animals were perfused with 0.5% glutaraldehyde in 0.1 M Pipes buffer pH 6.9 with 2 mM $MgCl_2$ and 5 mM EGTA, then the cerebellum incubated for 18 hr at 4 ^oC in PBS with 2 mM $MgCl_2$ and 30% sucrose, embedded in OCT, and cryostat sectioned at 20 mm.

Sections were postfixed 10', rinsed twice in PBS with 2 mM $MgCl_2$, then incubated for 10' in fresh buffer, followed by a 10' incubation in detergent solution (2 mM $MgCl_2$, 0.01% NaDeoxycholate, and 0.02% N-P40 in PBS). These steps were performed at 4 ^oC. To visualize the enzyme activity, the tissue was incubated at 37 ^oC in the detergent buffer with 5 mM $K_3Fe(CN)_6$, 5 mM $K_4Fe(CN)_6 \cdot 3H_2O$, and 1 mg/ml X-gal. Sections were allowed to react overnight to maximize the blue X-gal signal, even though this revealed a slight

endogenous activity in the Purkinje cells of the cerebellum. Sections were then rinsed 2 times in PBS, 3 times in H_2O, then dehydrated and mounted in Permount (Fisher).

Counting ^{3}H-Thymidine-Labelled Cells

Cells were labelled with ^{3}H-thymidine, a defined number implanted and analyzed autoradiographically as described above. Cerebellar sections were cut at 7 μm and hippocampal sections were cut at 10 μm. A radiolabelled cell was defined as a cell with 6 or more overlying silver grains. In the case of the hippocampus, phase contrast photomicroscopy was used to identify cells in the granule cell layer and labelled cells were counted. In the case of the cerebellum, the sections were stained with neutral red and labelled cells were counted separately in the molecular and the granular layers. In the two graphs shown (Figs. 5D, 9D), sample sections from an entire series of serial sections through the hippocampus and cerebellum were counted. These figures were then corrected for the systematic error generated by double counting of sectioned cells using the formula of Abercrombie (1946):

$$P=(A)[M/(L+M)],$$

where P is the corrected number of cells per section, A is the uncorrected number of cells per section, M is the section thickness, L is the average diameter of a cell in a section.

Results

Isolation of the HiB5 Cell Line

Hippocampal anlagen of E16 rats were dissociated and placed into tissue culture. This primary cell population is almost entirely nestin-positive, and can undergo extensive proliferation in either serum-containing or defined media before differentiating into neurons and glia after 3-7 days (data not shown). A total of 14.5 x 10^6 cells were infected approximately 18 hours after plating with a retrovirus transducing the *tsA58/U19* double-mutant T-antigen gene and a gene conferring neomycin-resistance (Frederiksen et al., 1988; Jat and Sharp, 1989; Almazan and McKay, 1988, Soc. Neurosci. Abstr. *14*, 1130). The cells were grown at 33 °C in the presence of the neomycin analog G418 for a minimum of three weeks, until drug-resistant colonies were observed. From three independent primary cultures and retroviral infections, 48 colonies of proliferating cells were picked and expanded into the "Hi" cell lines. Of these, 35 were tested, at both the permissive (33 °C) and non-permissive (39 °C) temperatures, for the expression of a set of cell-state markers, including the nestin antigen, characteristic of neuronal precursor cells, and others that indicate differentiation. Of the 35 lines tested, six were found to be strongly nestin-positive.

One of the nestin-positive lines, HiB5, had a flat morphology at 33 °C, with long, nestin-positive processes (Fig. 1A). At 39 °C, the cells changed their morphology; for example, some cell bodies reduced in size and their processes appeared more elaborate.

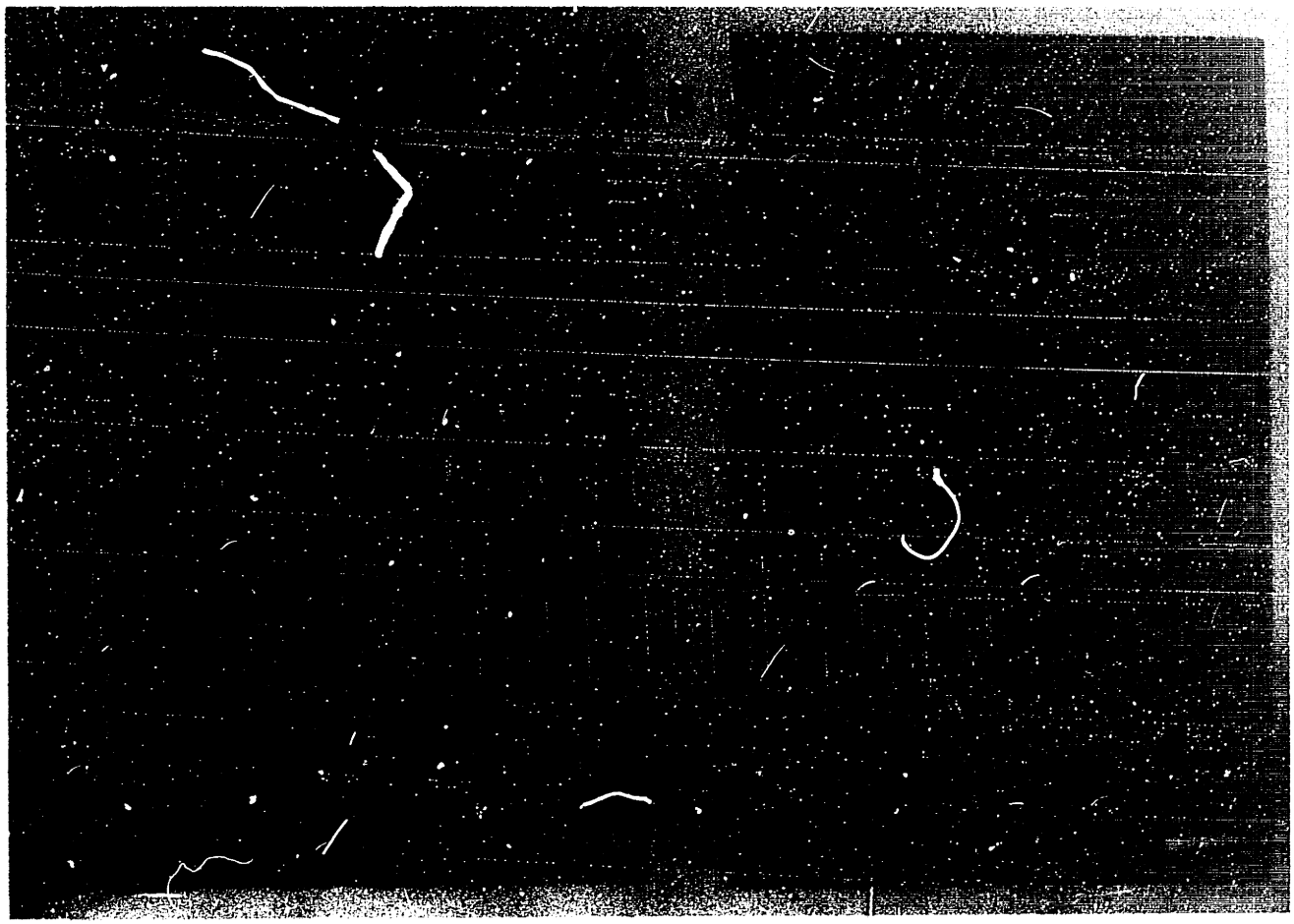

Figure 1. Morphology of HiB5 Cells In Vitro

(A) HiB5 cells at 33 °C are immunopositive for the nestin protein. Bar = 10 mm. (B) Double exposure under rhodamine and fluorescein optics to visualize cultured HiB5 cells labelled with DiI-C_{18}-(3) and green fluorescent latex microspheres (green beads). The DiI-C_{18}-(3) signal is orange-red and is localized on external and internal membranes. The green beads are endocytosed and often seen in perinuclear aggregates. Bar = 10 mm.

However, under all culture conditions tested, the cells continued to express the nestin antigen, and did not express markers such as neurofilament or glial fibrillary acidic protein, which are characteristically associated with neurons or glia, respectively (data not shown).

Implantation Strategy

The HiB5 cell line maintains certain characteristics that we observed in hippocampal precursor cells (see Experimental Procedures for details), and thus seemed a good candidate line to use for development of an implantation technique. In order to mark the HiB5 cells so that they could be identified within the host tissue, the cells were labelled by several techniques prior to implantation: tritiated thymidine (^{3}H-thymidine); 1,1'-dioctadecyl-3,3,3',3'-tetramethylindocarbocyanine perchlorate [DiI-C_{18}-(3)] (reviewed in Honig and Hume, 1989); green-fluorescent latex microspheres (green beads) (Katz et al., 1984; Katz and Iarovici, 1990); and by the expression of a transgene. The radioactive tracer was used to follow the distribution and measure the number of implanted cells and, in conjunction with retrograde filling, to show axonal projections. The two fluorescent markers were used to double-label the HiB5 cells, to show morphologies of implanted cells with a high level of confidence in their origin. Finally, the expression of an introduced marker gene (*lac*Z) was used to support further the results obtained by the other

labelling methods and to demonstrate the feasibility of introducing transgenes into the cell line.

Radioactively Labelled HiB5 Cells Are Associated with the Dentate Gyrus

To observe the localization of HiB5 cells after implantation into the developing hippocampus, cells undergoing mitosis in vitro were labelled with ^{3}H-thymidine. Then, 50,000-100,000 cells in a volume of 1 ml were implanted into the medial aspect of the dorsal hippocampal formation of P2 rats. After varying times postsurgery, radioactive label was visualized in tissue sections by emulsion autoradiography (Rogers, 1967). Clusters of silver grains were found over the nuclei of implanted cells.

In many experiments of this type, we routinely observed a large number of labelled nuclei in the dentate gyrus granule cell layer. For example, Figure 2 shows typical autoradiographic results from five experimental animals. In each case, the characteristic arc of the dentate gyrus contained many clustered silver grains located in the granule cell layer. Dark field photomicrographs showed that many of the implanted cells were intensely labelled with ^{3}H-thymidine, implying that the radioactive label was not greatly diluted. Some nuclei were located in the hippocampal fissure, just dorsal to the dentate gyrus, while others were seen in the space between the hippocampus and thalamus. Labelled nuclei were seldom seen in the CA1-CA3 subfields of the hippocampus (Fig. 2B, I), and those seen most often were not localized to the pyramidal cell

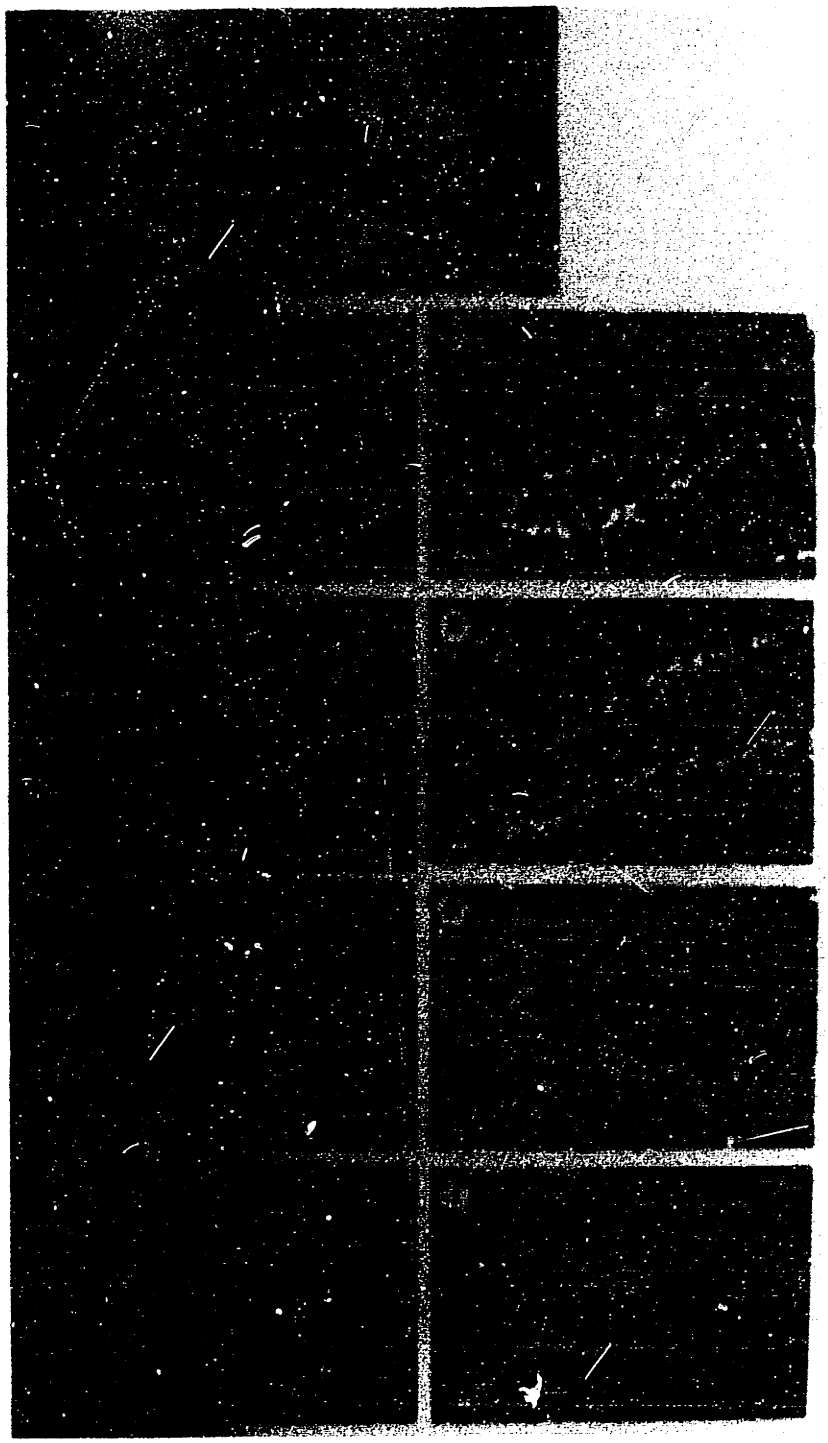

Figure 2. ^{3}H-Thymidine-Labelled HiB5 Cells Assume a Concentrated Distribution in the Dentate Gyrus Granule Cell Layer

(A) Schematic diagram of the rat dorsal hippocampal formation. The hippocampus proper contains pyramidal cells in regions CA1-CA3, with their cell bodies forming a layer. The dentate gyrus is a substructure of the hippocampus that arches around the terminal hippocampus proper and the hilar region (H); the hippocampal fissure (HF) lies dorsal to and the third ventricle (V) lies ventral and medial to the dentate gyrus. Three dentate granule neurons are drawn, with their cell bodies located in the granule cell layer (gcl). Their dendrites extend into the molecular layer (m), and their axons course via the mossy fiber pathway (mf) to terminate on CA3 pyramidal neurons. Displaced granule neurons have been described, whose cell bodies are located in the molecular layer, but their axons project normally. Bar = 50 mm.

(B-I) Hippocampal regions from five experimental subjects implanted with radioactively-labelled HiB5 cells, viewed using dark field illumination. In all, the dorsal surface is up as in the schematic.

When the whole hippocampal region is examined (B), silver grains are found dispersed across it, as well as in the ventricle and the hippocampal fissure. The silver grains are concentrated in both horns of the dentate gyrus. Bar = 100 mm.

When the same section is viewed at higher magnification (C), most of the silver grains are in round clusters and located in the granule cell layer. (D, E, F, and H) Views of the dentate gyrus of the remaining examples, each showing a similar concentration of HiB5 cells in the dentate gyrus granule cell layer. (G) Higher magnification view of example (F), illustrating that the radiolabelled cells are about the same size as the endogenous neurons. This result can be seen more clearly in Figure 3. (I) Region CA3 from example (H). Very few radiolabelled nuclei are seen in the CA3 pyramidal cell layer (indicated by the pair of brackets). In all cases, the section thickness = 20 mm. Bars (C, D, E, H, I) = 10 mm. Bar (F) = 20 mm. Bar (G) = 5 mm.

layer. Most of the cells that integrated into the host tissue were concentrated in the dentate gyrus, especially in the granule cell layer. At higher magnification (Fig. 2G), the radiolabelled cells were seen to be intimately associated with the endogenous granule cell neurons.

In one experimental animal (shown in Figure 3, and discussed below), the number of HiB5 cells localizing specifically to the granule cell layer was estimated six weeks after implantation by counting labelled nuclei in serial sections. Approximately 17,000 cells, out of about 70,000 initially implanted, were detected in the granule cell layer.

To control for the possibility of non-specific transfer of the radioactive label to host nuclei, other types of cells were similarly ^{3}H-thymidine-labelled and implanted: HiA4, a flat, nestin-negative cell line derived alongside HiB5; Rat2, a clonal embryonic fibroblast cell line (Topp, 1981); ^{3}H-thymidine-labelled HiB5 cells killed just prior to implantation. In all cases, few labelled cell nuclei were observed in the dentate gyrus granule cell layer (data not shown), demonstrating that the labelled nuclei seen in Figure 2 are those of implanted HiB5 cells.

Retrograde Filling of HiB5 Cells in the Dentate Gyrus with Fluoro-Gold

As diagrammed in Figure 2A, the major axonal projection of hippocampal granule neurons is the mossy fiber pathway, which connects them synaptically with the pyramidal cell neurons in the

hippocampal CA3 subfield (for reviews, see Brodal, 1981; Witter, 1989). If ^{3}H-thymidine-labelled HiB5 cells localized in the dentate gyrus granule cell layer are indeed similar to the endogenous neurons, some should have axons projecting to CA3. Therefore, six weeks after implantation, the retrograde tracer Fluoro-Gold (Schmued and Fallon, 1986) was injected into the CA3 region of five experimental subjects, and for 36 hours was allowed to fill the cell bodies innervating that region. In all subjects, fluorescence was observed at both the CA3 injection site and the adjacent dentate gyrus (Fig. 3). At the injection site, a general labelling of cellular structures was seen. In the ipsilateral dentate gyrus, Fluoro-Gold fluorescence was localized specifically to the granule cell neurons (Fig. 3B-E); fluorescence was not observed in the contralateral dentate gyrus (data not shown). Autoradiography of the Fluro-Gold-labelled tissue showed many radioactively-labelled HiB5 cell nuclei in the granule cell layer. Some of the fluorescent cells had clusters of silver grains above them, showing that the DNA of these backfilled cells had been radiolabelled in vitro. Many of the ^{3}H-thymidine-labelled HiB5 cells located in the granule cell layer were backfilled with Fluoro-Gold, indicating not only that HiB5 cells can survive for at least six weeks after implantation, but also that they can elaborate axons like those of endogenous dentate granule cell neurons of the dentate gyrus.

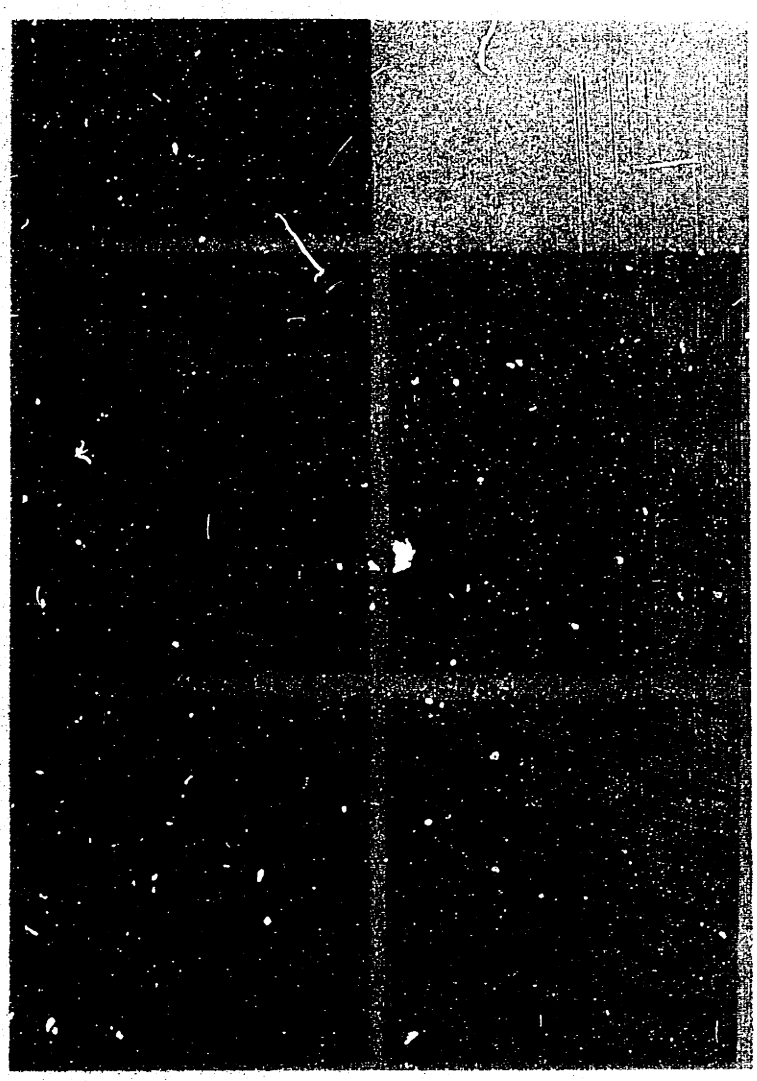

Figure 3. Radiolabelled HiB5 Cells in the Granule Cell Layer of the Dentate Gyrus Labelled by the Retrograde Tracer Fluoro-Gold from the CA3 Hippocampal Subfield

Six weeks after implanting radiolabelled HiB5 cells into the dentate gyrus, the retrograde tracer Fluoro-Gold was injected into the ipsilateral hippocampal subfield CA3, where the efferents of dentate granule neurons project. Since Fluoro-Gold can withstand processing for autoradiography, retrogradely-filled radiolabelled HiB5 cells in the dentate gyrus can be detected. [Dorsal is up; section thickness is 10 mm.]

(A) Low power view of the CA3 region and adjoining dentate gyrus is shown. The white-blue fluorescence of Fluoro-Gold indicates the injection site in CA3 and the cells in the dentate gyrus granule cell layer which have been retrogradely filled. Note the pair of fluorescent cells indicated by the arrow. Bar = 100 mm. (B) and (C) are magnified views of the cells indicated in (A) at two focal planes and with two forms of illumination. In (B), many granule neurons on the outer perimeter of the granule cell layer are fluorescent, including the pair of cells. The fluorescent signal reveals both the cell body and the dendritic processes extending from them into the molecular layer. (C) When viewed using a combination of fluorescent and transmitted light illumination, one of the pair (arrow) is labelled by both Fluoro-Gold and ^{3}H-thymidine.

(D,E) In an adjoining section, many cells in the center of the granule cell layer have been retrogradely labelled. By adjusting the plane of

focus, one of the backfilled cells in frame (D) (arrow) has a cluster of silver grains overlying it. This HiB5 cell has not only been labelled with a retrograde tracer placed in CA3, but also appears well integrated into the midst of the granule cell layer. Bar (B, C, D, E) = 8 mm.

Fluorescently Labelled HiB5 Cells Localize to the Granule Cell Layer of the Dentate Gyrus

In order to reveal the morphology of implanted cells without having to rely on backfilling, HiB5 cells were double-labelled with two fluorescent indicators prior to implantation. DiI-C_{18}-(3) is a lipid soluble dye that fluoresces orange-red when excited using a rhodamine filter set. Green beads are internalized and fluoresce green when excited using a fluorescein filter set. An example of double-labelled HiB5 cells in vitro is shown in Figure 1B, which is a double exposure using both methods of excitation. The fluorescent signal arising from DiI-C_{18}-(3) is spread throughout the entire cell, with several bright intracellular concentrations of dye presumably on endocytosed vesicles (Honig and Hume, 1986). The green fluorescence from the beads is entirely intracellular, with some individual and some bead aggregates contributing to the punctate signal.

To see if such double-labelled HiB5 cells persist in vivo, 50,000-100,000 HiB5 cells were implanted into the hippocampal formation of P2 rats. After one week in vivo, double-labelled cells were found distributed across the dentate gyrus of the hippocampal formation (Fig. 4A). Like the radioactively-labelled HiB5 cells, they were concentrated in the granule cell layer; the inset of Figure 4A shows that these cells were also bead-labelled. Despite inherent variability in the precise placement of cells, in a large number of

different experimental animals (see Experimental Procedures), HiB5 cells were integrated into the lateral and medial horns of the dentate gyrus, and into the hilar region. Comparatively few cells were observed in the hippocampal subfields CA1-3 and in the cortex dorsal to the hippocampus.

It is conceivable that many types of cells, when transplanted into a developing structure, can distribute themselves like host cells, for example owing to mechanical constraints. To investigate this possibility, the nestin-negative cell line HiA4 was double-labelled and implanted into the developing dentate gyrus (Fig. 4B). After one week in vivo, the distribution of HiA4 cells was unlike that of HiB5 cells: Double-labelled HiA4 cells neither became associated with the granule cell layer of the dentate nor transferred DiI-C_{18}-(3) to endogenous neurons, even though large numbers of double-labelled cells were seen immediately adjacent to the dentate granule cell layer.

The Rat2 fibroblast cell line (Topp, 1981) was similarly labelled and implanted (data not shown). Rat2 cells, like HiB5 and HiA4, are capable of surviving in the animal for many weeks. The Rat2 cells did not preferentially associate with the granule cell layer of the dentate gyrus, even when large numbers of Rat2 cells were implanted. The Rat2 cells remained separate from the host cells and exhibited uncontrolled growth, distorting the organization of the hippocampus. DiI-C_{18}-(3)-labelled cells with extensive processes were rare, being observed at least two orders of magnitude less frequently than when HiB5 cells were implanted.

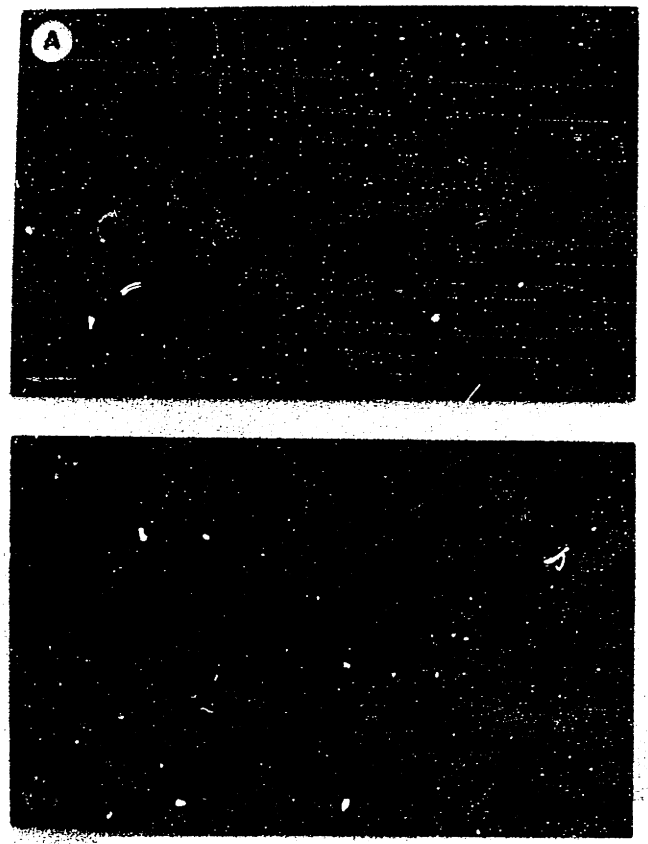

Figure 4.

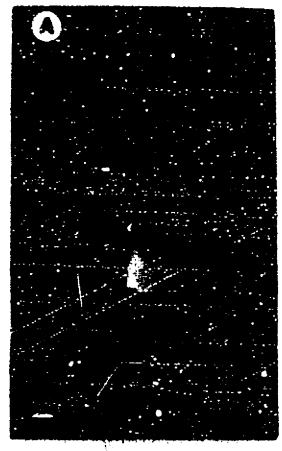

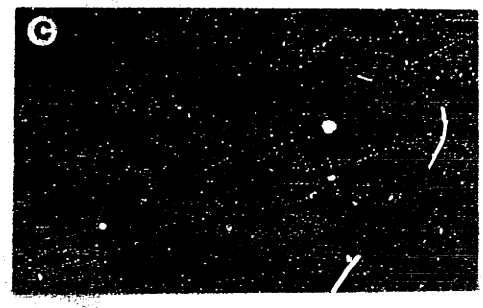

Figure 5.

Figure 4. Double-Labelling of Cells Using Two Fluorescent Markers Reveals their Distribution in the Hippocampus

Cells from line HiB5 (A) and HiA4(B) were double-labelled in vitro with DiI-C_{18}-(3) and green beads, then analyzed by fluorescence microscopy 10-14 days after implantation into the P2 hippocampus. In each frame, the granule cell layer is indicated by a trio of arrows. The double-headed arrow marks the apex of the gyrus, while the two single-head arrows point towards the apex along the lateral horns. Bar = 20 mm.

(A) The dentate gyrus of the hippocampus viewed with rhodamine optics shows the DiI-C_{18}-(3) signal from the double-labelled implanted HiB5 cells. The cells are concentrated in the granule cell layer. The same section viewed using fluorescein optics (inset) shows the green beads similarly concentrated in the granule cell layer. The fluorescence dorsal (up) to the dentate gyrus arises from cells in the hippocampal fissure.

(B) In a similar implant, the nestin-negative HiA4 cells, when viewed under rhodamine optics, can be seen in the dentate gyrus, but few labelled profiles are specifically present in the granule cell layer. Much of the fluorescent signal is located in the hilar region. In this example, dorsal is down.

Figure 5. Double-Labelled HiB5 Cells in the Granule Cell Layer of the Dentate Gyrus Have Neuronal Morphologies

(A-C) Three examples of a morphology HiB5 routinely adopt in the dentate gyrus granule cell layer as seen in double exposures. The cell body and processes appear orange-red, with the green beads appearing yellow. The dark oval in the center of each soma is the cell nucleus. In each panel, the molecular layer is up relative to the cell soma. The double-labelled cells are positioned in the granule cell layer, and each has multiple processes that branch upward into the molecular layer (full extension of these processes cannot be seen in a single plane of focus). In (A) and (B), a single fine process is observed that courses downward from the cell soma into the hilar region. A similar process was present in example (C), but was in a different focal plane. This morphology and orientation is typical of dentate gyrus granule neurons.

In (D), HiB5 cells were labelled and implanted similarly, but the cells were killed by hypotonic lysis followed by freeze/thaw before implantation. Little fluorescent material is found in the dentate gyrus per se. The double-labelled structures in the tissue, like this one, do not have a definable shape or bear processes. Bars (A, D) and (B, C) = 2 mm.

The Morphology of HiB5 Cells in the Granule Cell Layer

In Figure 5, three examples of a specific morphology we routinely observed for HiB5 cells in the dentate granule cell layer are shown in double exposures. The presence of green beads in the cells affirmed that the morphology revealed by the DiI-C_{18}-(3) arose from an implanted HiB5 cell and not from transfer of the dye between implanted and host cells. These cells looked remarkably like endogenous hippocampal dentate granule neurons. The double-labelled cell body was ovoid and was located in the granule cell layer. In all examples, the DiI-C_{18}-(3) fluorescence revealed several branched processes that extended from the cell soma to fan out in the host molecular region, which is the dendritic field of dentate gyrus. The orientation of the cell body and processes was like those described for granule cell neurons and their dendrites as visualized by other methods (for example, see Brodal, 1981; Frotscher and Zimmer, 1983; Lubbers and Frotscher, 1987; Claiborne et al., 1990). At the base of the cell body, one could often observe a fine process extending towards the hilar region, as shown in Figure 5A and B. This process is probably the axon of a granule neuron, since the axons of dentate granule neurons have a smaller diameter than their dendrites and they extend from the soma in a similar fashion. In the example shown in Figure 5C, the cell body was slightly displaced into the molecular layer, and the cell body was somewhat laterally elongated; this is precisely the morphology Ramon y Cajal (1894) described for displaced dentate granule neurons, identified as such

by their axonal projection along the mossy fiber pathway, *cf.*, Figure 3B,C. These data corroborate the autoradiographic and backfilling data, further indicating that implanted HiB5 cells differentiate into granule neurons.

To control for the transfer of either fluorescent label to host cells, HiB5 cells were double-labelled as in the previous experiment, but were killed prior to implantation. Bright fluorescent signals were detected in the extracellular spaces around the hippocampal region, like the hippocampal fissure. There was, however, a dramatic reduction of both fluorescent labels in the dentate gyrus per se, and little, if any, was found in the granule cell layer. Figure 5D shows one of the occasional double-labelled structures in the hippocampus of an animal implanted with hypotonically-lysed HiB5 cells. Processes were not observed around this structure. The lack of morphologically complex labelled cells at the implant site indicates that the dead HiB5 cells do not assume any of the shapes routinely seen with live HiB5 cell transplants, and that the markers are not being transferred from the labelled cell matter to the host cells.

Implantation of HiB5 Cells into the Postnatal Cerebellum

The cerebellum is one of the few regions of the rat CNS besides the hippocampus undergoing neurogenesis postnatally (Altman, 1972a, b, c). During the first week to ten days of postnatal life, large numbers of neurons are generated in the cerebellum; most of the neurons produced at this time are cerebellar granule neurons. Glial cells, including the morphologically distinct Bergmann glia, are also

generated during the first two weeks of postnatal life (for a review of cerebellar morphology, see Palay and Chan-Palay, 1974). A schematic diagram of the cerebellum (Fig. 6A) shows that it is divided into two distinct regions. The outer molecular layer is predominantly composed of the axons of granule neurons and their targets, the dendrites of Purkinje cells. To enable them to interact with Purkinje cells, the axons of granule neurons have a distinctive morphology, running parallel to each other and orthogonal to the dendritic fan of the Purkinje cells. The inner granular layer contains the cell bodies and dendrites of granule neurons, which have an average diameter of 5-7 μm (Palay and Chan-Palay, 1974).

To explore further the developmental potential of HiB5, the cells were labelled with ^{3}H-thymidine in tissue culture and implanted into the P2 cerebellum. After 2-3 weeks, autoradiographic analysis showed that labelled cells integrated into the cerebellar strata (Fig. 6B,C). Many intensely labelled nuclei were found in the granular layer and their morphology was similar to neighboring unlabelled nuclei of the host granule neurons.

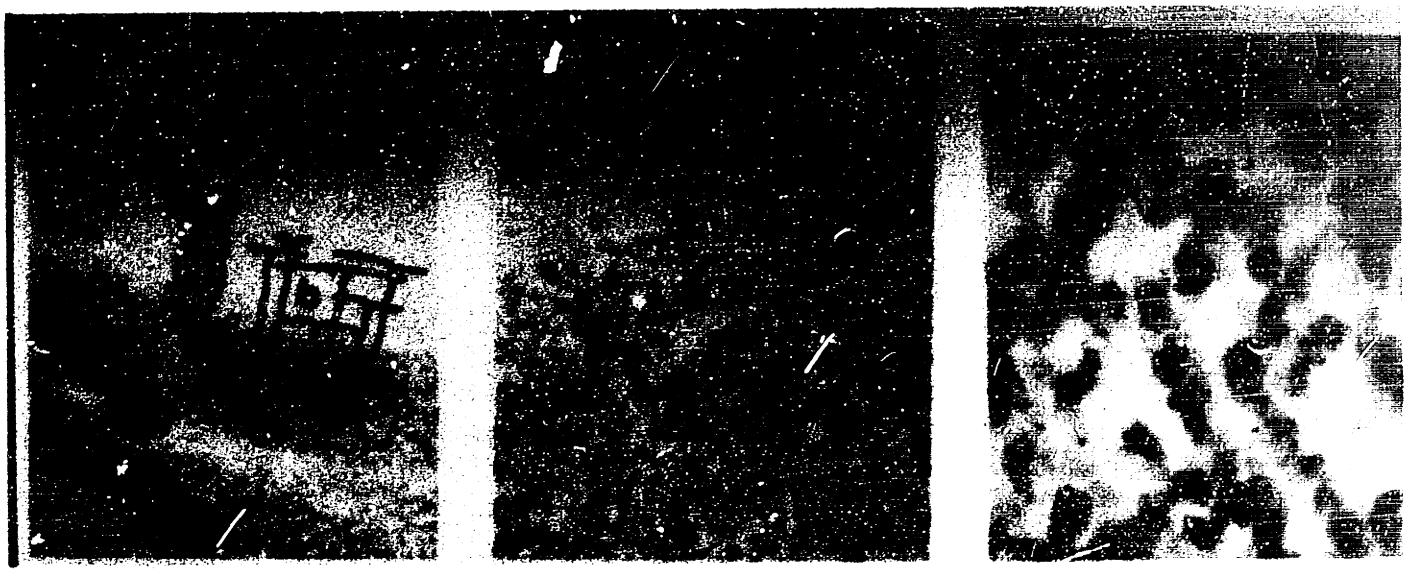

Figure 6. Radiolabelled HiB5 Cells in the Granular Layer of the Cerebellum

(A) A schematic diagram of the cerebellum illustrates the different layers. Just above the white matter (WM) is the granular layer (GL), which contains the cell bodies and dendrites of cerebellar granule neurons (a). The granule neuron axons (b) are oriented upwards, crossing the Purkinje cell layer (PCL), which contains the large Purkinje cell bodies and also Bergmann glial cell bodies. Just below the pial surface (P) lies the molecular layer (ML), which contains the T-shaped axons of granule neurons (b, parallel fibers), the dendrites of Purkinje cells, and two relatively rare types of cerebellar interneurons. It also has the distinctive processes from the Bergmann glial cells running to the pial surface. (B) A low magnification view of a cerebellar section three weeks after implantation with ^{3}H-thymidine-labelled HiB5 cells and counterstained with neutral red. The radiolabel appears as black silver grains. The molecular layer is uppermost and contains few cell bodies, while the granular layer, in the lower third of the micrograph, is densely populated with granule neuron cell bodies. Many small, intensely labelled cells can be seen in the granular layer. Bar = 25 mm. (C) Radiolabelled HiB5 cells in the granular layer are shown at a higher magnification. The silver grains are seen as a tight cluster, the diameter of which is identical to that of the endogenous granule neurons, which are stained red. Some HiB5 cells are less intensely labelled than others, having fewer silver grains overlying them. Bar = 6 mm.

By counting radiolabelled nuclei in the granular layer and in non-granular layers, we estimated that ~170,000 radiolabelled HiB5 cells were integrated into the cerebellum of a single animal. Since only 70,000 cells were implanted, some of the implanted cells must have divided. However, the intensity of labelling implies that the proliferation was not extensive. About 15% of the labelled cell bodies were found in the molecular layer, which lies above the Purkinje cell layer. Radiolabelled Purkinje cells were not observed. Some intensely labelled nuclei were found in the white matter below the granular layer. Strikingly, the remainder of the radiolabelled cells, about 80%, were found in the granular layer. Thus, a significant fraction of the HiB5 cells became integrated into the granular layer of the cerebellum.

Retrograde Filling of ^{3}H-Thymidine-Labelled HiB5 Cell Nuclei in the Granular Layer of the Cerebellum

Retrograde labelling experiments were again used in conjunction with radio-labelling of nuclei to determine if the small, intensely labelled cell bodies in the granular layer like those in Figure 6C extended axons into the molecular layer. Six weeks after implantation, the brains were fixed and removed for processing. Crystals of DiI-C_{18}-(3) were placed superficially in the molecular layer of a thick section of the cerebellum, to be taken up by axons that were in direct contact with the dye. Due to its hydrophobicity, the chromophore could diffuse in the cell membrane throughout the

length of the axon, eventually labelling the soma (Honig and Hume, 1986). Since the dye is not retained by cells during the processing required for autoradiography, the fluorescent signal was photoconverted to an insoluble brown product using diaminobenzidine (Sandell and Masland, 1988), which can be detected using white light. The low magnification image in Figure 7A shows labelled parallel fibers in the molecular layer, and backfilled cell bodies in the granular layer.

At higher magnification, the brown reaction product in cell bodies can be co-localized with silver grains in the overlying emulsion. In the three examples shown in Figure 7B,D,F, backfilled cell bodies contain the brown precipitate, while in Figure 7C,E,G, silver grains can be seen above the HiB5 cell nuclei. The colocalization of the precipitate and the grains indicates that HiB5 cells in the cerebellar granular layer can elaborate axons into the molecular layer.

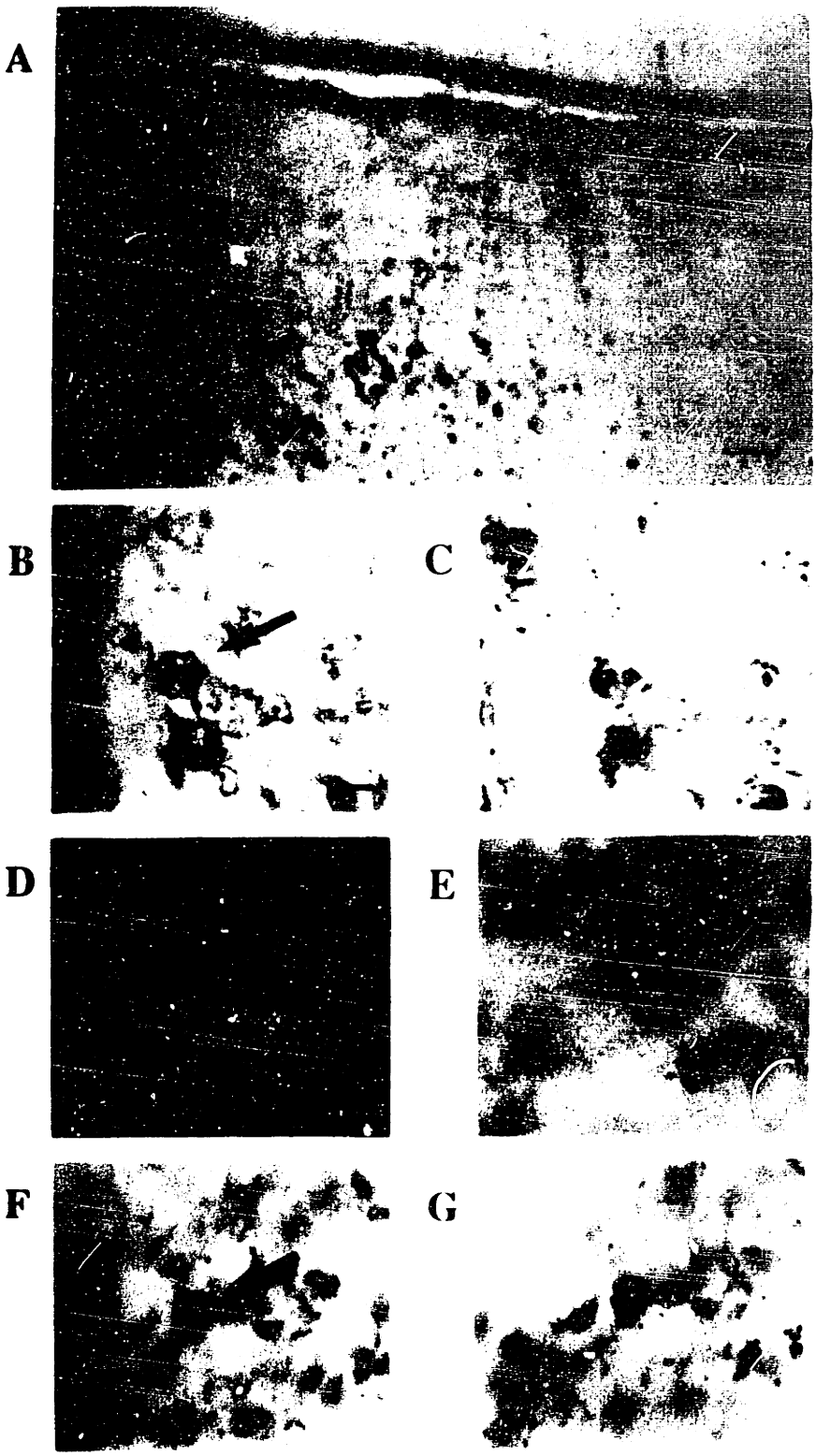
A
B
C
D
E
F
G

Figure 7. Small Radiolabelled HiB5 Cell Bodies in the Granular Layer Can be Backfilled by Applying a Tracer to the Axon-Rich Molecular Layer

Radiolabelled HiB5 cells in the granular layer can be detected by autoradiography, as shown in Figure 6. Retrograde tracing was used to determine if these radiolabelled cells extend axons into the molecular layer. DiI-C_{18}-(3), when converted to an insoluble diaminobenzidine product, serves as the retrograde tracer. (A) A low magnification photomicrograph showing the molecular layer comprising backfilled axons. These axons course past the Purkinje cells (open arrow). In the granular layer, many small, backfilled cell bodies are present. Section thickness is 7 mm. Bar = 48 mm.

In (B), one of the backfilled cell bodies (solid arrow) is shown at higher magnification. (C) is the same field as (B), but focussed in the emulsion to show the cluster of silver grains over it. (D-E) and (F-G) are pairs of photomicrographs showing additional examples of backfilled cells (D,F) and the silver grains (E,G) overlying some of them (indicated with arrows). Bar = 4 mm.

Morphological Profiles of HiB5 Cells in the Cerebellum

When labelled with the two fluorescent markers, HiB5 cells implanted into the cerebellum were observed to differentiate, as judged by morphological criteria. Many double-labelled HiB5 cells took on the morphology of cerebellar granule neurons (see Palay and Chan-Palay, 1974). In Figure 8, three such cells are shown. In each, a small, double-labelled cell body indicates that the cell originated from the HiB5 cell line. The extensive diffusion of DiI-C_{18}-(3) throughout the membrane of the cell revealed a fine process extending towards the molecular layer, where it branched into a T-shape. This bifurcation is a specific characteristic of cerebellar granule neuron axons, which form an elaborate network of parallel fibers in the molecular layer (Palay and Chan-Palay, 1974). In some samples, parallel fibers arising from transplanted HiB5 cells ran for hundreds of microns across the molecular layer of the host, although the characteristic bifurcation and/or the source of the parallel fiber could not always be identified, probably because of the orientation of the section. Occasionally, a green microsphere could be seen somewhere within a DiI-C_{18}-(3)-labelled parallel fiber (data not shown), confirming that parallel fibers were not labelled by spurious transfer of the lipid-soluble dye. In one example, shown in Figure 8A, the parallel fiber has varicosities like those seen at synaptic sites.

In some cases, like those shown in Figure 8A and C, we observed multiple short processes extending from the cell body into


A


B

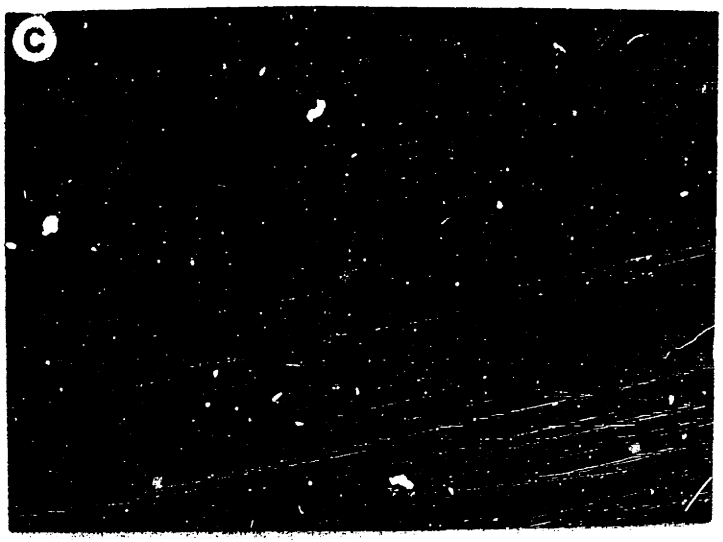
C

Figure 8. Double-Labelled HiB5 Cells Showing Morphological Features of Cerebellar Granule Neurons

Three typical examples are shown of a morphology seen when DiI-C_{18}-(3) and green bead-labelled HiB5 cells are implanted into the postnatal cerebellum. In each panel the pial surface of the cerebellum is oriented at the top of the figure. These HiB5 cells look like cerebellar granule neurons, i.e., small cell bodies and axons that extend towards the pial surface, bifurcating to give parallel fibers. (A) A collage of two photomicrographs shows the same cell in different focal planes. The HiB5 cell body lies in the host granular layer and has several short, branched processes, morphologically similar to granule neuron dendrites. From this cell is derived an axon-like process, which ascends into the molecular layer where it bifurcates. Varicosities are apparent on the parallel fiber. Bar = 5 mm. (B) A similar morphology is seen in another example. Bar = 5 mm. (C) A collage of another example. The cell body, seen to be double-labelled by the presence of an aggregate of green beads (double exposure, inset), has multiple, short, DiI-C_{18}-(3)-labelled processes resembling dendrites. The axon extends for about 50 mm before bifurcating into a parallel fiber in the host molecular region. Bar = 5 mm.

the granular layer; only some of these processes could be seen in a single plane of focus. These were larger in caliber than the ascending fiber and had the characteristic morphology of granule neuron dendrites. These data, like the autoradiographic and backfill results, suggest that HiB5 cells can adopt the morphology of cerebellar granule neurons.

Another cell type commonly observed when HiB5 cells were implanted into the cerebellum had a morphology like that of the Bergmann glial cell (Fig. 6A and 9). The cell bodies of Bergmann glia lie in or near the Purkinje cell layer, with highly stereotyped branched processes extending to the pial surface, where characteristic endfeet are formed (Palay and Chan-Palay, 1974). Labelled Bergmann glia-like cells were observed in all cerebellum implant experiments. We also observed cells whose morphology did not permit ready identification. Dead, double-labelled HiB5 cells were implanted into the P2 cerebellum (data not shown). Like the hippocampal implants, dead cells were not found in large numbers integrated into the host tissue, nor did they adopt the size or shape characteristic of endogenous cerebellar cells.

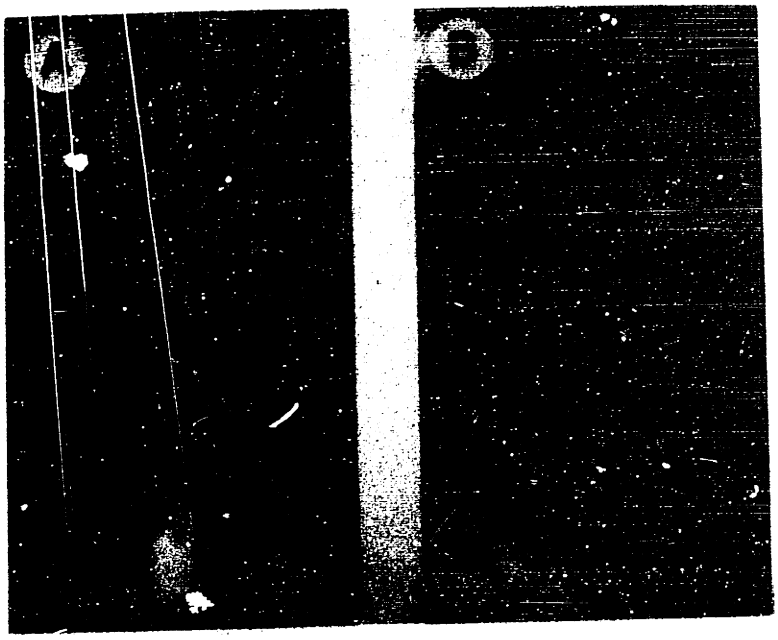

Figure 9. HiB5 Cells Can Also Adopt a Morphology like Cerebellar Bergmann Glial Cells

Another morphology commonly observed when HiB5 cells are implanted into the cerebellum resembles that of Bergmann glia. As reviewed in Figure 6A, the cell body lies near the Purkinje cell layer and has multiple long fibers, which run in and out of the plane of focus, extending up to the pial surface. In (A), a single example is shown, while in (B), a cluster of Bergmann glial cells is shown from another subject. In both panels, the pial surface is uppermost. Bars = 5 mm.

HiB5 Cell Bodies Integrated into the Cerebellum as Detected by an Intrinsic Gene Product

Marker genes such as those used to study the lineage properties of CNS stem cells might provide additional, independent evidence for the behavior of immortal cells after implantation. The *lacZ* gene from *Escherichia coli*, which has been widely used as a cell marker (Sanes et al., 1986; Price et al., 1987; Turner and Cepko, 1987; Gray et al., 1988; Price and Thurlow, 1988; Galileo et al., 1990; Turner et al., 1990), was introduced into HiB5 cells by infection with the BAG retrovirus (Price et al., 1987). *LacZ*-expressing cells were enriched from this population by fluorescence-activated cell sorting, using a substrate for b-galactosidase which, when cleaved, yields fluorescein (Nolan et al., 1988). This enriched population was then plated at limiting dilution, and many independent colonies were subcloned, among them the subclone HiB5B-27.

When HiB5B-27 cells were fluorescently tagged with DiI-C18-(3) and green beads and implanted into the P2 cerebellum, they behaved in the same way as HiB5 cells themselves (data not shown). When such transplanted cells were visualized using X-gal histochemistry, the implant sites were detected by the presence of intensely blue cells in a consecutive set of serial sections. A number of the blue cells were found associated with the cerebellar granular layer (Fig. 10A). Endogenous galactosidase activity was observed in Purkinje cells (Fig. 10B) throughout the cerebellum, i.e., in all of the serial sections, and thus was clearly distinguishable from the HiB5B-

27 signal. Small blue cell bodies were found in the granular layer at the implant site, and were the same size as adjacent unlabelled granule neurons. When HiB5B-27 cells were killed prior to implantation, small blue cells were not seen. The pattern of cells visualized by expression of the *lacZ* gene was consistent with the results observed with the other three labelling methods, as well as the retrograde filling experiment, further supporting the view that HiB5 cells integrated into the host tissue, where some differentiated into cerebellar granule neurons.

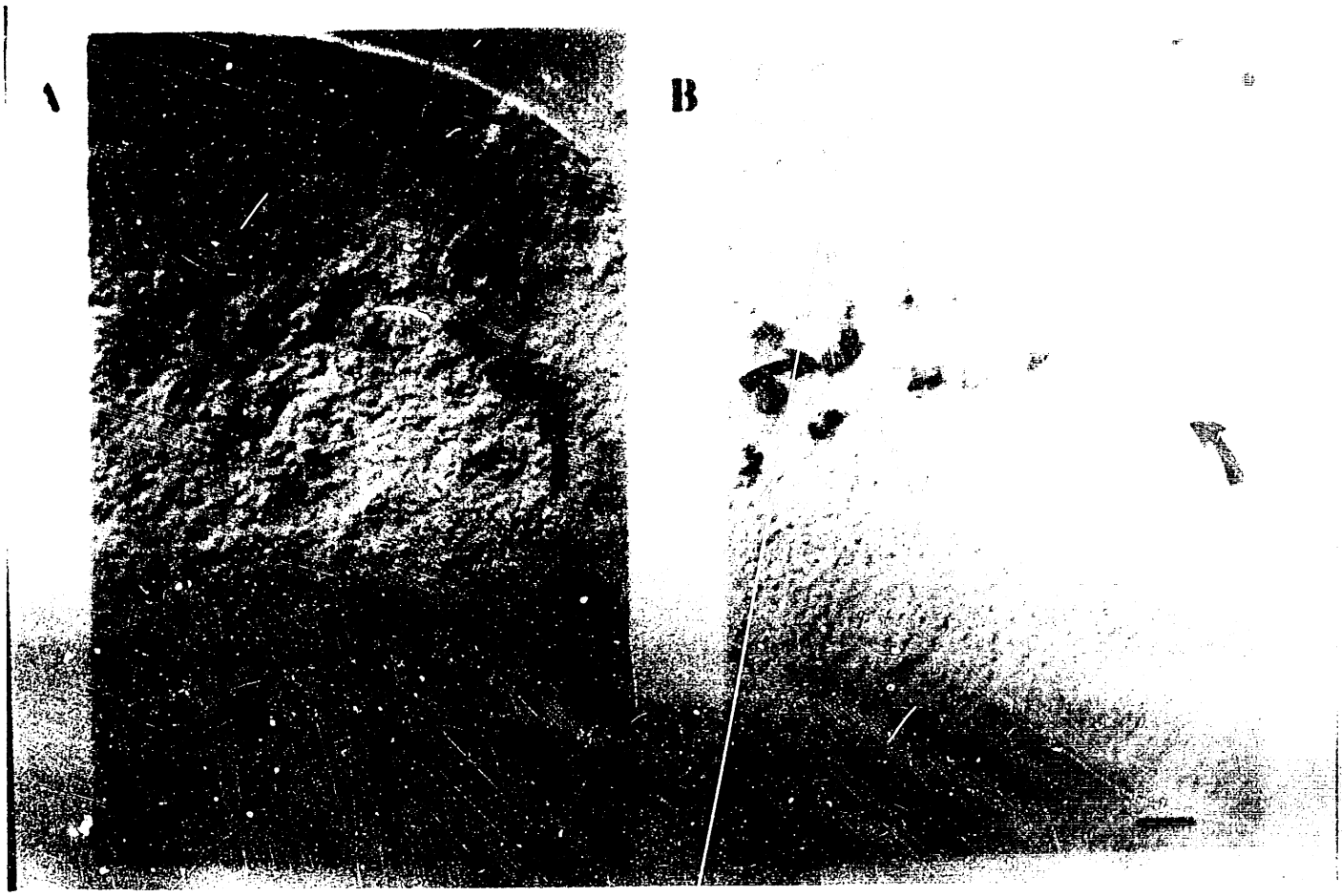
A
B

Figure 10. Implanted HiB5 Cells in the Cerebellum Detected by Expression of a Transgene

HiB5B-27, a subclone of HiB5 carrying the *E. coli lacZ* gene, was implanted into the P2 cerebellum. HiB5B-27 cells are detectable by X-gal histochemistry, which yields a blue product within the cells. (A) The distribution of blue cells seen in the tissue at the implant site. (B) The distribution of blue cells in tissue distant from the transplant site. Bar = 40 mm.

In both panels, the pial surface is in the upper right. The Purkinje cell layer, indicated by the pair of inward-facing arrows, curves across each folium. The large Purkinje cells react blue throughout the cerebellum, a consequence of endogenous galactosidase activity. Below the Purkinje cell layer is the granular layer, which is densely packed with granule neuron cell bodies. In (A), in contrast to (B), many small blue cells are present in the granular layer of the cerebellum only in the region of the implant. These blue cells are the same size as the neighboring, noncolored endogenous granule neuron cell bodies. In (B), the Purkinje cell layer is multiple-cell thick because the plane of section was slightly tangential to the pial surface.

The blue signal from HiB5B-27 cells correlates with, but is not identical to, the fluorescent and autoradiographic data. An explanation for this disparity is the observation that, in vitro, the blue signal decreases in the subclones with increasing time at 39 ^{o}C, possibly because of down-regulation of the viral promoter.

Discussion

HiB5 Cells Differentiate upon Implantation

In this paper, the in vivo behavior of a conditionally-immortalized progenitor cell line is described. The HiB5 cell line was one of 48 immortalized from the developing hippocampus of the E16 rat. HiB5 was expanded from a single colony that presumably arose from an individual hippocampal precursor cell infected by the retrovirus. Genomic DNA Southern blot analysis showed a single integrated retroviral genome (data not shown). Following extensive growth in tissue culture, HiB5 cells implanted back into the animal can still express the multiple differentiated phenotypes described here.

Since a temperature-sensitive variant of T-antigen was used, immortalized cells placed at the core body temperature of the rat should halt T-antigen-dependent cell division, and thus might differentiate if they retain the capacity to do so. The four labelling methods used [^{3}H-thymidine, DiI-C$_{18}$-(3), green fluorescent beads, and *lacZ* transgene] consistently showed that HiB5 cells integrated into the host tissue, where their proliferation was controlled. In the dentate gyrus of the hippocampus and the granular layer of the cerebellum, regions still undergoing neurogenesis at the time of implantation, many HiB5 cells assumed the shape of neurons, including the processes appropriate to their location. Retrograde filling and DiI-C$_{18}$-(3) labelling indicated that implanted cells in the dentate gyrus granule cell layer extended dendrites and axons like

those of native dentate granule neurons. Similarly, when placed in the cerebellum, labelled HiB5 cells were seen with axonal and dendritic morphology much like that of cerebellar granule neurons. At both implant sites, labelled cells with glial morphologies also were observed; this phenotype was especially apparent in the cerebellum, where the Bergmann glial cell has a distinctive morphology that makes it easy to recognize (Palay and Chan-Palay, 1974). The conclusion that HiB5 cells differentiate into glial cells is less well supported, though, because it relies exclusively on the fluorescent labels.

When autoradiography was used to follow implanted cells, HiB5 cells that localized to neuronal cell layers had nuclear morphologies similar to those of neighboring neurons, in both the granule cell layer of the hippocampal dentate gyrus and the granular layer of the cerebellar cortex. The identification of radiolabelled cells as neurons was further supported by the retrograde transport experiments, which showed that the HiB5-derived hippocampal and cerebellar granule neurons elaborated axons to the appropriate projection areas. Thus, HiB5 cells possess the capacity to express three important features of neuronal cells: the location and shape of the cell body, the projection of the axon, and morphological features of dendrites.

This analysis of implanted cells in the developing brain suggests that conditionally-immortal cells can respond to the developmental signals involved in the segregation of cell bodies, axons, and dendrites to specific zones. The molecular mechanisms

involved in the morphological differentiation of neurons appear to be intact in HiB5 cells. It remains to be seen, however, whether these cells are physiologically active.

Accuracy of the Different Labelling Techniques

The implant results have a number of interesting implications, whose validity depends on the labelling procedures. In the case of ^{3}H-thymidine, transfer of the radioactive nucleotide from one cell to another once it has been incorporated into DNA has not been described. This label has been used successfully mark primary stem cells for transplantation into the developing ferret brain (McConnell, 1988). Also, implants of radiolabelled live HiA4 and Rat2 cells and dead HiB5 cells did not result in labelled nuclei within neuronal cell layers (data not shown).

Although the two fluorescent dyes have not been used in this specific type of experiment, results from their use in other experiments suggests that they are unlikely to transfer to other cells. The beads were developed for retrograde tracing of afferents in the mammalian visual cortex, where little or no labelling secondary to the originally labelled cell has been noted (for example, Katz et al., 1984; Katz, 1987; Katz and Iarovici, 1990), nor has anterograde transport been observed. Thus, once the beads enter the cells by phagocytosis, they are unlikely to escape. Also, even if some were to escape, they would not diffuse very far through the tissue, given their relatively large size, 0.02-0.2 mm (Katz et al., 1984), and the

tight packing of cells in these tissues. Green bead-positive cells in the area of the implant are likely to be of cell-line origin.

A limitation of the beads is that they are concentrated in cell somata (Katz et al., 1984; Katz, 1987; Katz and Iarovici, 1990), so that the entire shape of the cell is not revealed. In contrast, DiI-C_{18}-(3) diffuses throughout the cell membrane (Schlessinger et al., 1977) to illuminate the morphology of the cell in detail (Honig and Hume, 1986; Thanos and Bonhoeffer, 1987; Honig and Hume, 1989). Given its highly hydrophobic character, the dye is unlikely to be transferred from one cell to another via the aqueous phase (Honig and Hume, 1986, 1989). However, in fixed tissue, dye transfer can occur (Godemont et al., 1987). We addressed this concern in two ways. First, the time period between fixation and examination was kept to a minimum, from 6 to 36 hours after fixation. Second, Godemont et al. (1987) showed that the signals arising from live- versus fixed-cell labelling are qualitatively different. In live cells, some of the dye is internalized into unidentified vesicles, leading to a punctate appearance in addition to surface labelling (Honig and Hume, 1986). In fills of fixed cells, only the external surfaces of the cells are labelled (Godemont et al., 1987), presumably because the endocytotic machinery relies on viability. In the double-labelled examples shown here, most cells contain internal dye. Further, there is no evidence in the literature, in connection with either live or fixed preparations, for transcellular labelling of the magnitude needed to explain our results. The probability of fluorescent indicator transfer was also addressed by implantation of double-labelled dead HiB5

cells and other types of live cells. In both cases, no evidence of DiI-C18-(3) or bead transfer to endogenous cells was observed.

The fourth labelling method, the stably-integrated marker gene encoding the *E. coli* b-galactosidase enzyme, showed subcloned HiB5 cells in the cerebellar granular layer at the implant site (Fig. 10). Although endogenous galactosidase activity was observed in Purkinje cells and in some cells associated with blood vessels, implanted cells were readily identifiable by their restricted distribution at the implant site.

The Efficiency of Integration

Our data support the view that implanted HiB5 cells integrate and differentiate in the host brain. The number of immortal cells that integrate can be estimated from the autoradiographic data (Figs. 2 and 6). In the hippocampus of a representative animal, ~17,000 radiolabelled cells were counted over a 4 mm length of the granule cell layer of the dentate gyrus, about 20% of the implanted population. Many other radiolabelled cells were located outside the granule cell layer, especially in the hippocampal fissure and the ventrical, but they were not counted. Few radiolabelled cells were detected in other subregions of the hippocampus. Implanted HiB5 cells also were widely distributed in the cerebellum, where about 170,000 radiolabelled cells were counted. Although this figure is larger than the number initially implanted, which suggests that some implanted cells divide in the host, this proliferation appears to be controlled, since intensely radiolabelled HiB5 cell nuclei can be seen

six weeks after implantation and there were no structural abnormalities seen at the implant site (Fig. 6). In contrast, radiolabelled Rat2 cells could not be detected after only two weeks in either implantation locale; also, in these experiments, the tissue was often grossly distorted (data not shown), together indicating that Rat2 cells continued to proliferate in vivo, unlike HiB5 cells. HiB5 cells must stop proliferating in vivo after a comparatively short time, and go on to survive for long periods without forming tumors or otherwise distorting the organization of the host brain.

Developmental Potential of HiB5 Cells

A variety of evidence suggests that HiB5 cells respond to endogenous cues within the local brain microenvironment. HiB5 cells implanted into neurogenic regions occupied the developing neuronal cell layers (Figs. 2 and 6), and the morphology these cells assumed was appropriate to the time and place of the implant. Also, in the cerebellum, HiB5 cells differentiated into a specific type of glial cell. Previous lineage studies documented multipotential precursors in the vertebrate brain in vivo (Turner and Cepko, 1987; Holt et al., 1988; Wetts and Fraser, 1988; Temple, 1989; Galileo et al., 1990). Furthermore, isolated, single CNS precursor cells grown in vitro have been shown to generate mixed neuronal and glial clones (Temple, 1989), suggesting that a progenitor capable of generating both types of cell exists, and might thus be immortalized.

In both the cerebellum and the hippocampus, many HiB5 cells localized specifically to a layer which, at the time of the surgery, was

being occupied by recently generated neurons (Figs. 2,3,4,6, and 7). Furthermore, these HiB5 cells extended axons and dendrites appropriately, assuming the specific features of neurons born at that time and location. These results suggest that HiB5 cells respond to the signals in different brain regions that establish the ordered structure of the central nervous system. Although there is no evidence to indicate that hippocampal and cerebellar neuronal precursors are alike, the HiB5 cell implants suggest a degree of similarity between them. By undertaking similar experiments using primary cells and cell lines derived from different brain regions, the features common to these precursors and the features that distinguish them might be elucidated.

References

Abercrombie, M. (1946). Estimation of nuclear populations from vibratome sections. Anat. Rec. *94*, 239-247.

Altman, J. (1963). Autoradiographic investigation of cell proliferation in the brains of rats and cats. Anat. Rec. *145*, 573-591.

Altman, J. (1972a). Postnatal development of the cerebellar cortex in the rat. I. The external germinal layer and the transitional molecular layer. J. Comp. Neurol. *145*, 353-398.

Altman, J. (1972b). Postnatal development of the cerebellar cortex in the rat. II. Phases in the maturation of Purkinje cells and of the molecular layer. J. Comp. Neurol. *145*, 399-464.

Altman, J. (1972c). Postnatal development of the cerebellar cortex in the rat. III. Maturation of the components of the granular layer. J. Comp. Neurol. *145*, 465-514.

Altman, J., and Bayer, S. A. (1990). Migration and distribution of two populations of hippocampal granule cell precursors during the perinatal and postnatal periods. J. Comp. Neurol. *301*, 365-381.

Altman, J., and Das, G. D. (1965). Autoradiographic and histological evidence of postnatal hippocampal neurogenesis in rats. J. Comp. Neurol. *124*, 319-336.

Angevine, J. B. (1965). Time of neuron origin in the hippocampal region: An autoradiographic study in the mouse. Exp. Neurol. Suppl. *13*, 1-70.

Banker, G. A., and Cowan, W. M. (1977). Rat hippocampal neurons in dispersed cell culture. Brain Res. *126*, 397-425.

Bartlett, P. F., Reid, H. H., Bailey, K. A., and Bernado, O. (1988). Immortalization of mouse neural precursor cells by the c-*myc* oncogene. Proc. Natl. Acad. Sci. USA *85*, 3255-3259.

Bayer, S. A. (1980). Development of the hippocampal region in the rat. I. Neurogenesis examined with [^{3}H]thymidine autoradiography. J. Comp. Neurol. *190*, 87-114.

Brodal, A. (1981). Neurological Anatomy (New York, NY: Oxford University Press), pp. 640-697.

Cattaneo, E., and McKay, R. D. G. (1990). Proliferation and differentiation of neuronal stem cells regulated by nerve growth factor. Nature *347*, 762-765.

Cepko, C. (1988). Immortalization of neural cells via oncogene transduction. Trends Neurosci. *11*, 6-8.

Cepko, C. L. (1989). Immortalization of neural cells via retrovirus-mediated oncogene transduction. Ann. Rev. Neurosci. *12*, 47-65.

Claiborne, B. J., Amaral, D. G., and Cowan, W. M. (1990). Quantitative, three dimensional analysis of granule cell dendrites in the rat dentate gyrus. J. Comp. Neurol. *302*, 206-219.

Frederiksen, K., and McKay, R. (1988). Proliferation and differentiation of rat neuroepithelial precursor cells in vivo. J. Neurosci. *8*, 1144-1151.

Frederiksen, K., Jat, P. S. , Valtz, N., Levy, D., and McKay, R. D. G. (1988). Immortalization of precursor cells from the mammalian CNS. Neuron *1*, 439-448.

Frotscher, M., and Zimmer, J. (1983). Lesion-induced mossy fibers to the molecular layer of the rat fascia dentata: Identification of postsynaptic granule cells by the Golgi-EM technique. J. Comp. Neurol. *215*, 299-311.

Galileo, D. S., Gray, G. E., Owens, G. C., Majors, J., and Sanes, J. R. (1990). Neurons and glia arise from a common progenitor in chicken optic tectum: demonstration with two retroviruses and cell type-specific antibodies. Proc. Natl. Acad. Sci. USA *87*, 458-462.

Godemont, P., Vanselow, J., Thanos, S., and Bonhoeffer, F. (1987). A study in developing visual systems with a new method of staining neurones and their processes in fixed tissue. Development *101*, 697-713.

Gray, G. E., Glover, J. C., Majors, J., Sanes, J.R. (1988). Radial arrangement of clonally related cells in the chicken optic tectum: lineage analysis with a recombinant retrovirus. Proc. Natl. Acad. Sci. *85*, 7356-7360.

Hockfield, S., and McKay, R. (1985). Identification of major cell classes in the developing mammalian nervous system. J. Neurosci. *5*, 3310-3328.

Holt, C. E., Bertsch, T. W., Ellis, H. M., and Harris, W. A. (1988). Cellular determination in the Xenopus retina is independent of lineage and birthdate. Neuron *1*, 15-26.

Honig, M. G., and Hume, R. I. (1986). Fluorescent carbocyanine dyes allow living neurons of identified origin to be studied in long-term cultures. J. Cell Biol. *103*, 171-187.

Honig, M. G., and Hume, R. I. (1989). DiI and DiO: Versatile fluorescent dyes for neuronal labelling and pathway tracing. Trends in Neurosci. *12*, 333-341.

Jat, P. S., and Sharp, P. A. (1989). Cell lines established by a temperature-sensitive simian virus 40 Large-T-Antigen gene are growth restricted at the nonpermissive temperature. Mol. Cell. Biol. *9*, 1672-1681.

Kaplan, M. P., Chin, S. S. M., Fliegner, K. H., and Liem, R. K. H. (1990). a-Internexin, a novel neuronal intermediate filament protein, precedes the low molecular weight neurofilament protein (NF-L) in the developing brain. J. Neurosci. *10*, 2735-2748.

Katz, L. C. (1987). Local circuitry of identified projection neurons in cat visual cortex brain slices. J. Neurosci. *7*, 1223-1249.

Katz, L. C., and Iarovici, D. M. (1990). Green fluorescent latex microspheres: A new retrograde tracer. Neuroscience *34*, 511-520.

Katz, L. C., Burkhalter, A., and Dreyer, W. J. (1984). Fluorescent latex microspheres as a retrograde neuronal marker for in vivo and in vitro studies of visual cortex. Nature *310*, 498-500.

Lee, H. J., Hammond, D. N., Large, T. H., Roback, J. D., Sim, J. A., Brown, D. A., Otten, U. H., and Wainer, B. H. (1990). Neuronal properties and trophic activities of immortalized hippocampal cells from embryonic and young adult mice. J. Neurosci. *10*, 1779-1787.

Lendahl, U., and McKay, R. D. G. (1990). The use of cell lines in neurobiology. Trends in Neurosci. *13*, 132-137.

Lendahl, U., Zimmerman, L. B., and McKay, R. D. G. (1990). CNS stem cells express a new class of intermediate filament. Cell *60*, 585-595.

Login, G. R., and Dvorak, A. M. (1985). Microwave energy fixation for electron microscopy. Am. J. Pathol. *120*, 230-243.

Lubbers, K., and Frotscher, M. (1987). Fine structure and synaptic connections of identified neurons in the rat fascia dentata. Anat. Embryol. *177*, 1-14.

McConnell, S. K. (1988). Fates of visual cortical neurons in the ferret after isochronic and heterochronic transplantation. J. Neurosci. *8*, 945-974.

Nolan, G. P., Fiering, S., Nicolas, J.-F., and Hersenberg, L. A. (1988). Fluorescence-activated cell analysis and sorting of viable mammalian cells based on b-D-galactosidase activity after transduction of *Escherichia coli lacZ*. Proc. Natl. Acad. Sci. USA *85*, 2603-2607.

Palay, S. L., and Chan-Palay, V. (1974). Cerebellar Cortex Cytology and Organization (Berlin: Springer-Verlag).

Price, J., and Thurlow, L. (1988). Cell lineage in the rat cerebral cortex: a study using retroviral-mediated gene transfer. Development *104*, 473-482.

Price, J., Turner, D., and Cepko, C. (1987). Lineage analysis in the vertebrate nervous system by retrovirus-mediated gene transfer. Proc. Natl. Acad. Sci. USA *84*, 156-160.

Rakic, P. (1974). Neurons in rhesus monkey visual cortex: Systematic relation between time of origin and eventual disposition. Science *183*, 425-427.

Ramon y Cajal, S. (1894). New Ideas on the Structure of the Nervous System in Man and Vertebrates. Translated from the French by N. Swanson and L.W. Swanson. (Cambridge: MIT Press).

Rogers, A. (1967). Techniques of Autoradiography (Amsterdam: Elsevier Printing Co).

Ryder, E. F., Snyder, E. Y., and Cepko, C. L. (1990). Establishment and characterization of multipotent neural cell lines using retrovirus vector-mediated oncogene transfer. J. Neurobiol. *21*, 356-375.

Sandell, J. H., and Masland, R. H. (1988). Photoconversion of some fluorescent markers to a diaminobenzidine product. J. Histochem. Cytochem. *36*, 555-559.

Sanes, J. R., Rubenstein, J. L. R., and Nicolas, J.-F. (1986). Use of a recombinant retrovirus to study post-implantation cell lineage of the mouse. EMBO J. *5*, 3133-3142.

Schlessinger, A. R., Cowan, W. M., and Gottlieb, D. I. (1975). An autoradiographic study of the time of origin and the pattern of granule cell migration in the dentate gyrus of the rat. J. Comp. Neurol. *159*, 149-176.

Schlessinger, A. R., Cowan, W. M., and Swanson, L. W. (1978). The time of origin of neurons in Ammon's horn and the associated retrohippocampal fields. Anat. Embryol. *154*, 153-173.

Schlessinger, J., Axelrod, D., Koppel, D. E., Webb, W. W., and Elson, E.L. (1977). Lateral transport of a lipid probe and labeled proteins on a cell membrane. Science *195*, 307-309.

Schmued, L. C., and Fallon, J. H. (1986). Fluoro-Gold: a new fluorescent retrograde axonal tracer with numerous unique properties. Brain Res. *377*, 147-154.

Temple, S. (1989). Division and differentiation of isolated CNS blast cells in microculture. Nature *340*, 471-473.

Thanos, S., and Bonhoeffer, F. (1987). Axonal arborization in the developing chick retinotectal system. J. Comp. Neurol. *261*, 155-164.

Topp, W. C. (1981). Normal rat cell lines deficient in nuclear thymidine kinase. Virology *113*, 408-411.

Turner, D. L., and Cepko, C. L. (1987). A common progenitor for neurons and glia persists in rat retina late in development. Nature *328*, 131-136.

Turner, D. L., Snyder, E. Y., and Cepko, C. L. (1990). Lineage-independent determination of cell type in the embryonic mouse retina. Neuron *4*, 833-845.

Wetts, R., and Fraser, S. E. (1988). Multipotent precursors can give rise to all major cell types of the frog retina. Science *239*, 1142-1145.

Witter, M. P. (1989). Connectivity of the rat hippocampus. In The Hippocampus New Vistas. V. Chan-Palay and C. Kohler, eds. (New York, NY: Alan R. Liss, Inc.), pp. 53-69.

Yen, S. E., and Fields, K. L. (1982). Antibodies to neurofilament, glia filament and fibroblast intermediate filament proteins bind to different cell types in the nervous system. J. Cell Biol. *88*, 115-126.

CHAPTER 6

IMMORTALIZED CLONAL STEM CELLS DIFFERENTIATE INTO HIPPOCAMPAL NEURONS AND ASTROCYTES

ABSTRACT

Immortal cell lines that behave as stem cells offer a powerful method to explore lineage mechanisms and neuronal function in the brain. We demonstrate that an immortalized cell is stable to sub-cloning *in vitro* and differentiates to neurons and astrocytes *in vivo*. A stem cell-specific gene is down regulated and neuronal or astrocytic genes are expressed when the clonal cells are grafted into the developing hippocampus or cerebellum. Moreover, the expression of *c-fos* is regulated similarly by endogenous granule neurons and the implanted neurons during seizure activity. These results show that the immortalized cell has stem cell properties and is stable for long periods *in vitro*. The differentiation of cultured cells into astrocytes or functional neurons that are fully integrated into the host tissue may provide powerful approaches to the analysis of brain development, function, and repair in mammals.

This chapter was adapted from a submitted manuscript authored by Miles G. Cunningham, Patricia J. Renfranz, Lisa Arel, & Ronald McKay.

Introduction

Immortalized cell lines have recently shown great potential as a tool to help elucidate the complex mechanisms controlling brain development and function. These cells can be precisely altered genetically, or their culture environment manipulated, and they can then be implanted into specific regions of the developing or adult brain. In a previous report, we demonstrated that an immortalized hippocampal stem cell line (HiB5) can differentiate into cells morphologically similar to neurons and astrocytes upon grafting into the developing brain (1). Snyder et al. (2) reported similar results based on transgene expresson, immunocytochemical staining, and electron microscopy for an immortalized cerebellar stem cell line grafted back into the developing cerebellum. There are important implications of these results for the use of such paradigms in studies of the molecular mechanisms of brain development, plasticity, and repair - particularly in light of the advancing technology in gene targeting. However, the future success of such approaches depends upon an understanding of many questions: Are the cells in culture genetically identical, that is, is the cell line clonal? Is the cell line stable for long periods in culture? Do the cells behave as progenitor cells - do they integrate into the host tissue and function normally? While our previous work demonstrated the differentiation of implanted HiB5 cells based on positional and morphological criteria, the clonality and stability of this cell line was not formally

established nor was gene expression or other indicators of normal functionality assessed. The present report addresses these issues.

In these experiments, we first establish unequivocally that HiB5 is a clonal cell line. Retovirally-infected subclones are shown to maintain the differentiation potential of the parent line through repeated passaging and cycles of cryopreservation. We demonstrate that implanted clonal cells differentiate to express neuronal and astrocytic genes indicating differentiation to multiple fates. Furthermore, we demonstrate that implanted cells integrated into the hippocampal circuitry show rapid responses in gene expression expected of normal hippocampal neurons.

MATERIALS AND METHODS

Southern Blotting Genomic DNA was prepared from the HiB5 cell line and its subclones following a modification of the proteinase K procedure. Approximately 25 mg of each of the genomic DNA samples was digested to completion with *Eco*R1. 5-10 mg of restriction-enzyme digested genomic DNA was separated by electrophoresis through an 0.8% agarose gel, then was transferred to GeneScreenPlus (Dupont/NEN) by capillary action. A standard curve derived from the 1 Kb DNA Ladder (Gibco/BRL) was used to estimate the size of restriction fragments. The Tag DNA insert and *lacZ* DNA insert were liberated from the appropriate plasmid vectors (gifts of T. Hayes) after digestion with *Bam*H1. The restriction fragments were purified from LMP agarose, and labelled with [^{32}P]-dCTP using the random priming

method (reagent mix gift of T. Hayes) to a specific activity greater than $3x10^8$ dpm/mg. Prehybridization, hybridization at 42° C, washing, and rehybridization were performed according to the manufacturer's directions. Probe and carrier DNA were added to a concentration of 2.5 x 10^6 dpm/ml and 200 mg/ml, respectively. The Southern blot was first probed with Tag, then, rehybridized with the *Bam*H1-fragment of the BAG7 vector.

Implantation and Analysis Prior to grafting, HiB5 cells were labeled in the culture dish with tritiated thymidine ([^{3}H]thymidine, New England Nuclear, Boston, MA) and with green fluorescent latex microspheres (green beads, Lumafluor, Inc., New City, NY) as described (1,4). Cell suspensions of each cell line (HiB5, HiB5B-21, and HiB5B-27) were prepared at a density of 3 x 10^4 cells per µl in calcium- and magnesium-free Hank's balanced salt solution. The subjects were postnatal day-2 (P2) Sprague-Dawley rats housed with their mothers in clear plastic cages, maintained on a 12 hr light/12 hr dark schedule with food and water provided ad libitum. For each cell line, 12-15 animals were grafted with 1 µl of the cell suspension into the right dentate gyrus and the right cerebellar hemisphere. In addition, 9 control animals received freeze-thaw killed labeled HiB5 cells. Grafting was performed using a stereotaxic technique (4,5). Animals were sacrificed at 3-4 and 6-8 weeks after grafting and perfused with isotonic saline followed by 4% paraformaldehyde in 0.1 M phosphate buffer. Seizures were induced 8 weeks after grafting with KA as described (6) or with PTZ

(7). These animals were sacrificed 1, 3, 12, and 24 hours after the onset of epileptiform behavior. Cryostat sections 10-30 μm thick were immunoreacted using standard procedures. The anti-Calbindin antiserum (Sigma Immunochemicals, St. Louis, MO) was diluted 1:200, anti-FOS antiserum (Cambridge Research, Wilmington, DE) was diluted 1:2000, and anti-GFAP antiserum (ICN ImmunoBiologicals, Irvine, CA.) was diluted 1:500. Nestin immunoreactivity was detected using the monoclonal antibody Rat 401 (8) and biotin-conjugated secondary antibody. Antibody complexes were visualized using Vectastain Avidin DH/Biotin-peroxidase complex kit (Vector Labs, Inc., Burlingame, CA). Control tissue for all immunoreactions was processed by deleting the primary antibody from the protocol. For tissue developed with diaminobenzidine, the sections were further processed using standard autoradiography methods (9). For epifluorescence microscopy, the primary antibody was visualized with the Texas Red Avidin D/Biotin Vectastain kit. Sections were observed as 1.8 μm-thick optical sections using confocal microscopy (Biorad MR600).

RESULTS

Southern analysis of HiB5 cells The HiB5 cell line was immortalized from an embryonic day-16 rat hippocampal primary culture by the *tsU19* allele of SV40 T-antigen (Tag) (1). Sub-lines of the parental line were isolated following infection with the BAG retrovirus (10). Genomic Southern analysis with DNA probes specific for the two retroviruses was used to determine whether the

sublines were independent clones (Figure 1). The T-antigen probe revealed only one site of retroviral insertion in the parent HiB5 line, as indicated by the presence of a single 8.8 kb *Eco*R1 fragment (Figure 1A). The same 8.8 kb fragment is present in both early- and late-passage cells. Each of the HiB5 sub-lines also carries this 8.8 kb *Eco*R1 fragment. Two of the sub-lines have an additional band of equal intensity to the 8.8 kb band; these bands are probably the result of a rearrangement common in Tag-immortalized cells (11,12,13). When the same blot is hybridized with a probe specific for the BAG retrovirus (Figure 1B), each sub-line is shown to have a different hybridizing band and therefore a unique integration site, demonstrating that the sub-lines are independent subclones.

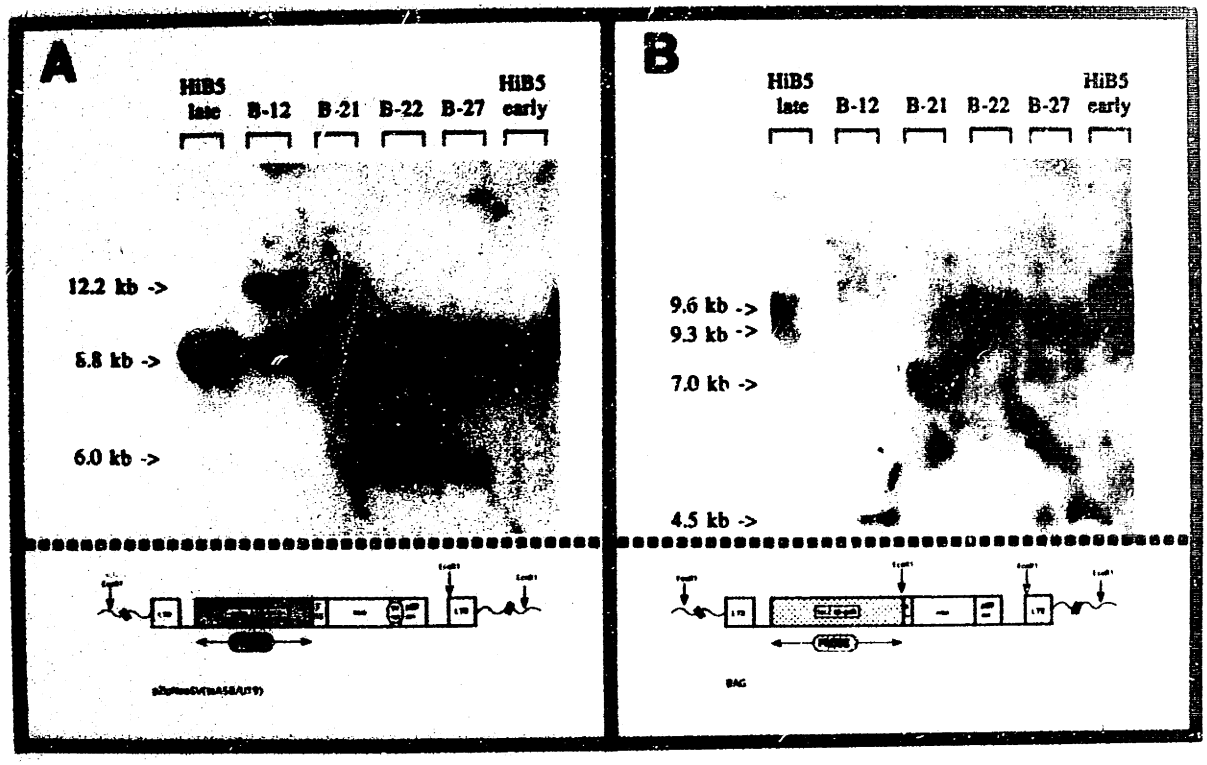
A
HiB5 late
B-12
B-21
B-22
B-27
HiB5 early
12.2 kb ->
6.8 kb ->
6.0 kb ->
B
HiB5 late
B-12
B-21
B-22
B-27
HiB5 early
9.6 kb ->
9.3 kb ->
7.0 kb ->
4.5 kb ->
BAC

FIGURE 1

Southern blot analysis of the HiB5 cell line and four of its subclones.

Genomic DNA was prepared from early- and late-passage HiB5 cells, and from the four subclones HiB5B-12, -21, -22, and -27, which were isolated after infection with the BAG retrovirus (1). DNA was digested with restriction endonuclease *Eco*R1, then analyzed by Southern blot. As shown in the diagrams, a genomic *Eco*R1 fragment that contains either the Tag or *lacZ* sequences will result from cleavage at one site within the provirus and one site from the left-side flanking DNA.

A. When the Southern blot was probed with the Tag insert, an 8.8 kb band was revealed in all the lanes. An additional 12.2 kb band was present in the HiB5B-12 genome, and a 6.0 kb band was present in the HiB5B-22 genome.

B. When the Southern blot was reprobed with *lacZ* DNA, a unique band was revealed in each of the subclones. Thus, each subclone is shown to be an independent derivative of the original parent HiB5 cell line.

Two of the subclones, HiB5B-21 and HiB5B-27, were chosen for grafting studies, as they do not show rearrangements in the retroviral genome. Cells were labeled in culture with [^{3}H]thymidine and with green fluorescent latex microspheres (green beads), and implanted into the postnatal day-2 (P2) rat dentate gyrus or cerebellum. After a survival time of three to eight weeks, brain sections were immunostained to test whether implanted cells could express neuronal or astrocytic antigens. HiB5, HiB5B-21, and HiB5B-27 cell lines gave identical results in these experiments.

Immunohistochemistry with neuronal and glial markers The intermediate filament protein, nestin, is expressed in neuroepithelial precursor cells (14,15) and HiB5 cells in culture (1). At the time of implantation, the hippocampus is nestin-positive as are the cells in the graft itself (Figure 2A). Within three weeks of implantation, the endogenous cells and the engrafted cells have lost their nestin immunoreactivity (Figure 2B & C). This observation is consistent with the down-regulation of the nestin gene normally seen during differentiation of the nervous system.

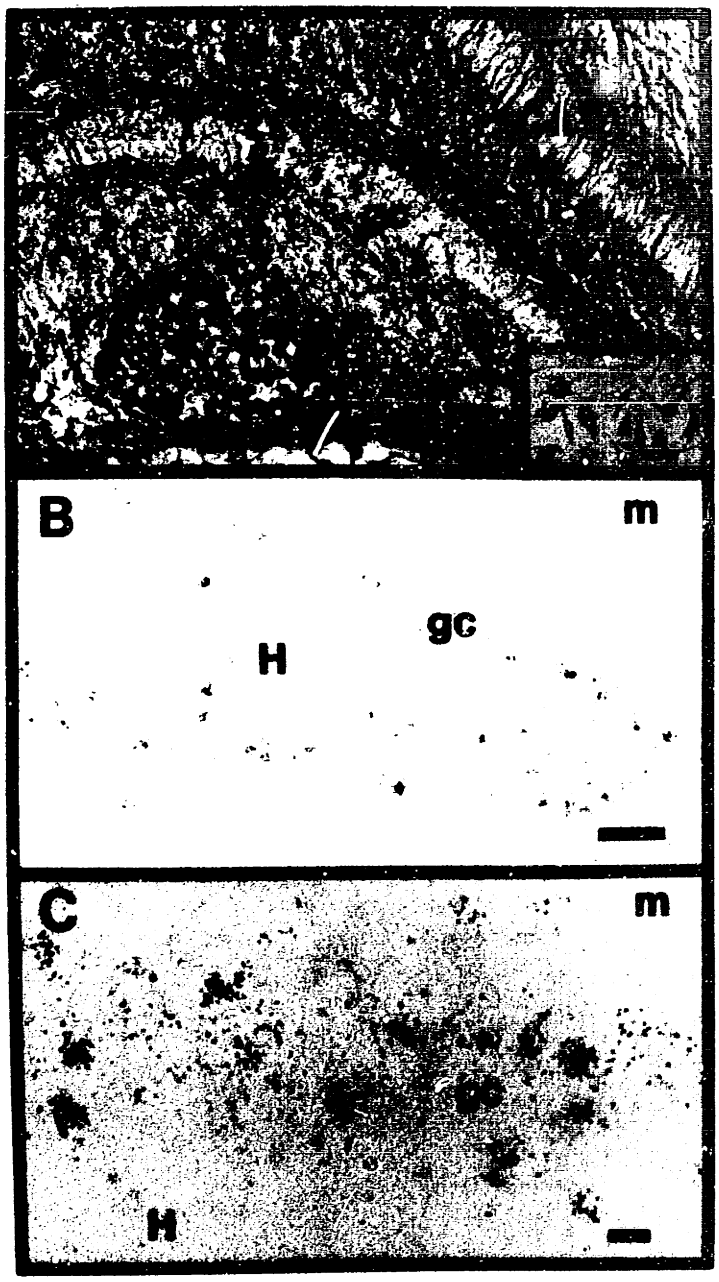
B
m
gc
H
C
m
H

FIGURE 2

Nestin is down-regulated during hippocampal differentiation

A. Immediately after implantation, the P2 dentate gyrus and the HiB5 cells contained in the graft (G) are strongly immunoreactive for the nestin protein. HiB5 cells are nestin-positive in culture (*inset*). Bars = 100 μm.

B. At 3 weeks of age, the dentate gyrus has completed its development and is no longer immunoreactive for nestin. Implanted [^{3}H]thymidine-labeled HiB5 cells have integrated into the granule cell layer and have also down-regulated nestin. Each grafted cell is represented by a cluster of silver grains overlying its soma. Bar = 100 μm.

C. High power view of granule cell layer three weeks after implantation showing integrated HiB5 cells devoid of nestin staining. Bar =10 μm.

CA1, CA1 field of the hippocampus; gc, granule cell layer; H, hilus; m, molecular layer.

Calbindin (CB) is a neuron-specific calcium binding protein expressed in some dentate gyrus granule neurons and in some pyramidal neurons but not in cerebellar granule neurons (16,17). In culture, HiB5 cells do not express this protein. After grafting, many implanted cells, identified by both [^{3}H]thymidine- and green bead-labeling, are found in the granule cell layer and are CB-positive (Figure 3A, B, C and E). Grafted cells found outside the granule cell layer (i.e., in the hilus and molecular layer) are CB-negative (Figure 3A, B and C). When HiB5 cells are implanted into the P2 cerebellum, they do not differentiate to express CB (Figure 3D). These cells preferentially localize to the granular layer (1) and, like endogenous cerebellar granule neurons, become immunoreactive for neuron-specific enolase (data not shown). These experiments demonstrate that the expression of CB in grafted HiB5 cells is differentially regulated in the hippocampus and the cerebellum. Neuronal antigen expression is consistent with previous morphological data suggesting that the HiB5 stem cell line generates neuronal types appropriate to the transplant site and stage of development (1).

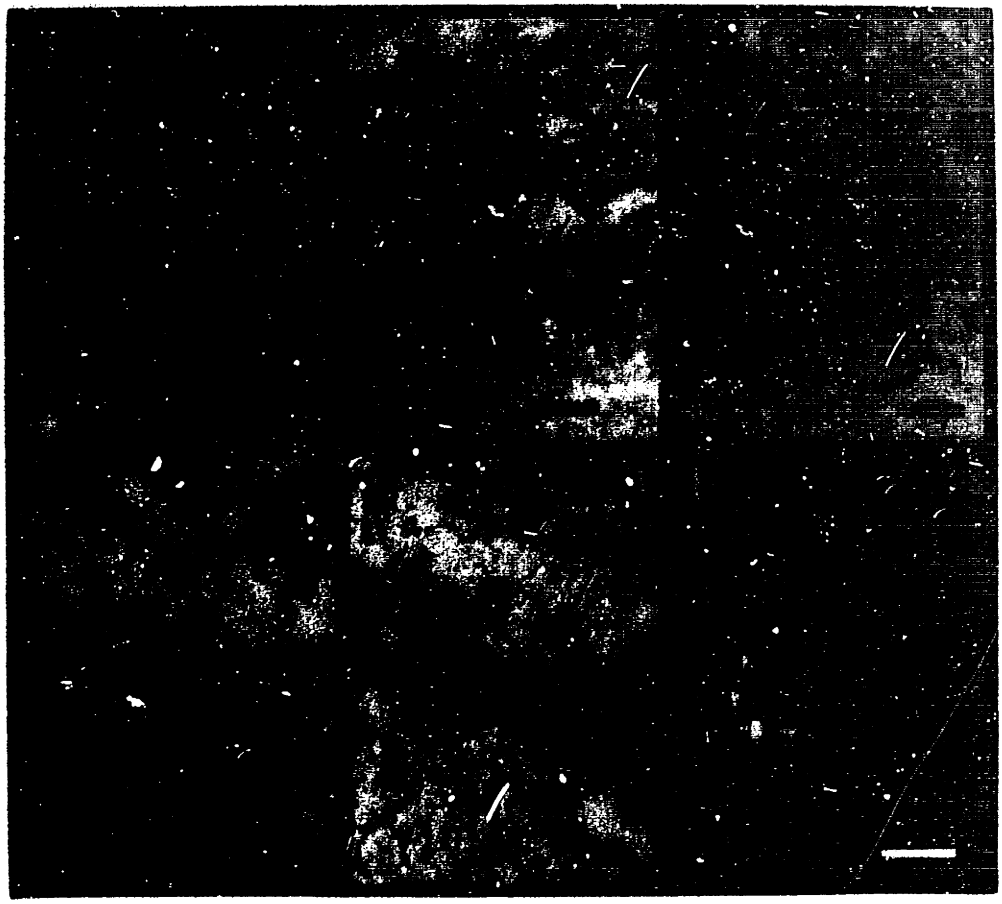

FIGURE 3

Calbindin (CB) immunostaining of grafted dentate gyrus and cerebellum.

A (HiB5), **B** (HiB5B-21), and **C** (HiB5B-27). Grafted cells located in the granule cell layer (gc) are CB-positive. Their cell bodies are immunoperoxidase-stained for CB and are overlaid with silver grains (arrows). Labeled cells outside the granule cell layer are CB-negative (arrowheads). At least 40% of the cells originally grafted are found in the granule cell layer (1). Of these, 80% are positive for CB.

D. HiB5 cells grafted into the cerebellum (arrows) do not express CB, unlike the strongly CB-positive Purkinje cells (arrowhead).

E. A confocal microscopic image of a green bead-labeled HiB5 cell (arrow) that has integrated into the granule cell layer of the dentate gyrus. The yellow-green microspheres can be seen in the same 1.8 μm - focal plane as the (red) cytoplasmic CB stain. Nuclei are devoid of stain and appear black. Bars: A = 50 μm, B-E = 10 μm.

g, granular layer of cerebellum. gc, granule cell layer of the dentate gyrus. H, hilus. m, molecular layer of the cerebellum. P, Purkinje cell layer of the cerebellum.

In the hippocampus, many grafted cells lie outside the granule cell layer. These cells are nestin- and CB-negative but express the astrocyte-specific intermediate filament protein, glial fibrillary acidic protein (GFAP) (18) (Figure 4A, B, & E). GFAP-positive HiB5 cells can also be identified in the cerebellum, where a specialized astrocytic cell type, the Bergman glia, is found (19). Bergman glial cells have a stereotypical morphology with radial, GFAP-positive processes running from their somas near the Purkinje cell layer, across the molecular layer toward the pial surface. Examples of [^{3}H]thymidine-labeled HiB5 cells with GFAP-positive processes like those of Bergman glia are shown in Figure 4, panels C and D. HiB5 cells thus acquire glial as well as neuronal fates appropriate to the implantation site.

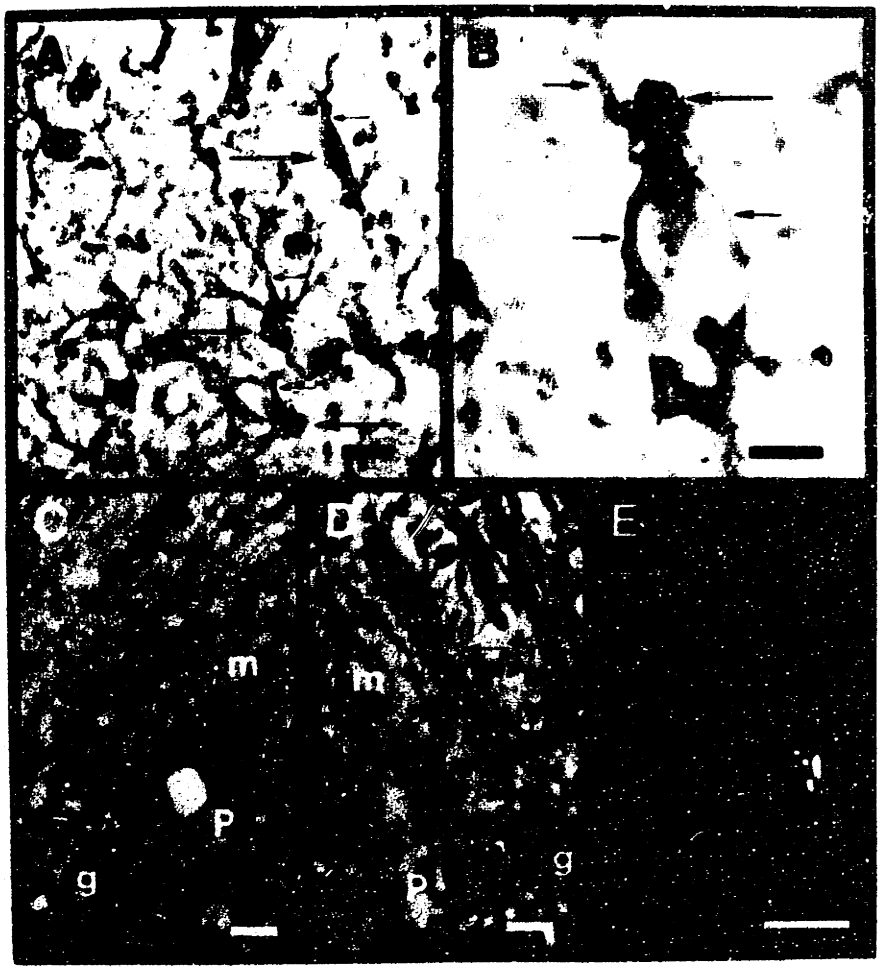
B
C
D
E
m
m
P
P
g
g

FIGURE 4

Implanted cells in the dentate gyrus and in the cerebellum express glial fibrillary acidic protein (GFAP).

A. [^{3}H]thymidine-labeled HiB5B-21 cell bodies (large arrows) in the molecular layer of the dentate gyrus extend GFAP-positive processes (small arrows). The nuclei are stained with cresyl violet. Many cells show GFAP expression; in the CA1 subfield 64±10% of the [^{3}H]thymidine-labeled cells were also GFAP-positive.

B. High power view of a GFAP-positive HiB5B-27 cell in the hilar region.

C (HiB5) & D (HiB5B-21). Cells grafted into the cerebellum assume positional, morphological, and antigenic characteristics of Bergmann glia.

E. A confocal image of a HiB5 cell in the hilus of the dentate gyrus labeled with green beads and positive for GFAP. All bars=10 μm.

g, granular layer of the cerebellum. m, molecular layer of the cerebellum. P, Purkinje cell layer of the cerebellum.

Kainic acid and PTZ induction of c-fos in grafted cells

Many experiments have shown that immediate early gene induction is a consequence of trans-synaptic stimulation (20,21,22). Up-regulation of the immediate early gene, *c-fos* , was used to further explore the properties of grafted cells in the granule cell layer. Seizure activity produced by kainic acid (KA) or pentylenetetrazol (PTZ) is known to induce c-*fos* protein(s) (e.g., FOS) in dentate gyrus granule neurons (6,7,23). Kainic acid, a glutamate agonist, produces a stereotyped limbic motor syndrome (24). In contrast, the GABA antagonist PTZ (25), produces a full-scale tonic-clonic seizure with a rapid onset. Both paradigms were used in the present studies to test the response of engrafted cells to these differing seizure etiologies.

Three hours after administration of KA, FOS is strongly expressed by dentate gyrus granule cells (Figure 5A). In animals carrying [^{3}H]thymidine or green bead-labeled HiB5 cells, only those cells that have integrated into the granule cell layer express FOS in response to KA (Figure 5B, C and E). Seizures produced with PTZ also result in the expression of FOS by grafted cells in the granule cell layer (Figure 5D). FOS staining peaks 3-4 hours after drug treatment and decreases over the following 10-12 hours. The time course and magnitude of FOS expression by HiB5 cells parallels that of endogenous granule neurons.

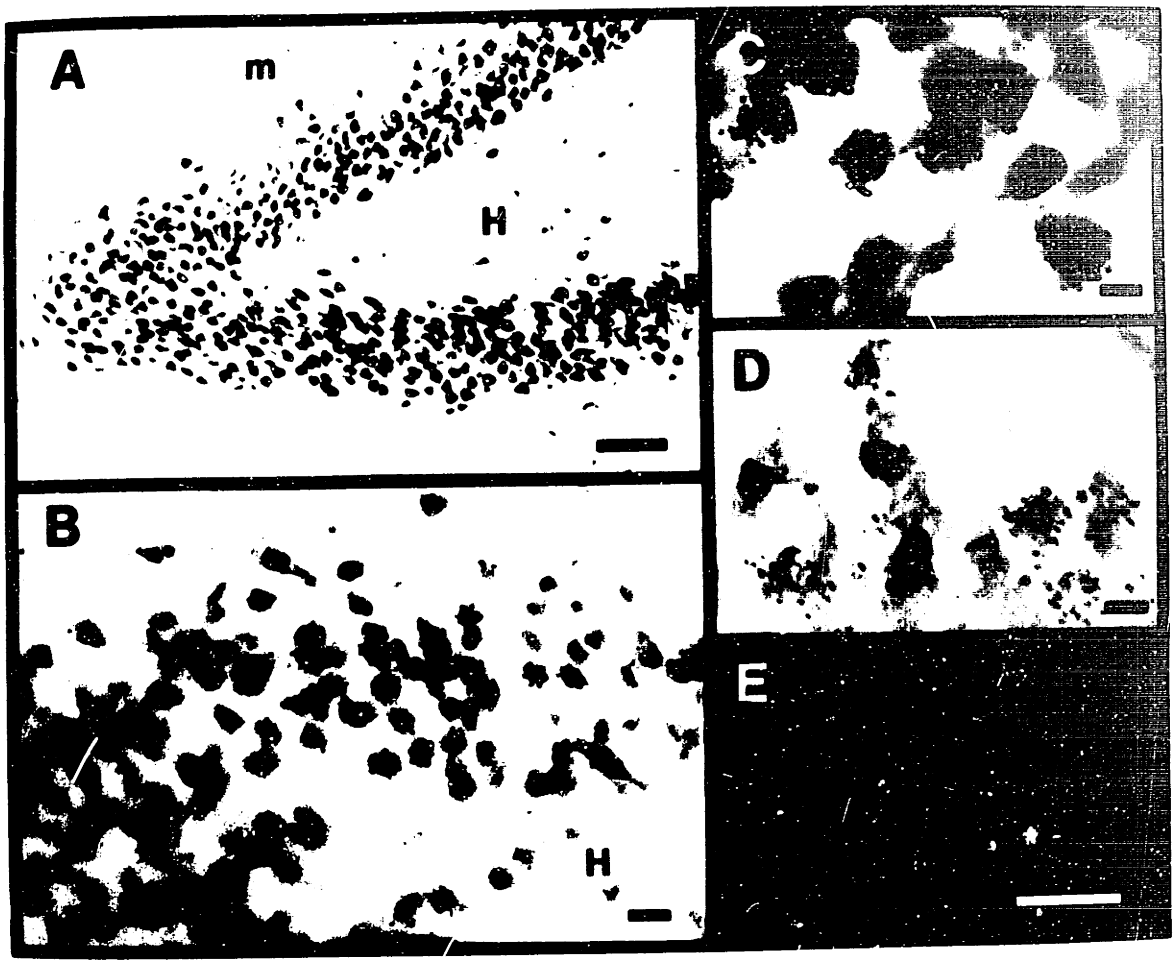
A
m
H
B
H
C
D
E

FIGURE 5

FOS immunostaining of dentate gyrus granule cells after KA and PTZ administration.

A. FOS immunostaining of the dentate granule neurons three hours after administration of kainic acid. In this section, counterstained with cresyl violet, Fos-negative granule cells can also be seen. Bar=100 μm.

B. [^{3}H]thymidine-labeled HiB5 cells which have integrated into the granule cell layer up-regulate Fos in response to KA; 66± 4% of the [^{3}H]thymidine-labeled HiB5 cells are Fos positive. Bar=10 μm.

C. High power view of HiB5B-27 cells which have up-regulated c-fos in response to KA. Bar = 5 μm.

D. High power view of HiB5B-27 cells which have up-regulated c-fos in reponse to PTZ. Expression of c-fos with PTZ treatment is weaker than with KA. Bar = 5 μm.

E. A confocal microscopic image of green bead-labeled HiB5 cells in the granule cell layer. The green microspheres are seen surrounding the (red) nuclear FOS stain. Bar=5 μm. *m, molecular layer. H, hilus.*

DISCUSSION

The experiments reported here use Southern blotting to establish the clonality of an immortalized hippocampal cell line. The differentiation of these stable, nestin-positive cells is demonstrated by the expression of cell type-specific antigens after transplantation. These results show that a clonal cell can differentiate efficiently into both neurons and astrocytes in the hippocampal dentate gyrus and in the cerebellum. Fate mapping studies have previously demonstrated that the astrocytic Muller glial cell and retinal neurons have a common precursor (26-28). Even though many other experiments show neurons and glia sharing a common progenitor (29-32), the origin of astrocytes in the central nervous system is still poorly understood. For example, fate mapping has shown that hippocampal pyramidal neurons and astrocytes are rarely in the same clone (33). The results presented here demonstrate that hippocampal neurons and astrocytes can efficiently arise from a common progenitor. They indicate that the stem cell properties of HiB5 cells are stable for long periods *in vitro*. Furthermore, astrocytes and neurons in the cerebellum can be derived from this hippocampus-derived clonal cell. These transplantation results extend previous fate mapping experiments and focus attention not only on the lineage of progenitor cells but on local signals in the developing brain that regulate fate choice by multipotential stem cells. The plasticity of differentiation

of HiB5 cells is similar to that observed for neuronal and glial stem cells in the peripheral nervous system (34, 35).

The dentate granule neuron is of great physiological interest as it exhibits long term potentiation and is a major component in the hippocampal circuit that mediates declarative learning in mammals (36, 37). Our previously published work suggested, on morphological grounds, that HiB5 cells differentiate into hippocampal granule neurons. The immunocytochemical data presented in this paper confirms this conclusion. The expression of calbindin by HIB5 cells implanted in the hippocampus, and the lack of calbindin expression in cells implanted into the cerebellum, shows that HiB5 cells differentiate to distinct neuronal fates in these two structures. This result raises the interesting possibility that only one neuronal progenitor type exits in the CNS. The response of hippocampal granule neurons in seizures induced by kainic acid or PTZ was used to more rigorously analyze the identity of the engrafted neurons. The up-regulation of c-*fos* during seizure activity suggests that implanted cells become functionally integrated into the neuronal circuitry.

REFERENCES

1. Renfranz, P. J., Cunningham, M. G. & McKay, R.D.G. *Cell* 66, 713-729 (1991).

2. Snyder, E.Y., Deitcher, D.L., Walsh, C., Arnold-Aldea, S., Hartwieg, E.A., & Cepko, C.L. *Cell* 68, 33-51 (1992).

3. Ausubei, F.M. et al., eds. Short Protocols in Molecular Biology: A Compendium of Methods from Current Protocols in Molecular Biology, John Wiley & Sons, New York (1989).

5. Cunningham, M.G. & McKay, R.D.G. (1993b)*Neuroprotocols* in press.

4. Cunningham, M.G. & McKay, R.D.G. (1993a) *J. Neurosci. Meth.* in press.

6. Popovici, T., Represa, A., Crepel, V., Barbin, G, Beaudoin, M, & Ben-Ari, Y. *Brain Research* 536, 183-194 (1990).

7. Dragunow, M. & Robertson, H.A. *Neuroscience Letters*, 82, 157-161 (1987).

8. K. Frederiksen & R.D.G. McKay,*J. Neurosci.* 8, 1144 (1988).

9. Rogers, A. Techniques of Autoradiography, Elsevier Printing Co., Amsterdam (1967).

10. Price, J., Turner, D. & Cepko, C. *Proc. Natl. Acad. Sci. USA*, 84, 156-160 (1987).

11. Bender, M.A., & Brockman, W.W. *J. Virol.* 38(3), 872-879 (1981).

12. Sagar, S. M., Sharp, F. R., & Curran, T. *Science* 240,1328-1331 (1988).

13. Gurney, T. & Gurney, E.G. *J. Virol.* 63(1), 165-174 (1989).

14. Frederiksen, K., & McKay, R.D.G. *J. Neurosci.* 8, 1144-1151 (1988).

15. Lendahl, U., Zimmerman, L.B., & McKay, R.D.G. *Cell* 60, 585-595 (1990).

16. Feldman, S. C., & Christakos, S. *Endocrinology,* Volume 112 (1), 290-302 (1983).

17. Baimbridge, K.G., & Miller, J.J. *Brain Res.* 245, 223-229 (1982).

18. Bignami, A., Eng, L.F., Dahl, D., and Uyeda, C.T. *Brain Res* 43, 429-435 (1972).

19. Palay, S.L., and Chan-Palay, V. Cerebellar Cortex Cytology and Organization, Springer-Verlag, Berlin (1974).

20. Hunt, S. P., Pini, A., & Evan, G. *Nature* 328, 632-634 (1987).

21. Sagar, S.M., Sharp, F.R,., Curran, T. *Science* 240,1328-1331 (1988).

22. Shin, C., McNamara, J. O., Morgan, J. I., Curran, T., Cohen, D. R. *J. Neurochem.* 55, 1050-1055 (1990).

23. Morgan, J.I., Cohen, D.R., Hempstead, J.L. & Curran, T. *Science* 237, 192-197 (1987).

24. Ben-Ari, Y., Tremblay, E., Riche, D., Ghilini, G., & Naquet, R. *Neuroscience* 6 (7), 1361-1391 (1981).

25. Corda, M.G., Giorgi, O., Longani, B., Orlandi, M., & Biggio, G. *J Neurochem* 55(4),1216-1221 (1990).

26. Wetts, R. & Fraser, S.E. *Science* 239,1142-1145 (1988).

27. Holt, C.E., Bertsch, T.W., Ellis, H.M., & Harris, W.A. *Neuron* 1, 15-26 (1988).

28. Turner, D.L. & Cepko, C.L. *Nature* 328, 131-136 (1987).

29. J.R. Sanes, J.L.R. Rubenstein, J.-F. Nicolas, *EMBO* J 5, 3133 (1986).

30. B.P. Williams, J. Read, J. Price, *Neuron* 7, 685 (1991).

31. E. Frank & J.R. Sanes, *Development* 111, 895 (1991).

32. M. Bronner-Fraser & S. Fraser, *Neuron* 3, 755 (1989).

33. E.A. Grove, T.B.L. Kirkwood, J. Price, *Neuron* 8, 217 (1992).

34. A. Baroffio, E. Dupin, & N.M. LeDouarin, *PNAS* 85, 5325 (1988).

35. D.L. Stemple & D.J. Anderson, *Cell* 71, 973 (1991).

36. Bliss, T.V. and Lømo, T., *J. Physiol.* 232, 331-356 (1973).

37. Morris, R.G.M., Garrud, P., Rawlins, J.N.P., O'Keefe, J., *Nature* 297, 681-683 (1982).

CHAPTER 7

FUNCTIONAL INTEGRATION OF AN IMMORTALIZED CELL LINE: AN ELECTRON MICROSCOPIC ANALYSIS AND ELECTROPHYSIOLOGICAL ASSAY

ABSTRACT

Previous work has shown that the hippocampal stem cell line, HiB5, immortalized with the temperature-sensitive allele, tsA58 of SV40 T-antigen, differentiates into granule neurons within the developing dentate gyrus. In the present studies, electron microscopy revealed that HiB5 cells, labeled with colloidal gold-conjugated latex microspheres, establish intimate contact with host cells and show ultrastructural features characteristic of dentate gyrus granule neurons. During the induction of long-term potentiation (LTP) of the perforant path-granule cell synapse, endogenous granule neurons specifically and consistently up-regulate the immediate early gene, NGFI-A. The mechanisms regulating LTP and the expression of NGFI-A appear to be closely associated, although the precise relationship is not known. The present report demonstrates that HiB5 cells engrafted into the granule cell layer express NGFI-A during the induction of LTP in a manner identical to host dentate gyrus granule neurons. These data illustrate the capability of HiB5 cells to integrate into the host structure and to establish appropriate synapses. Our results also exemplify the potential utility of such cell lines in the study of plasticity in the central nervous system, not only at the cellular or structural level, but also at the level of the synapse.

This chapter was adapted from a manuscript in preparation authored by Miles G. Cunningham, Ursula Staubli, Jeffrey Macklis, Carlos Vicario, & Ronald D.G. McKay.

INTRODUCTION

Tetanic stimulation of the perforant path-granule cell (pp-gc) synapse results in an increase in the postsynaptic response to subsequent baseline stimulation (Bliss & Lømo, 1973). This long-term potentiation (LTP) of synaptic efficacy is viewed as a model for neural plasticity and, more specifically, memory storage.

NGFI-A, synonomous with zif/268 (Christy et al.,1988), Egr-1 (Sakhatme,1988), and Krox 24 (Lemaire,1988), is an immediate early gene (IEG) which encodes a zinc finger protein homologous to other transcriptional regulatory proteins. In PC12 cells, NGFI-A is rapidly activated by nerve growth factor (NGF) concomitant to neurite extension and up-regulation of other genes, including c-*fos* (Milbrandt, 1987, Day et al., 1990). Immunostaining with antibodies against NGFI-A has shown that the protein is constituitively expressed by a variety of neurons in the central nervous system; moreover, cells in many brain regions up-regulate the gene in response to seizure activity (Mack et al.,1990). Sukhatme et al. (1988) showed that NGFI-A mRNA increases after membrane depolarization and speculated that NGFI-A may act as an early nuclear intermediary in signal transduction. Such immediate genomic responses may link short-term synaptic events to long-term or permanent events in neural plasticity (Dragunow & Robertson, 1987, Sheng & Greenberg, 1990).

It is now well established that NGFI-A mRNA and proteins increase in granule neurons with the induction of long-term potentiation (LTP) in the dentate gyrus (Wisden et al.,1990). The up-regulation is specific for this gene, as increases in NGFI-B, c-*fos*, c-

jun, *jun*-D, serum response factor, and PC4 are not detected. LTP induction is mediated through the NMDA receptor (Collingridge, 1983), which when antagonized by APV (Wisden, 1990) or MK801 or CGS-19755 (Cole, 1989), blocks the up-regulation of NGFI-A as well as the induction of LTP.

Cell lines derived from the central nervous system have shown promise in serving as tools in many areas of neurobiology, including development and cell replacement in cases of brain disfunction. The hippocampus-derived, immortalized stem cell line, HiB5, has previously been shown to integrate into the developing dentate gyrus and assume positional, morphological, and antigenic characteristics of granule neurons and astrocytes (Renfranz et al., 1991; Cunningham et al., submitted). Moreover, during drug induced seizure activity, HiB5 cells residing in the granule cell layer up-regulate the immediate early gene c-*fos*. thus suggesting that the cells have integrated into the neuronal circuitry. The present report addresses whether the implanted cells found in the dentate gyrus granule cell layer integrate normally on the ultrastructural level with endogenous cells and whether the engrafted cells establish functional synaptic connections. Electron microscopy was used to study the fine structure and the interactions of HiB5 cells with host cells. The capacity of transplanted cells to establish appropriate and functional synaptic connections was assessed by examining the up-regulation by engrafted cells of NGFI-A in response to electrical stimulation inducing LTP in dentate gyrus granule neurons. This approach, although indirect, has the benefits of inferring LTP induction in grafted cells within an intact system as well as assessing whether

normal gene regulation occurs in response to trans-synaptic activation of a specific neural circuit.

METHODS

The HiB5 cell line. The isolation of the HiB5 cell line has been previously described (Renfranz et al., 1991). Briefly, primary cultures of embryonic day-16 rat hippocampus were made and infected 18 hours after plating with a retrovirus transducing the tsA58/U19 double-mutant T antigen gene coupled to a gene conferring neomycin resistance (Frederiksen et al., 1988; Jat & Sharp, 1989). HiB5 was one of the expanded drug-resistant colonies which stained positively for the neural epithelial stem cell antigen (nestin). Southern blotting has demonstrated that the HiB5 cell line is clonal and stable indefinitely in culture (Cunningham et al., submitted).

Subjects. A total of 26 male and female Sprague-Dawley (Taconic, Germantown, NY) newborn rats were grafted. They were housed in clear plastic cages and maintained on a 12 hr light / 12 hr dark cycle. Food and water were provided *ad libitum*.

Implantation. Preparation of cell suspensions and implantation have been previously described (Renfranz et al., 1991; Cunningham & McKay, 1993). HiB5 cells were incubated with 0.2 µCi [^{3}H]thymidine (New England Nuclear, Boston, MA) per ml of DMEM+10% FCS over two days. [^{3}H]thymidine was renewed every 8 hours. Cells were labeled with red fluorescent microspheres (red

beads) (Lumafluor, Inc., NJ) or a 1:1 mixture of normal and colloidal gold-conjugated red nanospheres (Madison et al., 1990; gift of Prof. C. Thies, Washington University) diluted 1000-fold in DMEM+10% FCS for 12 hours. Labeled cells in culture were then rinsed three times with calcium and magnesium-free (CMF) Hank's solution, trypsinized, and centrifuged 5 min at 1000 rpm. The pellet was diluted with CMF Hank's to obtain a final density of 30,000 cells per µl. Viability of the grafting suspension was invariably $\geq$ 95% as determined with the trypan blue dye exclusion test. Postnatal-day-2 (P2) rats were hypothermically anesthetized and positioned in a hypothermic miniaturized stereotaxic instrument (Cunningham neonatal rat adaptor, Stoelting Co., Wood Dale, IL) combined with a standard stereotaxic instrument (Stoelting Co.). Hippocampal implants with a volume of 0.25 µl were placed bilaterally at the following coordinates: 1.8 mm lateral to midline, 1.2 mm posterior to bregma, and 2.1 mm below dura. Three weeks after grafting, 3 subjects were processed for electron microscopy, and eight weeks after grafting, 19 subjects underwent electrophysiological analysis.

Electron Microscopy. Subjects were deeply anesthetized and transcardially perfused with 4% paraformaldehyde and 0.5% glutaraldehyde in 0.1 M phosphate buffer. Brains were removed, blocked, and postfixed for 3 hrs in the same fixative. Sections 250 µm thick were cut on a vibrating microtome, cellular fluorescence was observed at low magnification in wet mounts, and regions containing transplanted cells were microdissected into PBS with 20% sucrose. Tissue was osmicated, dehydrated in serial ethanol grades,

embedded, and 60-80 nm thin sections were stained with uranyl acetate and lead citrate. Sections were viewed and photographed on a JEOL 1200 CX (80 kv) electron microscope.

Electrophysiology. Adult rats were anesthetized with 1.5 mg/kg i.p. urethane and placed in a stereotaxic instrument. A monopolar, 125 μm diameter, stainless steel stimulating electrode was positioned in the entorhinal cortex 8.1 mm posterior to bregma and 4.5 mm lateral to midline. A 75 μm diameter, platinum-iridium recording electrode was lowered in the rostral hippocampus 3.8 mm posterior to bregma and 2.4 mm lateral to midline. Stainless steel wires were placed in the frontal cortex (via skull screws) as reference and ground. The electrode positions were optimized so as to produce a maximal positive response using as a guide the laminar profile of field responses to stimulation of the perforant path. Stimulation pulses were provided by a custom built digital stimulator that allows precise and reproducible timing parameters and electrode current intensity. Responses recorded from the microelectrode in the hippocampus were amplified (X10) using a two-channel FET operational amplifier mounted onto the microdrive of the stereotaxic instrument and were then fed into a second stage amplifier set to a gain of X100 and a band pass of 1-3000 Hz. Evoked responses to single pulse and burst stimulation were digitized (5-20 KHz and analyzed on line with custom made software. Test pulses (biphasic, width of 150 μs) were delivered using a stimulation intensity (105 ± 5 μA) required to elicit a field potential with a minimal population spike. A test pulse was delivered every 40 s for 20 min to establish a stable baseline, upon

which high frequency stimulation (HFS) or low frequency stimulation (LFS) was initiated. For HFS, 12 bursts of 11 pulses at 500 Hz were delivered every 10 s. For LFS, 132 pulses were delivered at 0.1 Hz. During HFS and LFS, the current intensity was increased to 909 μA to produce a large population spike, ranging from 5-15 mV. Nine animals received HFS and six animals received LFS with these parameters. In addition, four animals received high frequency stimulation but at the stimulus intensity used for the test pulses. All animals were sacrificed 90 minutes after onset of high or low frequency stimulation.

Immunocytochemistry. Standard immunohistochemical methods were used to visualize NGFI-A and FOS antigens. Animals were deeply anesthetized and transcardially perfused with 100 ml of normal saline followed by 200 ml 1% paraformaldehyde in 0.1 M phosphate buffer. Brains were immersion fixed for 1 hr and transferred to 30% sucrose in phosphate buffer. After cryoprotection, the brains were rapidly frozen and 10 and 30 μm cryostat sections were thaw-mounted onto poly-lysine coated glass slides (1 mg poly-L-lysine/ml water). Sections were air dried 3 hrs, permeabilized with 0.4% triton in PBS for 1 hr, blocked with 10% normal goat serum (NGS) in PBS for 1 hr, and then incubated with primary antibody (a-NGFI-A or a-FOS) for 12 hours at 4°C. Anti-NGFI-A (generously provided by Dr. Jeffrey Milbrandt) was diluted 1:1000 and anti-FOS (Santa Cruz Biotechnology, Inc., Santa Cruz, CA) was diluted 1:2000 both in 1% NGS in PBS. Control tissue for all immunoreactions was processed by including with each immunoreaction naive hippocampal sections (negative control) and hippocampal sections from animals given pharmacologic seizures

(positive control) (Popovici et al., 1990), as seizure activity robustly up-regulates both FOS and NGFI-A. Control tissue was also processed by deleting the primary antibody from the protocol. Antibody complexes were visualized using Vectastain Avidin DH/Biotin-peroxidase complex kit (Vector Labs, Inc., Burlingame, CA). For tissue developed with diaminobenzidine, the sections were further processed using standard autoradiography methods (Rogers, 1967). For confocal microscopy, the primary antibody was visualized with the Texas Red Avidin D/Biotin Vectastain kit. Sections were observed as 1.8 μm-thick optical sections using confocal microscopy (Biorad MR600).

RESULTS

The ultrastructural features of engrafted nanosphere-labeled HiB5 cells is shown in Figure 1. Transplanted cells are identified by the presence of the extremely electron-dense colloidal gold-conjugated nanospheres, approximately 30-70 nm in diameter, which are typically compartmentalized within lysosomal vesicles approximately 400-500 nm in diameter. The labeled cells show features characteristic of their endogenous granule neuron counterparts, including pale nuclei that are large relative to the cytoplasm, dispersed nuclear chromatin, abundant rough endoplasmic

N_3

Figure 1. Electron micrographs of HiB5 cells engrafted into the dentate gyrus granule cell layer.

A. A labeled cell with characteristic neuronal features, such as numerous mitochondria (arrowheads) and dispersed chromatin within a pale, large nucleus (N) (see also N_1 & N_3 in panel C). The nanospheres are typically compartmentalized into cytoplasmic lysosomal granules (arrow). The cell is fully integrated with the surrounding endogenous cells. Numerous dendrites (d) are seen coursing nearby, many of which are in contact with the labeled cell. Scale bar = 500 nm. **Inset**, High power micrograph of lysosomal granule containing normal (arrowhead) and colloidal gold-conjugated (arrow) nanospheres. Gold particles are seen as punctate densities covering the nanosphere. Scale bar = 200 nm.

B. Labeled neuron (asterisk) with numerous nanosphere-containing lysosomal granules (arrows). The labeled cell is in contact (arrowhead) to a dendrite (d), nestled between the neuron and an underlying protoplasmic astrocyte, which is characterized by large and elongated mitochondria, short cisternae of granular endoplasmic reticulum, and distinct condensations of karyoplasm beneath the nuclear envelope (Peters et al., 1991).

C. An nanosphere-labeled (small arrow) appendage (asterisk) from a nearby neuron is shown in intimate contact with three surrounding neurons (N_1, N_2, & N_3). The contacts between the labeled cell and N_1 (arrowhead) and N_2 (large arrow) appear to be zonulae adhaerens; however, their assymetry suggests that they may be synaptic junctions. Numerous punctate adhesions (puncta adhaerentia) can be seen along the interface of the labeled cell and N_3.

reticulum and ribosomes, lysosomes, microtubules, and numerous mitochondria (Peters et al., 1991). Furthermore, the integration and intimate contact with surrounding cells suggests functionally normal interaction with the host tissue.

Figure 2 portrays the typical electrophysiological profiles of animals receiving HFS and those receiving LFS. After HFS, the slope as a percentage of the mean slope recorded during baseline remains elevated throughout the remainder of the recording session. Tissue from the subject represented in Figure 2A was processed and immunostained for NGFI-A. The confocal image of this tissue in Figure 3B shows red bead-labeled implanted cells positively stained with NGFI-A. Panel A of this figure is an image from a previous, non-grafted, positive control animal representing normal expression of the protein by granule neurons after induction of LTP.

LFS does not induce LTP nor is there seen expression of NGFI-A beyond what is seen with constituitive expression in naive animals. The dentate gyrus from an animal which received LFS is shown in Figure 4A. Rarely are positively-stained cells found in the granule cell layer, while a number of positive cells can be found in the hilus. The present experiment included a subgroup of animals (N=4) in which LTP was induced with HFS, but at the same current level used for baseline recording (105 $\pm$ 5 μA). These animals demonstrated clear expression of NGFI-A with a much lower stimulus intensity, thus indicating that up-regulation is independent of current level. Figure 4B illustrates immunostained tissue from a typical high frequency/low intensity (HF/LI) subject. Panels C-E are high power

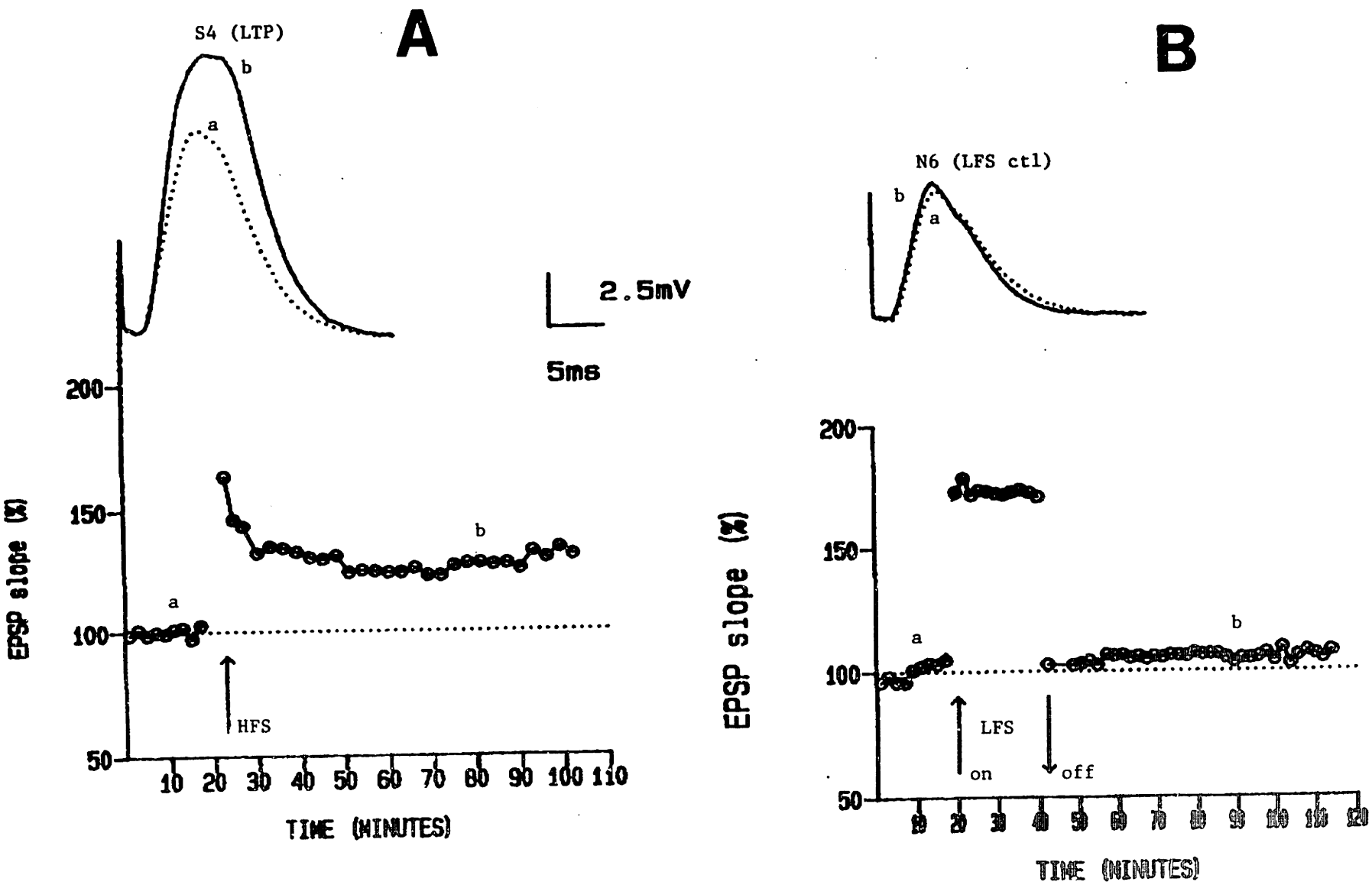
A
S4 (LTP)
b
a
2.5mV
5ms
200
150
100
50
EPSP slope (%)
a
b
HFS
10 20 30 40 50 60 70 80 90 100 110
TIME (MINUTES)
B
N6 (LFS ctl)
b
a
200
150
100
50
EPSP slope (%)
a
b
LFS
on
off
TIME (MINUTES)

Figure 2. Induction of LTP (in subject, S4) with high frequency stimulation (HFS) , **A**, and lack of induction (in subject, N6) with low frequency stimulation (LFS), **B**. Upper traces represent the epsp's prior to ("a", dotted lines) and after ("b", solid lines) HFS (A) and LFS (B). Graphs under their respective traces give the slope as a percentage of the mean slope value. Upward arrows represent onset of stimulation; downward arrow represents offset.

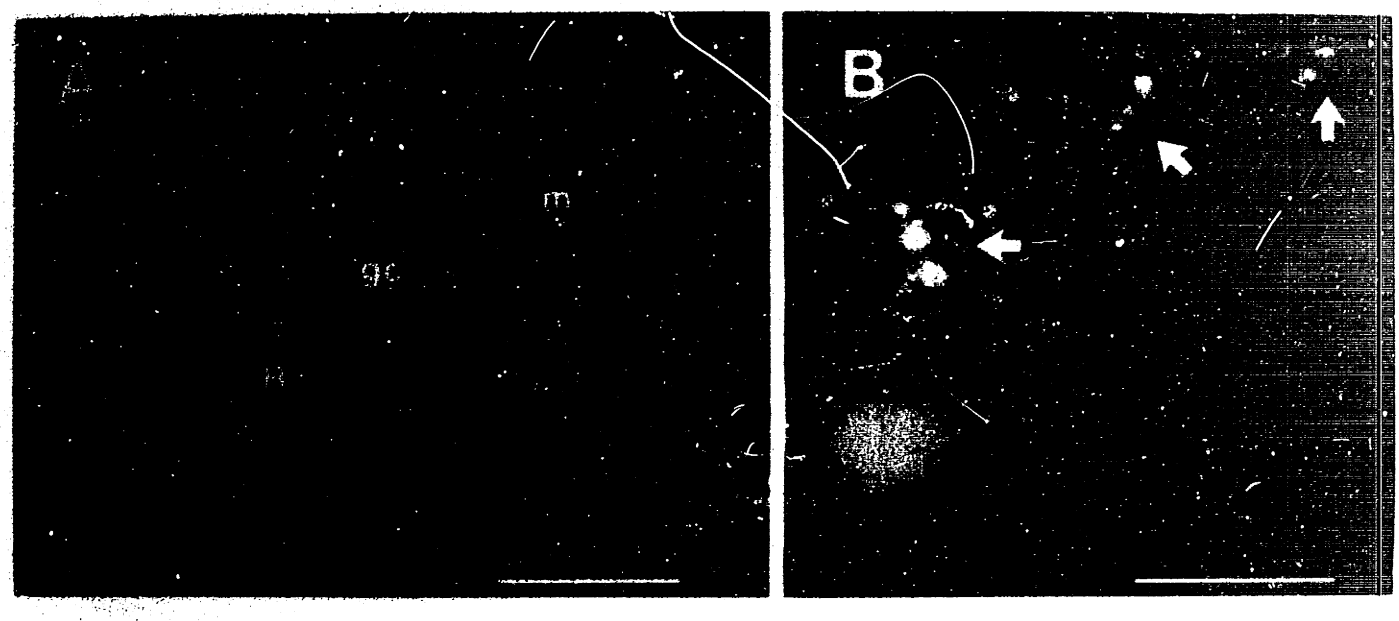
B

Figure 3. Confocal images of NGFI-A expression by endogenous granule neurons and grafted cells in the dentate gyrus ipsilateral to stimulation.

A. Typical expression pattern of NGFI-A after LTP induction. The gene is expressed strongly and consistently in granule neurons ipsilateral to stimulation. A minority of granule neurons contralateral to stimulation also stain positively for NGFI-A (data not shown). Scale bar = 100 μm.

B. Red latex microsphere-labeled HiB5 cells (arrows) are readily seen which have integrated into the granule cell layer and express NGFI-A in response to HFS. In this confocal microscopic image, the microspheres appear red or yellow-red and surround the (green) nuclear NGFI-A stain. Scale bar = 10 μm; H, hilus; gc, granule cell layer; m, molecular layer.

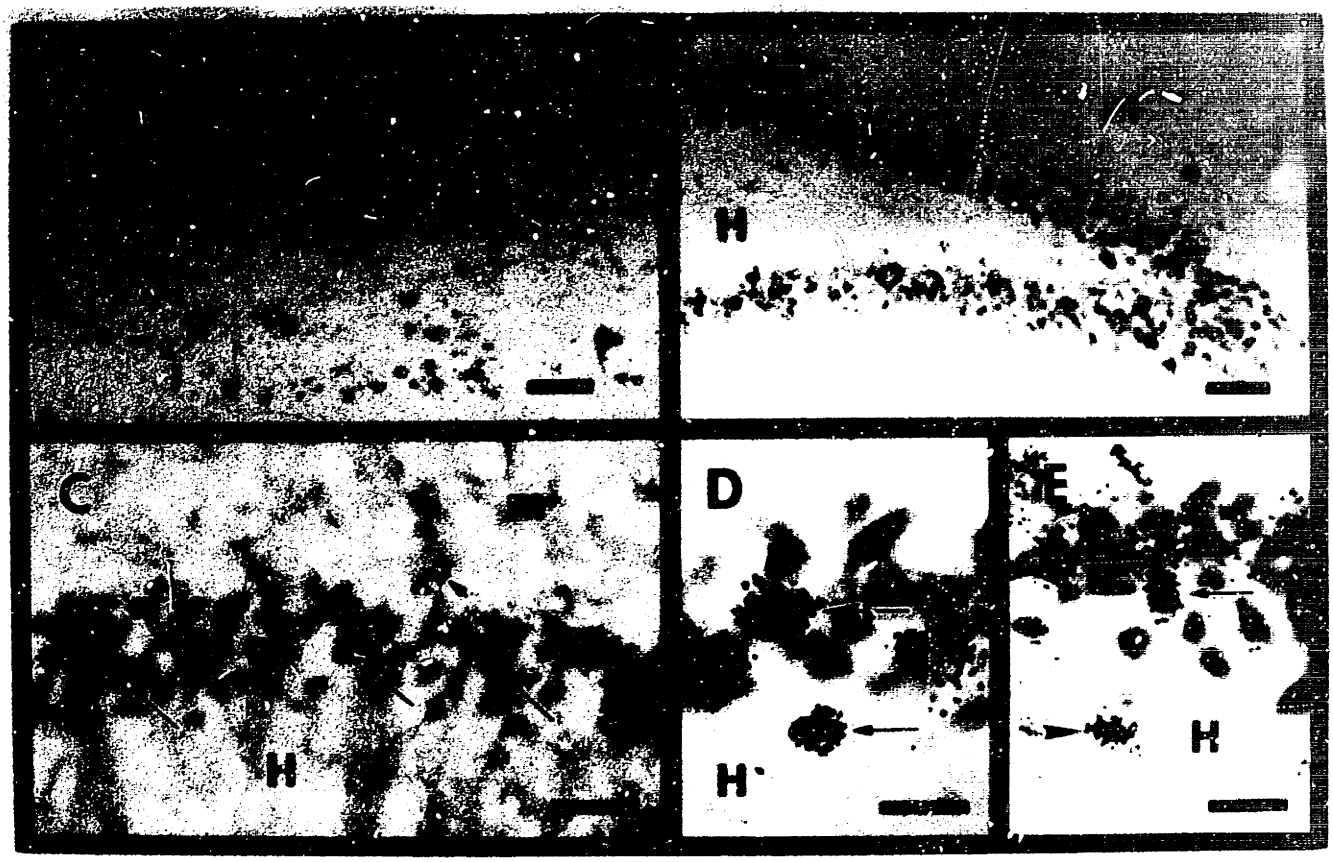
H
C
H
D
H
E
H

Figure 4. Bright field micrographs of NGFI-A immunostaining after control and experimental stimulation.

A. Low frequency stimulation results in a staining pattern indistinguishable from that seen with constituitive NGFI-A staining (not shown). Granule neurons are devoid of staining while many hilar neurons have dense staining. The peroxidase reaction product appears brown and [^{3}H]thymidine-labeled cells are represented by clusters of black silver grains overlying their nuclei. Scale bar = 50 μm.

B. LTP induced with high frequency/low intensity stimulation results in expression of NGFI-A by endogenous and grafted cells with a staining density and pattern similar to that seen with high frequency/high intensity stimulation (panels C-E). Scale bar = 50 μm.

C - E. NGFI-A - positive grafted cells can be identified by their peroxidase stained nuclei overlaid by silver grains (arrows). A subpopulation of cells appear to be less densely stained (small arrow in panel D), while other cells are negative for the protein.

micrographs of cells which express NGFI-A. Engrafted cells, overlaid with clusters of silver grains, are integrated with endogenous cells, and like their host counterparts, can stain with variable densities.

DISCUSSION

The induction of long-term potentiation (LTP) and the up-regulation of the immediate early gene, NGFI-A, have in common a number of features. They both require high-frequency stimulation, while both fail to be elicited with low-frequency stimulation; they both require a similar stimulus intensity; they both are blocked by NMDA antagonists; and neither response is seen with the administration of convergent synaptic inhibitory inputs (Cole et al., 1989). Therefore, it appears that the synaptic mechanisms which regulate LTP apparently regulate expression of NGFI-A as well.

That engrafted HiB5 cells express NGFI-A in response to perforant path stimulation indicates that they establish functional synapses with the appropriate afferents. Furthermore, in light of the correlation between LTP and NGFI-A expression, it strongly suggests that engrafted cells participate in long-term potentiation. This is supported by electron microscopy data demonstrating that HiB5 cells differentiate into neuronal phenotypes and appear to interact normally within the host. However, the present report does not illustrate engrafted cells with distinct synapses. This may be due to the mild tissue fixation conditions used (note the indistinct fine structure of cytoplasmic organelles, such as mitochondria), the relatively early age at which electron microscopy was conducted,

and/or simply not enough tissue analyzed. Further ultrastructural analysis using alternative methods in mature animals is ongoing.

Cole et al. (1989) found more intense immunostaining in the dorsal hippocampus and attributes this to stimulating electrode placement (angular bundle) as opposed to our entorhinal cortex placement in which the intensity of the stain was highest in the caudal aspect of the hippocampus (data not shown). Moreover, Wisden et al. (1990) reported that an increase in stimulus intensity resulted in increased expression of NGFI-A. Furthermore, the minimum stimulus intensity required to establish LTP was similar to that required to produce an increase in NGFI-A.

Our results support previous conclusions by demonstrating, using high and low stimulus intensities, that NGFI-A is up-regulated, by endogenous and grafted cells, with the induction of LTP, and the protein is not detectable when LTP fails to be established or during low frequency control stimulation. Although the lower intensity stimuli inducing LTP were sufficient to detect increased expression of NGFI-A, high-intensity stimuli resulted in a greater number of cells expressing NGFI-A and their staining density was higher as well.

In addition to demonstrating the ability of HiB5 cells to functionally integrate in the developing dentate gyrus, the present studies suggest that such cell lines may serve to elucidate the mechanisms controlling synapse formation and plasticity, and perhaps learning and memory.

REFERENCES

Cunningham, M.G. & McKay, R.D.G. *J. Neurosci. Meth.* (in press) A hypothermic miniaturized stereotaxic instrument for surgery in newborn rats.

Cunningham, M.G., Renfranz, P.J., Arel, L., & McKay, R.D.G. (submitted) Immortalized clonal stem cells differentiate into hippocampal neurons and astrocytes.

Cole, J.A., Saffen, D.W., Baraban, J.M., & Worley, P.F. Nature 340, 474-476 (1989) Rapid increase of an immediate early gene messenger RNA in hippocampal neurons by synaptic NMDA receptor activaiton.

Frederiksen, K. & McKay, R. *J. Neurosci.* 8, 1144-1151 (1988). Proliferation and differentiation of rat neuroepithelial precursor cells in vivo.

Jat, P.S. & Sharp, P.A. *Mol. Cell. Biol.* 9, 1672-1681 (1989). Cell lines established by a temperature-sensitive simian virus 40 large-T-antigen gene are growth restricted at the nonpermissive temperature.

Lemaire, P., Revelant, O., Rodrigo, B., & Charnay, *P. Proc. Natl, Acad. Sci. USA* **85**, 4691-4695 (1988). Two mouse genes encoding potential transcription factors with identical DNA-binding domains are activated by growth factors in cultured cells.

Madison, R., Macklis, J., & Thies, C. Brain Res 522, 90-98 (1990) Latex nanosphere delivery system (LNDS): novel nanometer-sized carriers of fluorescent dyes and active agents selectively target neuronal subpopulations via uptake and retrograde transport.

Milbrandt, J. *Science* **238**, 797-799 (1987). A nerve growth factor-induced gene encodes a possible transcriptional regulatory factor.

Popovici, T., Represa, A., Crepel, V., Barbin, G., Beaudoin, M., Ben-Ari, Y., *Brain Research*, 536, 183-194 (1990) Effects of kainic acid-induced seizures and ischemia on c-fos-like proteins in rat brain

Renfranz, P.J., Cunningham, M.G., & McKay, R.D.G. *Cell* 66, 713-729 (1991). Region-specific differentiation of the hippocampal stem cell line HiB5 upon implantation into the developing mammalian brain.

Rogers, A. Techniques of Autoradiography (Amsterdam: Elsevier Printing Co., 1967)

Sukhatme, V.P. et al. *Cell* **53**, 37-43 (1988). A zinc finger-encoding gene coregulated with c-fos during growth and differentiation, and after cellular depolarization.

Wisden, W., Errington, M.L., Williams, S., Dunnett, S.B., Waters, C., Hitchcock, D., Evan, G., Bliss, T.V.P., & Hunt, S.P. *Neuron* 4, 603-614 (1990) Differential expression of immediate early genes in the hippocampus and spinal cord.

CHAPTER 8

FATE SHIFTING OF CEREBELLAR PRIMORDIAL CELLS UPON TRANSPLANTATION INTO THE DEVELOPING FASCIA DENTATA

ABSTRACT

Discordant views have been taken as to whether cell fate is determined by cell-autonomous or environmental factors. The latter has become the more favored view in light of transplantation and fate mapping studies showing the diversity in the range of phenotypes that a neural stem cell may ultimately express. However, the limitations of such pluripotency is unclear. In the present study we have challenged the notion of pluripotency to an extreme, testing for fate restrictions at the level of the individual cell transplanted to a phylogentically isolated site. Single cell suspensions were prepared from cerebellar primordia either from newborn rats which had received injections of tritiated thymidine or from transgenic mice carrying the *lacZ* gene driven by a neuron-specific enolase promoter. The cells were stereotaxically grafted into the fascia dentata of newborn rats and mice, whereupon they differentiated into neurons and astrocytes characteristic to the heterotopic site. Our results demonstrate the striking plasticity of these precursors and the powerful influence that developing brain regions have over the differentiation of individual cells.

This chapter was adapted from a manuscript in preparation authored by Miles G. Cunningham, Carlos Vicario, and Ronald D.G. McKay.

INTRODUCTION

It has been well documented that cells destined to become sympathetic or parasympathetic neurons are capable of shifting their phenotype in response to environmental conditions (see Patterson, 1978; Le Douarin, 1986 for review). In the neocortex the parcellation of distinct areas, and the fate of the cells comprising these areas, appear to be established by epigenetic factors. Transplantation of embryonic perirhinal or sensorimotor cortex prior to, but not after, neurogenesis into newborn hosts results in the grafted cells expressing limbic-system-associated membrane protein (LAMP) appropriate to the host site as opposed to their site of origin (Barbe & Levitt, 1991). Furthermore, when fetal occipital cortex is grafted heterotopically to the newborn rostral region or somatosensory cortex, the transplanted neurons develop in a manner appropriate to their new locale (O'Leary & Stanfield, 1989; Schlaggar & O'Leary, 1991).

At very early stages in development in the chick (10-12 somites embryos) a portion of the mesencephalic alar plate transplanted to the diencephalic alar plate is capable of developing into a laminated structure appearing to be a supernumerary optic tectum (Martinez & Alvarado-Mallart, 1989). However, other regions, notably the caudal and rostral metencephalon, when grafted to the mesencephalon and diencephalon, respectively, maintained their cerebellar fate (Alvarado-Mallart et al., 1990). This latter result is in agreement with earlier studies in which cerebellar primordia was transplanted as aggregated cells or solid grafts into

ectopic sites in the newborn or adult rat. These grafts survived and developed the cytoarchitectural features characteristic of the cerebellum (Alvarado-Mallart & Sotelo, 1982; Wells & McAllister, 1982; Kromer et. al, 1983; Ezerman & Kromer, 1985).

It should be considered that in the experiments describe above, the immediate environment has been transplanted along with the cells. To what level are individual cells from one region (e.g., the cerebellum) competent to respond appropriately to the inductive signals in a developmentally disparate region? We have previously shown that an immortalized stem cell line derived from hippocampus differentiates into cerebellar granule neurons and Bergmann glia when implanted heterotopically into the developing cerebellum (Renfranz et al., 1991; Cunningham et al., 1993). This plasticity may be a feature unique to this particular cell line, or perhaps it is a general characteristic of most, if not all, stem cells.

The present studies address these questions by transplanting micro-volume suspensions of single cells from one developing region to a distant, phylogenetically distinct developing region. The cerebellum, which arises from the rhombencephalon (Jacobson, 1978), was chosen as the donor region as it continues to develop for some three weeks postnatally (Altman, 1972c) and offers ample, easily accessible tissue. The dentate gyrus, which arises from the telencephalon (Jacobson, 1978), was chosen as the implantation site since this structure is also actively developing postnatally (Altman & Das, 1965), and, with maturation, allows for a variety of assays to characterize grafted cells.

Two paradigms were used in these experiments. Cell suspensions were made from the cerebella of newborn rats which were injected with thymidine-[methyl-3H] (tritiated thymidine), and cell suspensions were made from the cerebella of newborn transgenic mice carrying a *lacZ* gene driven by a neuron-specific enolase (NSE) promoter (Forss-Petter, 1990). These suspensions were stereotaxically placed into the dentate gyri of newborn rats and mice (Renfranz et al., 1991; Cunningham and McKay, in press). This allowed transplanted cells to be identified using two methods: with autoradiography transplanted cells have a dense cluster of silver grains overlying their nuclei (Rogers, 1967), and with the X-Gal (5-Br-4-Cl-3-indolyl-b-galactoside) reaction the cells which carry the *lacZ* gene produce a blue reaction product (Price and Thurlow, 1988) The phenotype of the transplanted cells was determined based on expression of cell-specific antigens as well as ultrastructural characteristics as seen with electron microscopy. Immunohistochemistry was performed for the neuron-specific calcium binding protein, calbindin (CBP) which is expressed by dentate gyrus granule neurons but not cerebellar granule neurons, neuron-specific enolase (NSE), the astrocyte-specific glial fibrillary acidic protein (GFAP), and the FOS protein(s), which is strongly expressed by dentate gyrus granule neurons (but not cerebellar cells) during seizure activity produced by kainic acid (KA) (Popovici, 1990).

METHODS

Subjects. Rats were purchased from Taconic (Germantown, NY), Black 6 and CB6/SJL mice from Jackson Laboratory (Bar Harbor, ME) and NSE-*lac*Z transgenic mice from J.G. Sutcliffe's laboratory (Research Institute of Scripps Clinic, La Jolla, CA). They were housed in plastic cages and maintained on a 12h light / 12h dark cycle. Food and water were provided *ad libitum*. A total of 22 newborn rats and 12 newborn mice were grafted in this series of experiments. Animal care was as approved by the Massachusetts Institute of Technology in accordance with National Institute of Health guidelines.

Cell suspensions. Cells were prepared from 2-day-old (P2) male and female Sprague-Dawley rat pups, and 3 day-old (P3) male and female F1 hybrid CB6/SJL transgenic mice carrying a 1.8 kb rat neuron-specific enolase (NSE) promoter fragment fused to an *E. coli lacZ* gene (Forss-Petter et al., 1990). Prior to removing cerebellar primordia, P1 rats were injected intraperitoneally every six hrs over a 24 hr period with [H^3]thymidine at a dosage of 15 mCi/g. Animals were then hypothermically anesthetized and their cerebella removed. The tissue was placed in calcium and magnesium-free Hank's balanced salt solution (CMF-HBSS) (Gibco BRL, Grand Island, NY) at 4°C and cleaned of meninges and blood vessels under a dissecting microscope. The cerebella were then placed in CMF-HBSS containing 0.01% deoxyribonuclease (Worthington, Freehold, NJ) and chopped in small pieces (about 1mm^3). The tissue was incubated in the presence of 0.025% trypsin (200-300 U/mg protein, Worthington) and 0.1% DNAse for 5 min at 37°C and the trypsin

activity was quenched with Dulbecco's Modified Eagle Medium containing 10% fetal calf serum (DMEM + 10% FCS). After centrifugation at 1,000 rpm for 5 min at 4°C the tissue was triturated in CMF-HBSS containing 1% DNAse using a P-1000 followed a P-200 Pipetteman. The resulting cell suspension was centrifuged at 2,000 rpm for 5 min at 4°C and the cell pellet was resuspended in CMF-HBSS. The cells were counted and their viability was invariably ≥85% according to the trypan blue dye-exclusion test (Sigma, St. Louis, MO). The final volume of the cell suspension was adjusted to obtain a cell density of 100,000 cells/ul. Red fluorescent latex microspheres (red beads) (Lumafluor, Inc., NJ) were added at a concentration of 5% (v/v) in order to follow the graft after transplantation. For each host animal a 0.5 ul volume of cell suspension was implanted into the dentate gyrus or into the right cerebellar hemisphere.

Implantation. Transplantation was performed using a previously described technique (Cunningham and McKay, 1993). Animals were hypothermically anesthetized. Each animal was then fixed in a hypothermic miniaturized stereotaxic instrument (Cunningham neonatal rat adaptor, Stoelting Co., Wood Dale, IL) combined with a standard stereotaxic instrument (Stoelting Co.). A midline cranial incision was made, the skull surface was cleaned of connective tissue and bregma was determined. At the site of the appropriate coordinates for the hippocampus or the cerebellum, a 1mm diameter area of skull was removed using a low-speed drill equipped with a dental burr. Hippocampal implants were placed 1.8 mm lateral to midline, 1.2 mm posterior to bregma, and 2.1 mm

below dura in P-2 rat pups or 1.4 mm lateral to midline, 0.8 mm posterior to bregma, and 1.4 mm below to dura in P4 mouse pups. Cerebellar implants were placed 1 mm lateral to midline, 1 mm caudal to the parietal fissure, and 0.8 mm below dura in P2 rat pups. Using a pulled glass pipette (with a tip internal diameter of approximately 70 mm) connected to a Hamilton syringe, 0.5 ml of the cell suspension was injected over 2 min. The pipette was left in this position for 2 min and then withdrawn over 3 min. Gel foam was placed in the skull cavity, the animal was sutured, revived on a heating pad, and returned to its mother.

At variable periods after grafting (1-8 months) animals were deeply anesthetized with ethyl ether and then transcardially perfused. For CBP, NSE, GFAP or FOS immunostaining the animals were perfused with 0.9% NaCl followed by 2-4% paraformaldehyde in phosphate buffer pH=7.4. For *lac*Z histochemistry animals were perfused with phosphate-buffered saline containing 2 mM MgCl2 followed by 2% paraformaldehyde/2 mM MgCl2/5mM EGTA/0.2 % (v/v) glutaraldehyde in pipes pH=6.9.

Some animals were previously injected intraperitoneally with kainic acid (Sigma) at a dosage of 10-12 mg/kg in order to induce the synthesis of c-Fos proteins in the hippocampus, as previously described (Popovici et al., 1990). Three hours after the injection of kainate, the animals were deeply anesthetized and perfused as described above. The brains were immersed overnight at 4°C in 30% sucrose, embedded in OCT (Miles, Elkhart, IN) and10-30 mm cryostat sections were thaw-mounted onto coated glass slides coated with 1mg/ml poly-L-lysine (Sigma).

Immunohistochemistry. Air dried sections were permeabilized with 0.2-0.4% triton X-100, and incubated overnight at room temperature with the primary antibodies against CBP (monoclonal anti-calbindin-D, Sigma) (1:200) and neuron-specific enolase (polyclonal anti-NSE, Polysciences, Inc., Warringtown, PA) (1:500), or overnight at 4°C with the primary antibody against FOS (polyclonal anti-FOS proteins, Cambridge Res. Biochem., Cambridge, MA) (1:2000) and GFAP (monoclonal anti-GFAP, ICN, Costa Mesa, CA) (1:500). The sections were then incubated with the corresponding biotinylated secondary antibody (1:200) followed by avidin-biotin-horseradish peroxidase complex and processed with 3,3' diaminobenzidine (DAB) and H_2O_2. Finally, the sections were rinsed with H_2O, dried, dehydrated and mounted in Permount (Fisher Scientific, Fair Lawn, NJ).Cambridge Res. Biochem., Cambridge, MA). Then the sections were incubated with the corresponding biotinylated secondary antibody (1:200) followed by avidin-biotin-horseradish peroxidase complex and processed with 3,3' diaminobenzidine (DAB) and H_2O_2. Finally, the sections were rinsed with H_2O, dried, dehydrated and mounted with Permount

X-Gal staining. The method described by Price and Thurlow (1988) was followed for lacZ histochemistry. Air dried sections were postfixed with 0.5% glutaraldehyde in PBS/2mM $MgCl_2$ for 15 min at 4°C. After two rinses with PBS/2mM MgCl2 the sections were permeabilized with detergent solution (0.01% sodium deoxycholate, 0.02% nonidet P-40 in PBS/2mM MgCl2) during 15 min at 4°C. To visualize the B-galactosidase activity, the sections were incubated overnight at 37°C in detergent containing 5mM $K_3Fe(CN)_6$, 5mM

$K_4Fe(CN)_6$ and 2.5mM (1mg/ml) 5-Br-4-Cl-3 indolyl-B-galactoside (X-Gal) (GIBCO BRL). Sections were then rinsed twice with PBS and dehydrated and mounted with Permount. When antibody immunostaining and *lac*Z histochemistry was performed on the same sections, the tissue was first incubated to visualize the B-galactosidase activity although the step of postfixation with glutaraldehyde was omitted. Then the sections were incubated with the antibodies and mounted as described.

Electron microscopy. For electron microscopy analysis, animals were perfused with phosphate-buffered saline containing 2 mM MgCl2 followed by 2% paraformaldehyde/2.5% (v/v) glutaraldehyde in phosphate-bufered saline/2mM MgCl2. Sections 250 μm thick were cut on a vibrating microtome and reacted with XGal.regions containing transplanted cells were microdissected caco buffer. Tissue was osmicated, dehydrated in serial ethanol grades, embedded, and 60-80 nm thin sections were stained with uranyl acetate and lead citrate. Sections were viewed and photographed on a JEOL 1200 CX (80 kv) electron microscope.

RESULTS

Our observations based on immunocytochemistry combined with [H^3]thymidine autoradiography are illustrated in Figure 1. Cerebellar primordia were taken from postnatal-day 2 (P2) rats which had received a series of [H^3]thymidine (cumulative labeling) injections over the previous 24 hours. The vast majority of cerebellar cells originating during this labeling period are the granule cells; glial cell proliferation comprises a small minority (Margolis,

1969). Purkinje cells are born prenatally while the basket and stellate cells are born during post-natal days 6-11 (Altman, 1972c). Single cell suspensions were prepared and injected into the dentate gyrus of P2 rats, and the animals were allowed to survive 4-6 weeks. Four hours prior to sacrificing, the animals received injections of kainic acid. Adjacent tissue sections of the grafted hippocampi were immunoreacted for CBP, FOS, and GFAP. Stained tissue was then processed with a standard autoradiographic protocol (Rogers, 1967).

Figure 1, panels A and D, illustrate the normal immunostaining of granule neurons in the dentate gyrus for CBP and FOS, respectively. [H^3]thymidine-labeled cerebellar cells transplanted to the dentate gyrus integrate into the granule cell layer and, like endogenous granule neurons, express CBP (Fig. 1B & C). These cells also strongly express FOS as a consequence of seizure activity (Fig. 1E & F), as they are FOS-negative when seizures are not elicited (data not shown). GFAP immunostaining illustrates that many transplanted cerebellar cells are capable of differentiating into astrocytes (Fig. 1G & H), albeit the lineage of these cells can only be speculated. When cells were grafted back into the P2 cerebellum they dispersed primarily in the granular layer. The grafted cells are indistinguishable from the surrounding cerebellar granule neurons and astrocytes and do not express CBP (Fig. 1I) while most stain positively for neuron specific enololase (NSE) (data not shown).

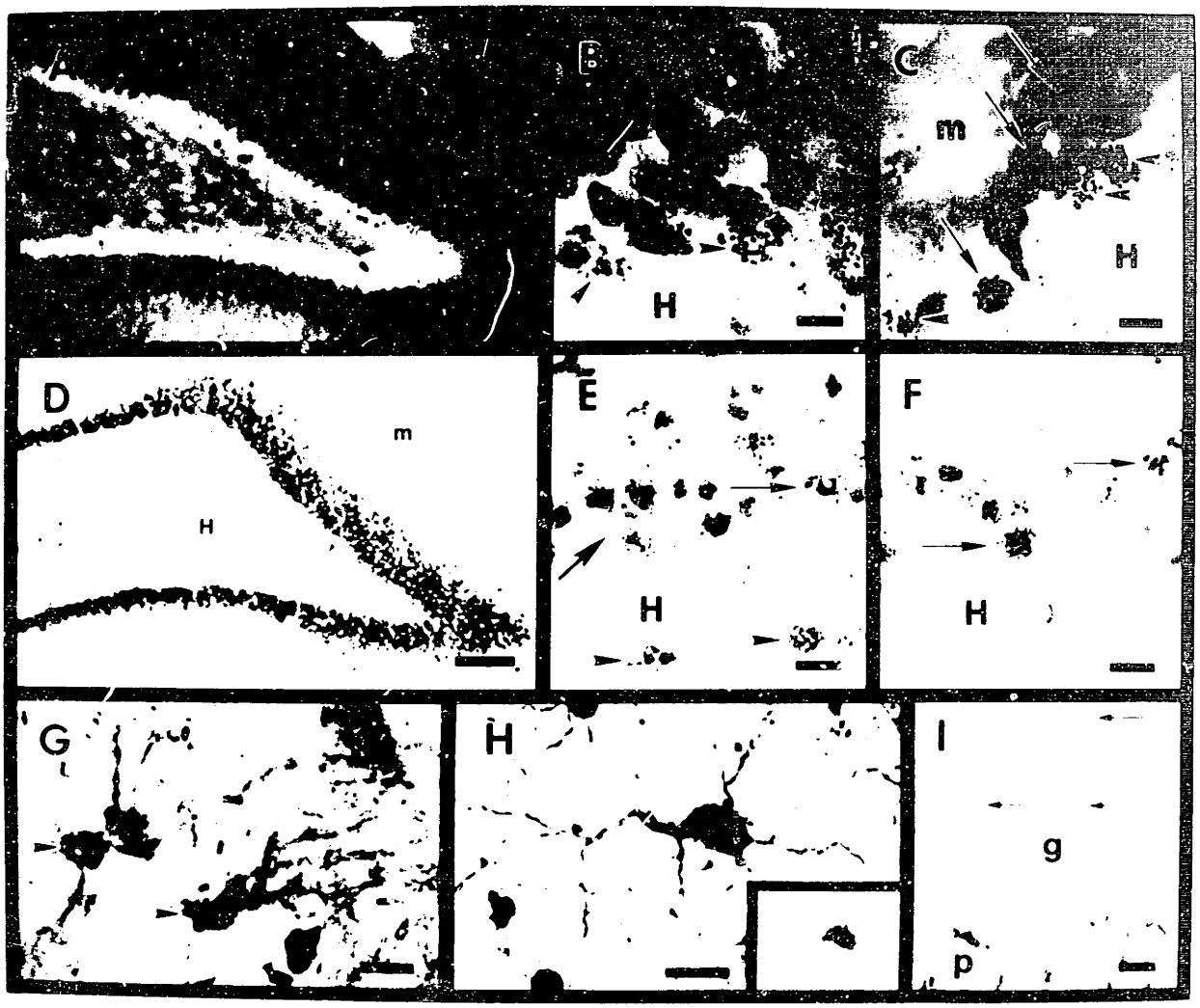
A
B
H
C
m
H
D
m
H
E
H
F
H
G
H
I
g
p

Figure 1. [H^3]thymidine-labeled cerebellar cells engraft into the developing dentate gyrus and differentiate to express locale-specific neuronal or astrocytic markers. *A*, Normal CBP-staining in the dentate gyrus. Note the immunopositive granule cells (gc) and their dendritic network in the molecular layer (m). *B & C*, Transplanted cells can be identified by clusters of silver grains overlying their somata. CBP-positive (arrows) as well as CBP-negative (arrow heads) transplanted cells are readily found near the graft site. *D*, Typical immunostaining of kainate-induced FOS in granule neurons. *E & F*, Transplanted cells (arrows) appear to up-regulate c-*fos* in a manner identical to endogenous granule neurons. FOS-negative transplanted cells (arrow heads) are usually found outside the granule cell layer, in the hilus (H) or in the molecular layer (m). *G & H*, GFAP-positive transplanted cells can be found throughout the grafted tissue, such as the two examples (in panel *G*) in the molecular layer (arrow heads) and the stereotypical astrocytic cell located in the hilus (panel *H*) (inset shows overlying silver grains). *I*, Cells grafted back into the cerebellum are found predominantly in the granular layer (g) and are not immunoreactive for CBP as the cerebellar Purkinje cells (p) or the transplanted cells in the dentate gyrus. Scale bars *A & D* = 100 μm. Scale bars *B*, *C*, *E-I* = 10 μm.

Similar results were seen with grafts of cerebellar primordia prepared from NSE-*lacZ* transgenic mice. The mice were generated from CB6xSJL hybrids and express a fusion gene (NSE-*lacZ*) containing a 1.8 kb NSE promoter fragment linked to the E. coli *lacZ* gene. The expression of this transgene is neuron-specific and pan-neuronal (Forss-Petter et al., 1990).

Transplantation of P3 NSE-*lacZ* cerebellar cells into the the P2 rat or P4 CB6xSJL mouse dentate gyrus results in cells integrating into the tissue, particularly the granule cell layer, and assuming morphologies of neurons characteristic to the dentate gyrus (Fig. 2A & B). Immunocytochemistry reveals that most of these integrated cells express CBP (Fig. 2D & E), and after seizure activity, FOS (Fig. 2F & G). However, a subset of integrated cells do not stain for these proteins and their position and morphology resemble local circuit neurons, notably the pyramidal basket cell (Fig. 2B). Most local circuit neurons are born postnatally and are GABAergic, probably providing GABA-mediated, tonic inhibition to other neurons (Ribak & Anderson, 1980). When NSE-*lacZ* cerebellar cells are grafted into the rat cerebellum, they integrate primarily into the granular layer and do not immunostain for CBP (Fig. 2H) while they are strongly immunoreactive for NSE (Fig. 2I).

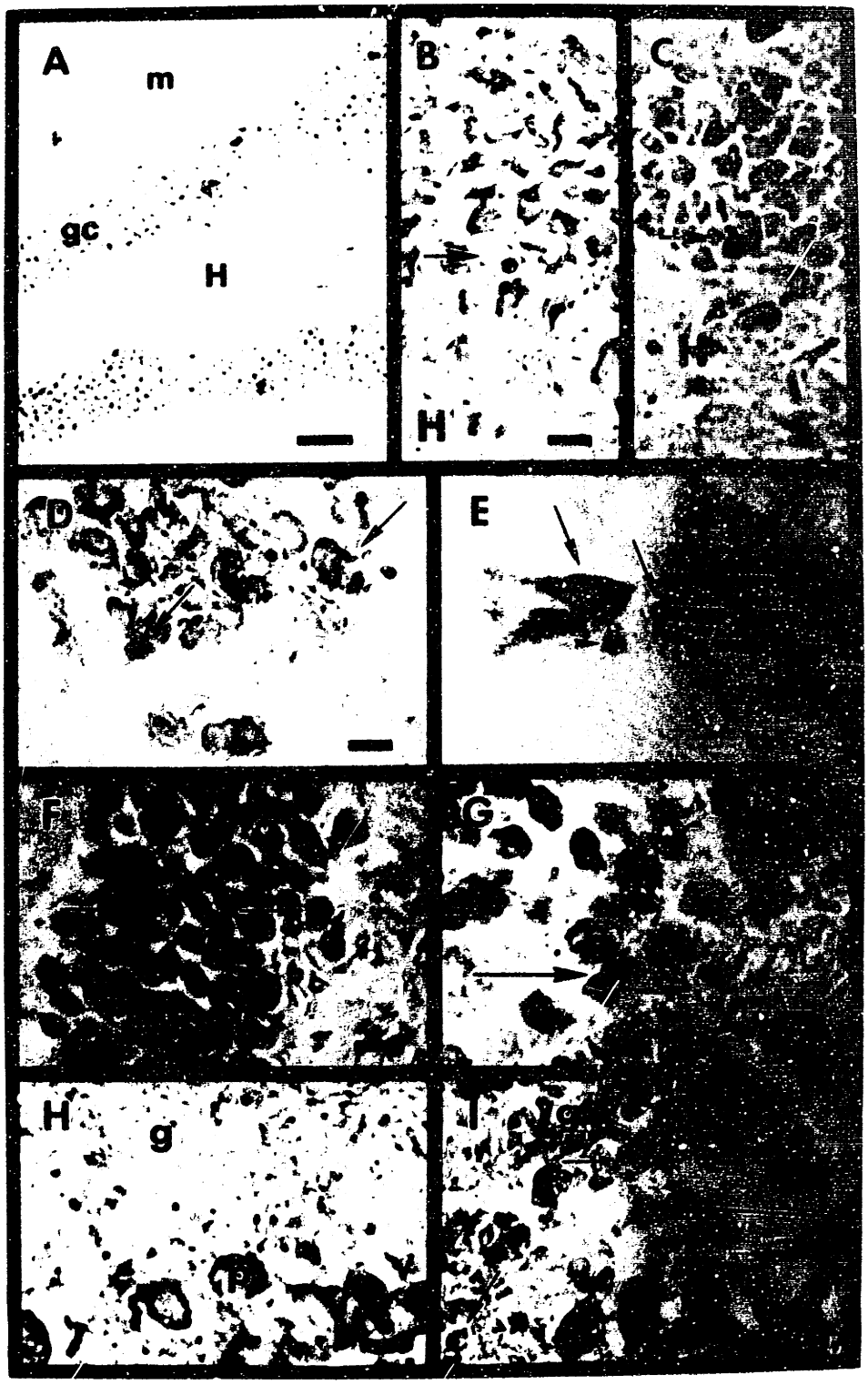
A
m
gc
H
B
H
C
D
E
F
G
H
g
P
I

Figure 2. Transplanted transgenic cerebellar cells which express the NSE-*lacZ* transgene integrate into the host fascia dentata, assume neuronal morphologies, and express neuron-specific antigens. *A*, Low power view of X-gal reacted grafted dentate gyrus. Transplanted cells (arrows) produce a dense blue reaction product and are seen distributed in the granule cell layer (gc) as well as the hilus (H) and the molecular layer (m). *B & C*, High power view of engrafted cells (arrows) which resemble in their somatic morphology a granule cell (*B*) and a pyramidal basket cell (*C*). *D & E* CBP-immunostaining reveals transplanted cells (arrows) residing in the granule cell layer express this locale-specific neuronal marker. Transplanted cells can also be identified as CBP-negative (arrow heads in *E*). Note the stereotyped "displaced granule neuron" morphology (described by Ramon y Cajal in 1894) in *E* (large arrow). Transgenic cells lying outside the granule cell layer were invariably negative for CBP. *F & G* Transgenic cerebellar cells (arrows) up-regulate c-*fos* appropriately upon challenge with kainic acid. *H*, Transgenic cells (arrows) grafted into the rat cerebellum populate the granular layer (g) and are not immunoreactive for CBP as are the Purkinje cells (p). *I*, Transgenic cells (arrows) grafted into the rat cerebellum strongly express NSE. Scale bar *A* = 100 mm. Scale bars *B* - *I* = 10 mm.

To further assess the differentiation state of transplanted cerebellar cells, the electron-dense X-gal reaction product was utilized to identify engrafted cells with electron microscopy. The very dense reaction product is seen associated with the nuclear membrane, endoplasmic reticulum, and other organelles (see inset, Fig. 3D). Most cells which were found integrated into the dentate gyrus granule cell layer (Fig. 3, panels D-F) showed ultrastructural features characteristic to endogenous granule neurons and distinguishing them from cerebellar granule neurons. Hippocampal granule neurons are 8-12 μm in diameter with a nuclear envelope which is rarely indented. They have uniformly dispersed chromatin, an eccentric nucleolus, and have sparse cytoplasm with common neuronal organelles such as mitochondria, Golgi apparatus, dense bodies and free and membrane-bound ribosomes (Laatsch, 1966). In contrast, cerebellar granule neurons (see Figure 3A) have small, 5-8μ diameter tightly packed cells with sparing cytoplasm and few organelles often nested within indentations in the nucleus, which has characteristically large masses of condensed chromatin arranged around the inner wall of the nuclear envelope (Palay & Chan-Palay, 1974).

Less frequently the ultrastructure of engrafted cells resembled that of local circuit neurons. These cells, of which the pyramidal basket cell is well characterized, have an infolded nuclear envelope, a prominent nucleolus, intranuclear rods and sheets, symmetric and asymmetric synapses, and an abundance of cisternae of granular endoplasmic reticulum and other perikaryal organelles (Ribak, 1980).

The endogenous cell shown in Figure 3C and the transplanted cell shown in Figure 3G illustrate many of these features. Although the hippocampal local circuit neuron shares features with the cerebellar basket cell, such as an infolded nuclear envelop, the transplanted cells were observed to be larger than expected of cerebellar basket cells (approximately 12 mm in diameter as opposed to approximately 7 mm) and further, the chromatin of engrafted cells was not widely dispersed as it is in cerebellar basket cells (Palay & Chan-Palay, 1974).

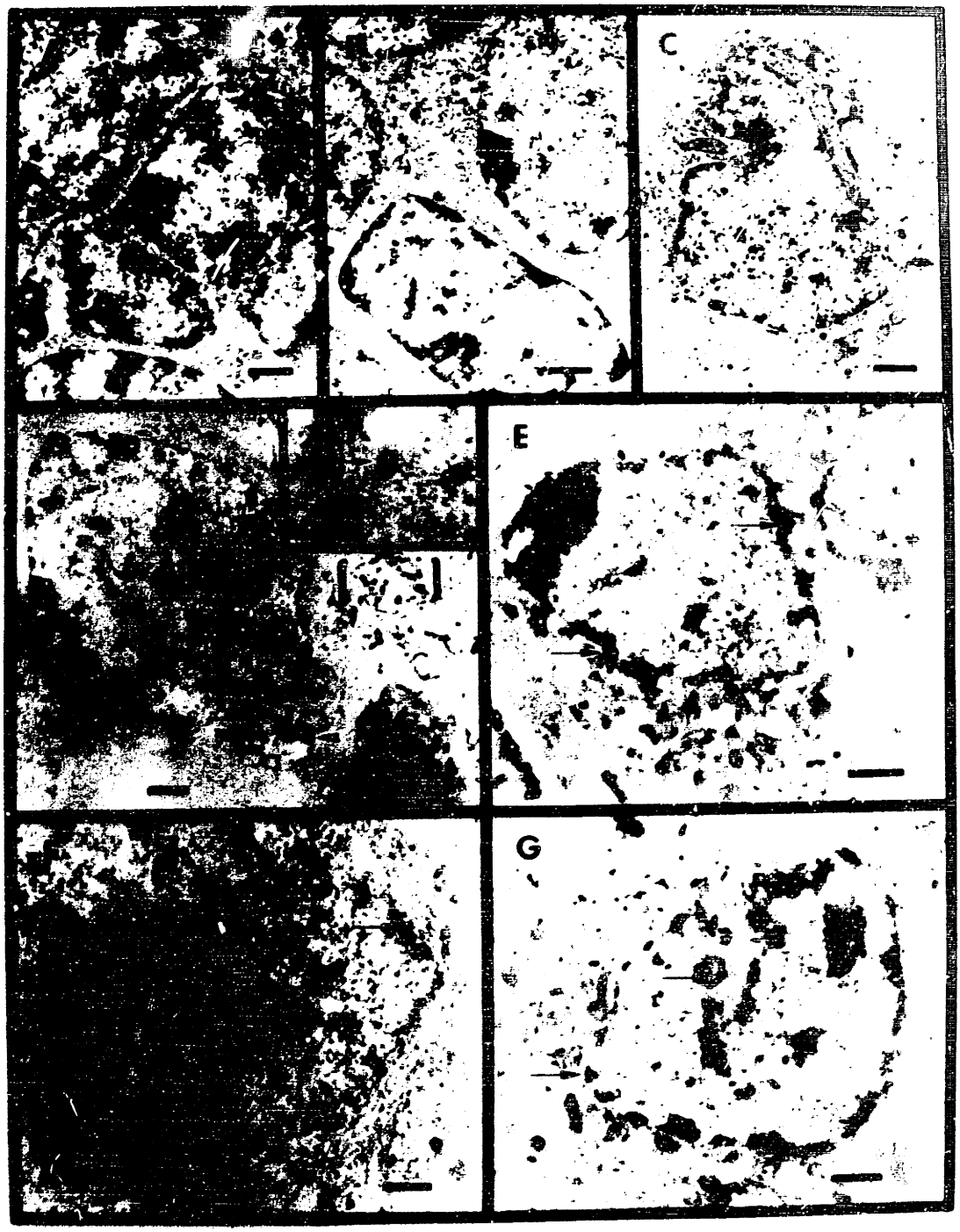
C
E
G

Figure 3. Ultrastructural features of transplanted cells are characteristic of endogenous dentate gyrus granule and local circuit neurons. *A, B, & C,* Electron micrographs of normal cerebellar granule neurons, dentate gyrus granule neurons, and a dentate gyrus local circuit neuron *in situ*, respectively. *D - G,* Engrafted cells are identified by their electron dense, crystalline X-gal precipitate which is typically associated with the nuclear membrane and subcellular organelles, such as the endoplasmic reticulum (*D*, inset). Transplanted cells have integrated intimately within the host tissue and appear to interact normally as indicated by their close cell-to-cell contact and and other features, such as myelinated fibers coursing nearby (arrow heads, *D*). A process of another transplanted cell (brackets) can be seen associated with the cell shown in *D*. Panel *G* illustrates a transplanted cell with an infolded nuclear envelope and dispersed chromatin (and, although not evident in this micrograph, a soma diameter of 11 mm) characteristic of local circuit neurons. Scale bars = 1 mm. Inset scale bar = 200 nm.

DISCUSSION

Our results have shown that cells from the newborn cerebellum, when grafted into the developing dentate gyrus, integrate and differentiate into neurons and astrocytes characteristic of this heterotopic site. The experiments described herein have demonstrated, using two independent assays, the profound plasticity of cells taken from the newborn cerebellum in that they can differentiate into cells distinct to the dentate gyrus. That the grafted cells become immunoreactive for CBP or GFAP indicates their neuronal or glial phenotype, respectively. Their up-regulation of the immediate early gene, *c-fos*, as a consequence of seizure activity induced by kainic acid strongly suggests that the grafted cells are functionally integrated into the normal circuitry. This is supported by a number of studies which have shown that up-regulation of *c-fos* is a consequence of trans-synaptic activity (Greenberg et al., 1986; Dragunow & Robertson, 1987; Shin et al., 1990; Hunt et al., 1987; Sagar et al., 1988). And finally, electron microscopy confirms that the transplanted cells integrate into the host tissue and strongly supports that cerebellar primordial cells can differentiate into dentate gyrus granule and local circuit neurons.

The two approaches used in this study differ in that the [H^3]thymidine-labeled cells represent newly born or mitosing precursors to cerebellar glial cells, granule neurons, or the more distant precursors of basket and stellate cells (Altman, 1972), while the cells taken from transgenic mice comprise a heterogeneous population of all cerebellar cell types or precursors. Therefore, the

lacZ-positive cells identified after transplantation may have derived from pre-existing Purkinje or Golgi neurons through a process of countermandation. This possibility is unlikely since the preparation of single cell suspensions axonomizes and traumatizes differentiated neurons. This mechanical insult appears to markedly decrease these cell's viability (unpublished observations; Brundin, 1988).

The present studies exemplify the use of tissues from transgenic animals for transplantation experiments producing chimeric tissue. The advantage of using transgenic cells which express a genetic marker is that this technique allows unequivocal identification of the grafted cells. This marker is reliable and stable indefinitely, as we have identified cells many months post-transplantation. Furthermore, there is evidence that the expression of NSE is not only an indicator of neuronal differentiation but is also associated with functional activity (Marangos & Schmechel, 1987). This technology therefore provides a powerful approach to the study of lineage and function.

Previous studies have reported that cerebellar primordia retains its original fate when transplanted to an ectopic site (Alvarado-Mallart, 1990; Alvarado-Mallart & Sotelo, 1982; Wells & McAllister, 1982; Kromer et al., 1983; Ezerman & Kromer, 1985). An exception to this was observed when 2-day-old avian rostral metencephalon shifted its fate to a tectal phenotype when transplanted to the mesencephalon (Alvarado-Mallart et al., 1990). It should be noted, however, that the rostral metencephalon arises from the caudal mesencephalic vesicle (Martinez & Alvarado-Mallart, 1989), and therefore the mesencephalon and the rostral

metencephalon arise from common neuroepithelia. Our results provide another exception to previous reports. We attribute this discrepancy to the method of tissue preparation and delivery as well as the developmental stage of the site of implantation. Single cell suspensions, instead of tissue pieces or aggregates, were prepared and micrografted (Nikkhah et. al, 1993) within an actively developing brain region. With this method, suspended cells are not adhered to or otherwise in close contact with other cells from the same region. Rather, they remain isolated when immersed into a foreign environment. Under these conditions, it appears that the individual cells are more susceptible to the influences of their new surroundings. Thus, our results indicate that the fate of early postnatal cerebellar cells is shifted, or countermandated, when transplanted as single cell suspensions into the developing fascia dentata. The*in vitro* control and manipulation of such cells with seemingly limitless developmental versatility may provide a powerful tool in the analysis of development and the reconstruction of the damaged central nervous system.

REFERENCES

R.-M. Alvarado-Mallart & C. Sotelo, J Comp Neurol 212, 247-267 (1982) Differentiation of cerebelar anlage heterotopically transplanted to adult rat brain: a light and electron microscopic study.

R.-M. Alvarado-Mallart, S. Martinez, C.C. Lance-Jones, Dev Biol 139, 75-88 (1990) Pluripotentiality of the 2-day-old avian germinative neuroepithelium.

J. Altman, J. Comp. Neurol. 145, 465-514 (1972c) Postnatal development of the cerebellar cortex in the rat. III. Maturation of the components of the granular layer.

M.F. Barbe and P. Levitt, J Neuroscience 11(2) 519-533 (1991) The early commitment of fetal neurons to the limbic cortex.

M. G. Cunningham & Ronald D.G. McKay, J. Neurosci. Meth. in press (1993) A Hypothermic miniaturized stereotaxic instrument for surgery in newborn rats.

M.G. Cunningham, P.J. Renfranz, L. Arel, R.D.G. McKay (submitted) Immortalized clonal stem cells differentiate into hippocampal neurons and astrocytes.

M. Dragunow & H.A. Robertson.*Neuroscience Letters*, 82, 157-161 (1987) Generalized seizures induce c-*fos* protein(s) in mammalian neurons.

E.B. Ezerman & L.F. Kromer, Dev Brain Res 23, 287-292 (1985) Development and neuronal organization of dissociated and reaggregated embryonic cerebellum after intracephalic transplantation to adult rodent recipients.

S. Forss-Petter, P.E. Danielson, S. Catsicas, E. Battenburg, J. Price, M. Nerenberg, & J.G. Sutcliffe, Neuron 5, 187 (1990) Transgenic mice expressing B-galactosidase in mature neurons under nouron-specific enolase promoter control.

M.E. Greenberg, E.B Ziff, & L.A. Greene *Science* 234, 80-83 (1986) Stimulation of neuronal acetylcholine receptors induces rapid gene transcription.

S.P. Hunt, A. Pini, & G. Evan *Nature* 328, 632-634 (1987) Induction of c-*fos*-like protein in spinal cord neurons following sensory stimulation.

M. Jacobson, Developmental Neurobiology (Plenum Press, New York) (1978)

L.F. Kromer, A. Bjorklund, & U. Stenevi *J Comp Neurol* 218, 433-459 (1983) Intracephalic embryonic neural implants in the adult rat brain. I. Growth and mature organization of brainstem, cerebellar, and hippocampal implants.

R.H. Laatsch & W.M. Cowan *J Comp Neurol* 128, 359-396 (1966) Electron Microscopic studies of the dentate gyrus of the rat

N.M. Le Douarin, Science 231,1515-1522 (1986) Cell line segregatioon during peripheral nervous system ontogeny

P.J. Marangos, and D.E. Schemechel, Ann Rev Neurosci. 10, 269-295 (1987) Neuron specific enolase, a clinically useful marker for neurons and neuroendocrine cells.

S Martinez and R.-M. Alvarado-Mallart, Dev Brain Res 47, 263-274 (1989) Transplanted mesencephalic quail cells colonize selectively all primary visual nuclei of chick diencephalon; a study using heterotopic transplants.

S.K. McConnell, Ann. Rev. Neurosci. 14, 269-300 (1991) The generation of neuronal diversity in the central nervous system.

D.D.M. O'Leary and B.B. Stanfield, J Neurosci 9(7), 2230-2246 (1989) Selective elimination of axons extended by developing cortical neurons is dependent on regional locale: experiments utilizing fetal cortical transplants.

S.L. Palay & V. Chan-Palay, Cerebellar Cortex, Cytology and Organization, Heidelberg: Springer-Verlag, (1974).

P.H. Patterson, *Ann. Rev. Neurosci.* 1, 1-17 (1978) Environmental determination of autonomic neurotransmitter functions

T. Popovici, A. Represa, V. Crepel, G. Barbin, M. Beaudoin, Y. Ben-Ari, *Brain Research*, 536, 183-194 (1990) Effects of kainic acid-induced seizures and ischemia on c-fos-like proteins in rat brain

J. Price and L. Thurlow, *Development* 104, 473-482 (1988) Cell lineage in the rat cerebral cortex: a study using retroviral-mediated gene transfer.

P.J. Renfranz, M.G. Cunningham, R.D.G. McKay, *Cell* 66, 713-729 (1991) Region-specific differentiation of the hippocampal stem cell line HiB5 upon implantation in the developing mammalian brain.

D.E. Ribak & L. Anderson, *J Comp Neurol* 192, 903-916 (1980) Ultrastructure of the pyramidal basket cells in the dentate gyrus of the rat.

A.W. Rogers, Techniques of Autoradiography (Elsevier Publishing Co., London) (1967)

C. Shin, J.O. McNamara, J.I. Morgan, T. Curran, & D.R. Cohen *J. Neurochem.* 55, 1050-1055 (1990) Induction of c-*fos* mRNA expression by afterdischarge in the hippocampus of naive and kindled rats.

S.M. Sagar, F.R. Sharp, & T. Curran *Science* 240,1328-1331 (1988) Expression of c-*fos* protein in brain: metabolic mapping at the cellular level.

B.L. Schlaggar and D.D.M. O'Leary, Science 252, 1556-1560 (1991) Potential of visual cortex to develop an array of functional units unique to somatosensory cortex.

J. Wells & J.P. McAllister II, Dev Brain Res 4, 167-179 (1982) The development of cerebellar primordia transplanted to the neocortex of the rat.

FINAL COMMENTS

The idea of transplanting brain tissue as a cure for incapacitating neurodegenerative diseases is, among lay people and scientists alike, an intriguing prospect that resonates with futuristic scientific romanticism. For those afflicted with such incurable brain diseases, and their loved ones, the prospect offers new and exciting hope. For the physicians, the prospect offers the power to successfully treat patients for disorders in which the clinician has previously been powerless. The sobering truth is that neural transplantation for the treatment of neurodegenerative disease in humans is confronted with a number of major problems. These include increasing the efficiency of the grafts in order that precious tissue is utilized to it fullest, determining the most appropriate sites for engraftment of tissue, and improving access to fresh tissue and/or developing an alternative tissue source. In addition, a possible trend that must be avoided is that of diverging from the fundamental question: What is the etiology of these disorders and how can we stop the disease process? However, regardless of these critical problems, the fact remains that the deplorable quality of life of patients urges immediate intervention. As basic research continues and more patients are grafted, neural transplantation will likely become more effective. One example of such progress is that future grafting protocols for transplantation into humans will consist

of depositing multiple grafts using a small gauge cannula (Dr. Thomas Freeman, University of South Florida College of Medicine, personal communication).

Most Parkinson's research has focused primarily on the striatum as the important site of action for grafts as well as various drugs, such as L-dopa. However, it has been shown that the effects of L-dopa in Parkinson's patients and in animal models is partly due to elevation of dopamine levels in the substantia nigra (Robertson & Robertson, 1989). Recent studies in which multiple micrografts of embryonic ventral mesencephalon were placed into the substantia nigra of the 6-OHDA-lesioned adult rat demonstrated striking survival and integration of these grafts within the host structure (G. Nikkhah, M. Cunningham, C. Bentlage, & A. Björklund, unpublished). Upon administration of the mixed D1-D2 agonist apomorphine, the D1 agonist SKF38393, or the D2 agonist quinpirole, rotation asymmetry was significantly reduced. This compensation was strongly correlated with the number of surviving TH-positive cells in the substantia nigra. These results suggest that a more comprehensive behavioral recovery may be obtained with the engraftment of cells into the substantia nigra in addition to the striatum. Experiments involving multiple micrografts placed in both of these structures are now being conducted (G. Nikkhah, C. Bentlage, & A. Björklund). The results of these studies will assuredly prove to be important for future transplantation therapy in human patients.

The present experiments have demonstrated that CNS progenitor cells can be cloned, express stem cell properties, and upon transplantation, differentiate to neuronal and astrocytic fates. The response of HiB5 cells to seizure activity, and their participation in long-term potentiation, are consistent with the conclusion that the implanted cells integrate into the circuitry of the host. Furthermore, recent anatomical and behavioral studies have indicated that the irradiation-lesioned newborn dentate gyrus can be partially reconstructed with the HiB5 cell line. That is, animals which were irradiated as newborns, and shortly thereafter received multiple bilateral deposits of HiB5 cells in the dentate gyri, perform better in a spatial learning task than lesion only or control grafted animals (See Appendix I) (J. Sørensen, M. Cunningham, T. Rasmussen, & J. Zimmer, in preparation).

That embryonic brain tissue has remarkable abilities to differentiate and function following transplantation into the adult animal is now a matter of fact (for example, see Björklund et al., 1976). The therapeutic value of immortalized cells which are capable of differentiating in the adult brain would be immense. The results reported here indicate that conditionally-immortalized cell lines hold considerable promise towards this end.

Since it appears that the HiB5 cell line can differentiate normally in vivo, one could now attempt to define the interactions that are necessary to promote differentiation in vitro. This could also include the study of variations on the extracellular matrix and the

analysis of axon guidance mechanisms, which is the focus of a great deal of effort (for review, see Lander, 1987). Furthermore, factors which contribute to aberrant proliferation and differentiation may be readily investigated. For example, cells could be infected with various oncogenes or exposed to toxins or carcinogens prior to grafting. Oncogenesis could thereby be modeled.

Several reports have shown that the mRNAs for the neurotrophins NT-3, BDNF, and NGF are widely expressed in the developing and adult hippocampus (Ernfors et al., 1990b; Friedman et al., 1991a). Moreover, BDNF and NGF have been shown to support the differentiation and survival of the cholinergic neurons projecting from the septum to the hippocampus (Hefti, 1986; Hofer & Barde, 1988). Current *in vitro* studies have shown through Northern blotting that the HiB5 line expresses high levels of BDNF and NT-3 mRNA as well as detectable levels of NT-3 receptor (TrkC) mRNA (Diana Collazo, personal communication). On the other hand, the nestin-negative hippocampal line, HiA4, used for negative control grafts in Chapter 4, does not express BDNF, NT-3, or TrkC mRNA at 39°C, and its expression of NGF mRNA is weak (See Appendix II). These data set the stage for experiments in which the expression of neurotrophins and there receptors can be genetically altered. The consequences of such manipulation can then be assessed *in vitro* and through transplantation.

The genetic manipulation of mammalian systems has been greatly extended by recent work making use of transgenic mice and embryonic stem cells (see Gossler et al., 1986; Robertson et al., 1986). An example relevant to the LTP data presented here is the recent gene knock-out experiments in which mutant mice deficient for CAM kinase C were produced. These animals demonstrate poor induction of LTP and their performance in a spatial learning task (Morris water-maze) is compromised as well (Asa Abeliovich, personal communication). However, undesirable effects are commonly seen with these and other transgenic animals, including a high neonatal morbidity and retarded development. Implanting genetically manipulated immortal cells into specific sites in the brain may therefore offer some unique advantages over manipulating the genome of the entire animal. Introduction of genetic changes into an immortalized cell line, which is then transplanted in relatively small numbers into the brain, may allow for the investigation of developmental and physiological questions in an otherwise normal environment. In comparison, transgenic mice have the disadvantage that the whole animal is genetically altered, raising potential problems with pleiotropic genetic effects. These effects may be especially acute in the CNS, where many features of function depend on interactions between different neurons.

It is therefore conceivable that the mechanisms underlying complex phenomena such as LTP can be investigated by genetically modifying and then implanting cell lines like HiB5. Since there is now compelling evidence that these cells integrate into the normal

circuity and establish synapses which can be potentiated, the mediators of this potentiation can be systematically evaluated. For example, gene modification or knock-outs can be conducted for one or a combination of genes such as NMDA receptor subtypes, protein kinase C, and the previously mentioned CAM kinase C, as well as the Ca^{2+}/calmodulin-, Ca^{2+}/phospholipid-, and cAMP-dependent protein kinases, which are thought to be involved in short-term synaptic plasticity (Reichardt & Kelly, 1983).

A case in point is the AMPA subclass of glutamate receptors. The perforant path - granule cell synapse exhibits a decremental form of LTP which decays over a period of several weeks (Barnes, 1979). It is believed that LTP at this synapse is a consequence of a change in channel kinetics of the AMPA receptors (Staubli et al., 1992). Since the genetic sequence of the AMPA receptor is known, the number of the receptors expressed by the cell may be increased and/or the receptor can perhaps be altered, enhancing the kinetic properties and strengthening baseline transmission and the stability of LTP. Increasing the efficiency of the AMPA channels of existing granule neurons or of cells engrafted into the fascia dentata may be of particular value for degenerative diseases such as Alzheimer's Disease, in which the number of synapses is markedly decreased.

The neonatal grafting studies presented here have not only helped characterize a cell line in the normal developing system, but also have provided information about lineage. The nestin-positive, clonal HiB5 cells appear to be instructed by their microenvironment to differentiate into distinct fates. Their pluripotency is observed on two levels. They are pluripotent within the same structure, differentiating into neurons and astrocytes characteristic to that site, and they are pluripotent across different developing structures; that is, they are capable of differentiating into a completely different set of neurons and astrocytes characteristic to a disparate region into which they are implanted. The differentiation of cerebellar primordial cells into dentate gyrus neurons and astrocytes suggests that the multipotentiality seen with HiB5 is a general feature of stem cells, as opposed to a culturing artifact. In addition to demonstrating the striking developmental potential of neural precursors, the cell line and the fresh tissue transplantation data raise a provoking developmental question: Do different regions of the brain contain an equivalent multipotential precursor cell type? If so, the identification and isolation of such a cell becomes an intriguing initiative for future research.

The studies presented here have in common a novel perspective on transplantation research for the study of brain plasticity. New methods and revised techniques have shown promise for improving the engraftment of tissue as well as focusing attention on the possible value of studies conducted in the newborn. With

contemporary gene targeting strategies, immortalized cells may prove to be valuable tools in virtually every aspect of neurobiology - including serving as a tissue source for transplantation therapy in neurodegenerative diseases. These approaches, however, are in their infancy and, if and when developed, will become extremely powerful. The data presented in this thesis testify to the importance of actualizing the potential of cultured stem cells for the analysis of the determinants of cell fate, neuronal physiology, and repair in the mammalian central nervous system.

REFERENCES

Björklund A., Stenevi U., & Svengaard, N.-A. (1976) growth of transplanted monoaminergic neurons into the adult hippocampus along the perforant path. Nature 262, 787-790.

Ernfors, P., Wetmore, C., Olson, L., & Persson, H. (1990b) Identification of cells in the rat brain and peripheral tissues expressing MRNA for members of the nerve growth factor family. Neuron 5, 511-526.

Friedman, W., Ernfors, P., & Persson, H. (1991a) Transient and persistent expression of NT-3/HDNF MRNA in the rat brain during postnatal development. J. Neurosci. 11, 1577-1584.

Gossler, A., Doetschman, T., Korn, R., Serfling, E., & Kemler, R. (1986) Transgenesis by means of blastocyst-derived embryonic stem cell lines. Proc. Natl. Acad. Sci. USA 83, 9065-9069.

Hefti, F. (1986) Nerve growth factor promotes survival of septal cholinergic neurons after fimbrial transections. J. Neurosci. 6, 2155-2162.

Hofer, M.M. & Barde, Y.-A. (1988) Brain-derived neurotrophic factor prevents neuronal death *in vivo*. Nature 331, 261-262.

Lander, A.D. (1987) Molecules that make axons grow. Mol. Neurobiol. 1, 213-245.

Reichardt, L.F. & Kelly, R.B. (1983) A molecular description of nerve terminal function. Ann. Rev. Biochem. 52, 871-926.

Robertson, E., Bradley, A., Kehn, M., & Evans, M. (1986) Germ-line transmission of genes introduced into cultured pluripotential cells by retroviral vector. Nature 323, 445-448.

Robertson, G.S. & Robertson, H.A. (1989) Evidence that L-dopa-induced rotational behavior is dependent on both striatal and nigral mechanisms. J. Neuroscience 9(9), 3326-3331.

Staubli, U., Ambros-Ingerson, J., and Lynch, G. (1992) Receptor changes and LTP: An analysis using aniracetam, a drug that reversibly modifies glutamate (AMPA) receptors. Hippocampus 2, 49-58.

Transplantation Strategies for the Analysis of Brain Development and Repair

Appendix

I

HiB5 Grafts Improve Water-Maze Performance in the Irradiation-Lesioned Neonatal Rat.

X-irradiation of the postnatal day 2 (P2) rat selectively eliminates dividing cells, and when focused upon the hippocampus, reduces the granule cell population to approximately 15% of normal (as more than 80% of the granule cells are born postnatally) (Sunde et al., 1984). Experimental animals (P2 male Wistar rats) received bilateral X-irradiation of the hippocampi and within 24 hours were implanted with three, 250 nL suspensions of HiB5 cells into each hippocampus (see Chapter 7 for preparation of cell suspension and grafting procedure). One implant was placed in the dorsal dentate gyrus, one in the ventral dentate gyrus, and one midway between the two. Twelve weeks after grafting, animals were tested for spatial learning and memory using the Morris water-maze as described elsewhere (Morris, 1984).

Preliminary data for representative animals are presented in the following water-maze traces representing the swim patterns of the subjects. Panel A represents the performance of animals in the non-irradiated control group. Note the searching behavior evident by the extensive area explored by the animal. After 3-4 days of testing, the animal is able to find the platform quickly. In contrast, irradiated-only animals, represented by the traces shown in panel C,

rarely find the platform. Furthermore, they demonstrate a lack of searching behavior as indicated by their swimming pattern around the periphery of the pool. The performance of sham grafted animals (which received "implants" of cell suspension medium only) was equally as poor as the irradiated-only animals (data not shown). Subjects which received grafts of HiB5 cells appeared to perform better than sham or irradiated-only animals, although their performance was clearly inferior to non-irradiated controls. Interestingly, grafted animals demonstrated searching behavior resembling non-irradiated animals although "periphery swimming" was evident.

These results suggest that the performance of grafted animals is intermediate to irradiated-only and non-irradiated animals. This may reflect a partial repopulation of the granule cells in the hippocampi. Animals are presently being evaluated histologically. The number of granule cells or the extent of reinnervation required to achieve normal water maze performance is not known. The trend of the present data indicates such a threshhold may be attainable, perhaps by increasing the number of cells grafted into the dentate gyri.

A Non-irradiated control rat "C/06", 1st trial, day 1–10, spatial reference memory:

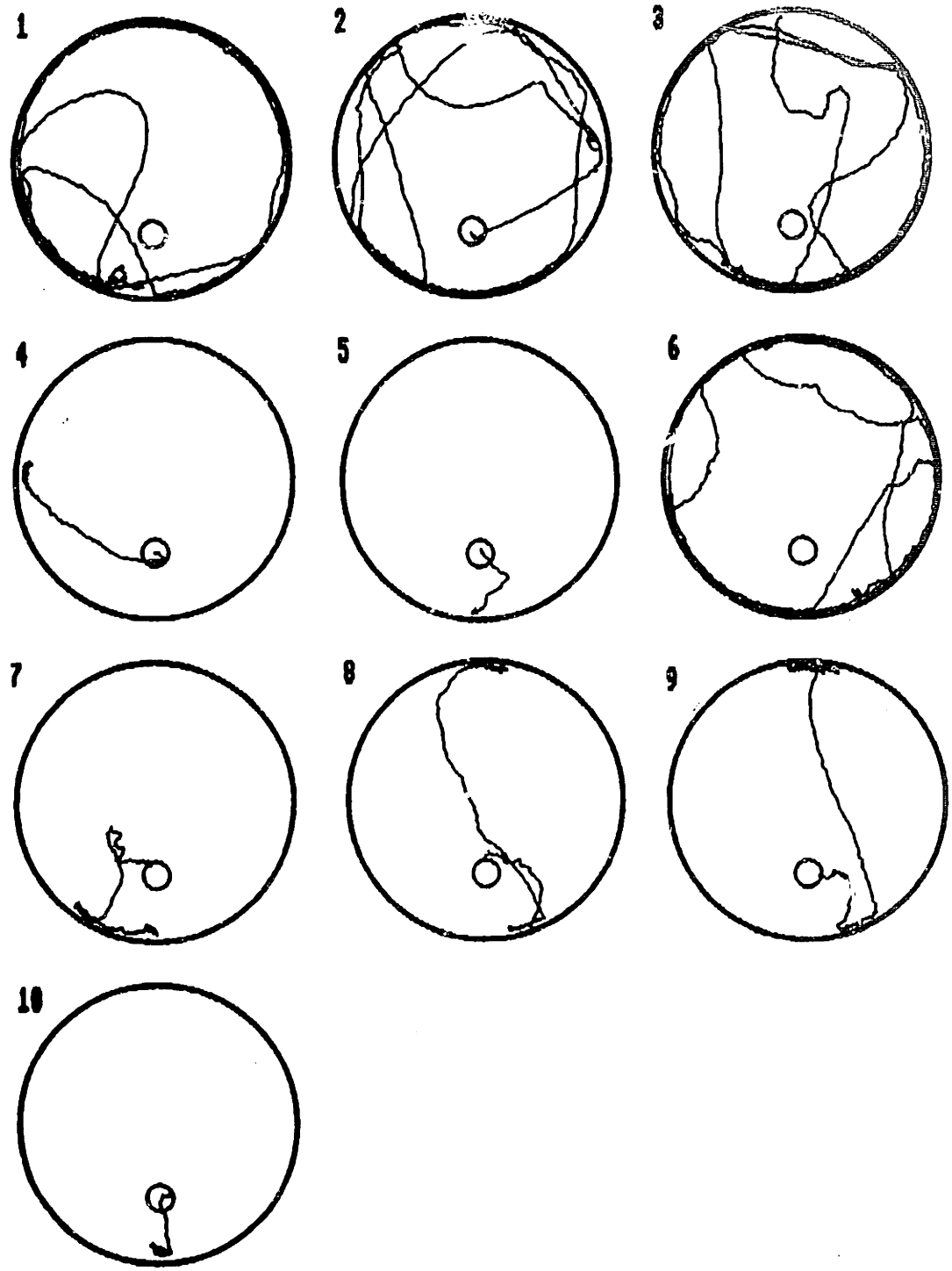

B Irradiated and transplanted rat "B/02", 1st trial, day 1–10, spatial reference memory:

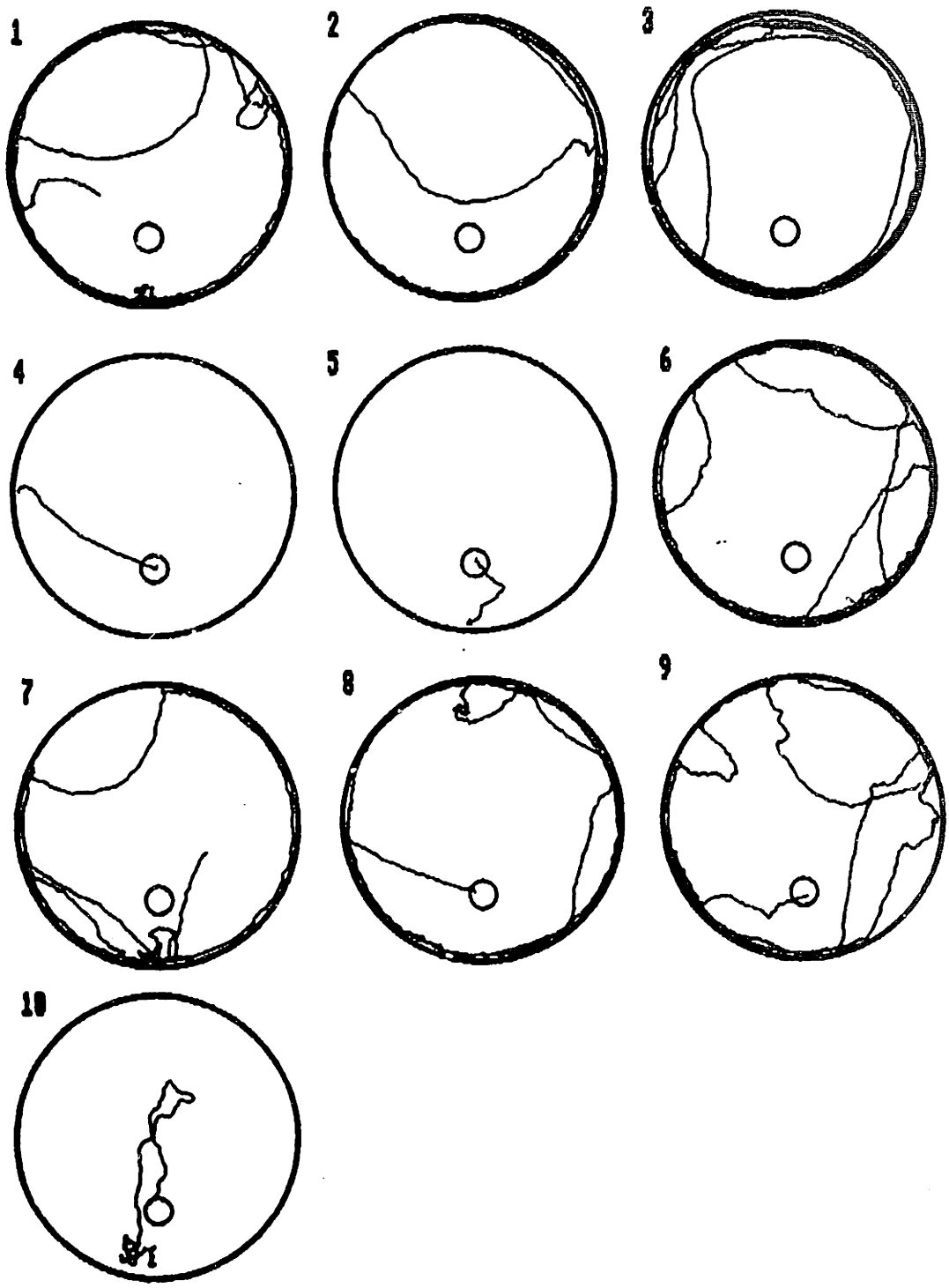

C Irradiated-only rat "D/05", 1st trial, day 1–10, spatial reference memory:

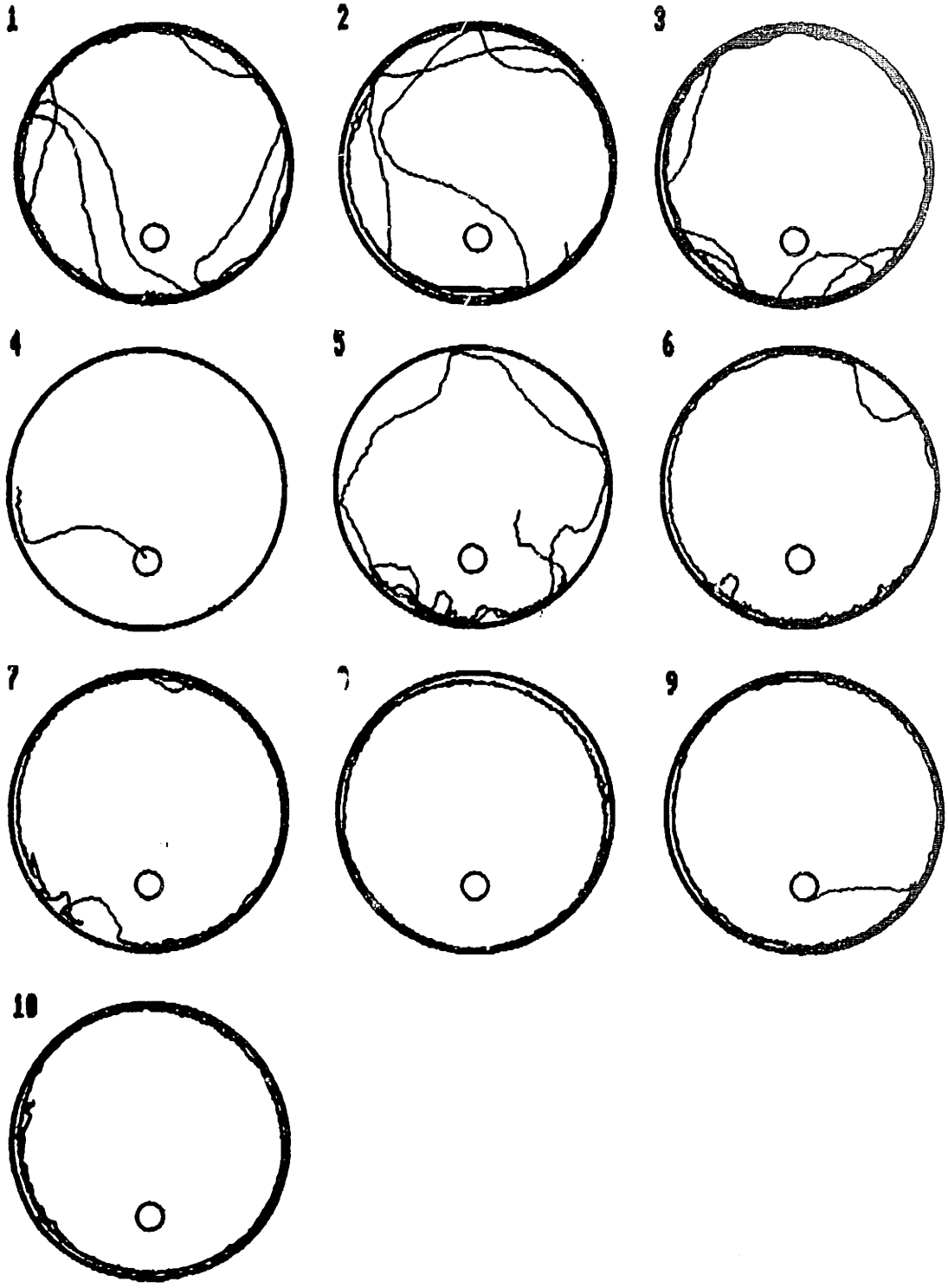

References:

Sunde, N., Laurberg, S., & Zimmer J. (1984) Brain grafts can restore irradiation-damaged neuronal connections in newborn rats. Nature 310, 51-53.

Morris, R.G.M. (1984) Developments of a water-maze procedure for studying spatial learning in the rat. J. Neurosci. Meth. 11, 47-60.

II

***In Vitro* Expression of Neurotrophins by Immortalized Hippocampal Cell Lines.**

cell line	nestin mRNA	BDNF mRNA	NT-3 mRNA	NGF mRNA	TrkC mRNA
HiB5 33°C	+	+++	++	-	+
HiB5 39°C	+	++	++	-	++
HiA4 33°C	-	+	-	+	-
HiA4 39°C	-	-	-	+	-

+++ strong expression
++ moderate expression
+ weak expression